A Structure-Activity Relationship Study of Dihydroajoenes as Anti-Cancer Agents

James Biwi

University of Cape Town

June 2014

A Structure-Activity Relationship Study of Dihydroajoenes as Anti-Cancer Agents

A dissertation submitted to the University of Cape Town

in fulfilment of the requirements for the degree in

Masters in Chemistry

by

James Biwi

Supervisor: Professor Roger Hunter

Co-supervisor: Dr Catherine Kaschula

Department of Chemistry

University of Cape Town

Rondebosch, 7701

Cape Town

South Africa

June 2014

ABSTRACT

Ajoene ((*E*-/ *Z*)-4,5,9-trithiadodeca-1,6,11-triene-9-oxide), a constituent of garlic is known to possess *in vitro* and *in vivo* anticancer activity based on the presence of a vinyl disulfide as its pharmacophore. This thesis reports on the synthesis of dihydroajoenes, a novel set of ajoene analogues, containing a saturated double bond, in which the intention was to study the influence of removing the double bond on biological activity and metabolic stability, since ajoenes are unstable in blood. A divergent synthetic route to 6 new dihydroajoene analogues has been developed in which a phenolic hydroxyl group at the disulfide end served as a platform for modulating aqueous solubility. The dihydroajoene analogues synthesized retained good *in vitro* anti-proliferation activity against a WHCO1 oesophageal cancer cell line, with the phenol derivative showing the greatest activity, with an IC_{50} of 4.1 μM as about 7-times more active than the parent ajoene. In addition the dihydroajoenes were found to be significantly more stable in the red blood cell fraction of mouse blood, when compared with ajoene analogues retaining the double bond. This opens up the possibility of exploring them as anti-cancer agents in an *in vivo* setting.

This thesis also describes a preliminary study towards the synthesis of an ajoene-drug (fludarabine) conjugate for chemosensitization studies, in which an advanced synthetic intermediate was secured.

Declaration

I am presenting this dissertation in full fulfilment of the requirements for my degree.

I know the meaning of plagiarism and declare that all the work in

A Structure-Activity Relationship Study of Dihydroajoenes as Anti-Cancer Agents, save for that which is properly acknowledged is my own.

_____

James Biwi

June 2014

Acknowledgements

I would like to thank the following people for their contribution to this thesis:

Firstly, un-ending gratitude to my supervisor Professor Roger Hunter, for his support, patience and guidance for the duration of this dissertation. Dr Catherine Kaschula for valuable insights and for giving direction to the biological component of this project. Professor Iqbal Parker for allowing me to make use of the ICGEB laboratories at the Institute of Infectious Disease and Molecular Medicine (IDM), UCT. Dr Carmen De Kock for all the pharmacological work she conducted as part of this project.

Special thanks to the members of the Hunter group, Dr Sophie Rees-Jones, Thobela Bixa, Mandla Mabunda, Cathyrn Driver, Fabrizio L'abbate, Wade Petersen, Rudy Cozett, John Woodland, Greg Bowden, Ana Andrijevic, Kathryn Wicht, Athi Msutu, Shankari Nair, Nomakhwezi Mvumvu, Valerie Ramaotsoa and Mpho Mafata. Guys all those long days, late nights and six day weeks would have been unbearable without your presence and warm smiles. Munnerah Smith for nudging me through "the joys" of tissue culture. My colleagues in IDM your company and science discussions were most welcome. My friend, Thobela Bixa - it's been a long journey but your support and never ending kindness has helped me navigate the "struggle".

Mr Pete Roberts and the University of Stellenbosch CAF for the analytical Services.

Many thanks to the Mellon Mays Undergraduate Fellowship, for mentoring and financial support during my academic stay at UCT. A special mention goes out to Kathy Erasmus and Gideon Nomdo, who were instrumental in my growth both emotionally and academically.

My mother and sister for being patient during what has been a very long academic journey.

Rutendo Jessica Kasiamhuru, thank you for your enormous support during a very stressful period of my life.

LIST OF ABBREVIATIONS

aq	aqueous
ar	aromatic
brs	broad singlet
cat.	catalytic
d	doublet
dd	doublet of doublets
ddd	doublet of doublets of doublets
dt	doublet of triplets
equiv	equivalents
EtOAc	ethyl acetate
EtOH	ethanol
g	grams
h	hours
Hz	hertz
HPLC	high pressure liquid chromatography
HRMS	high-resolution mass spectroscopy
IDM	Institute of Infectious Disease and Molecular Medicine
IR	infra-red spectroscopy
J	coupling constants
m	*meta*
m-CPBA	*meta*-chloroperbenzoic acid
m	multiplet
min	minute
m/z	mass-to-charge ratio

mp	melting point
mg	milligrams
ml	millilitres
mmol	millimole(s)
mol	mole(s)
Me	methyl
NMR	nuclear magnetic resonance
OMe	methoxy
o	ortho
p	para
Pet ether	petroleum ether
Ph	phenyl
ppm	parts per million
*p*MBCl	*para*-methoxybenzyl chloride
q	quartet
RBC	red blood cell
rt	room temperature
s	singlet
t	triplet
td	triplet of doublets
THF	tetrahydrofuran
TLC	thin layer chromatography

Contents

Chapter 1: Review of Biological and Chemical Aspects of Ajoene

1.1 Introduction

This thesis describes the synthesis of ajoene analogues designed for a Structure-Activity Relationships (SAR) study. The project spans several research fields thus this chapter will give a background of some of the interesting aspects of ajoene.

1.1 Garlic Overview

Garlic (*Allium sativum*) is a plant species of the genus *Allium*, to which onion, shallot and chive belong. Garlic has been known throughout history from as early as the ancient Sumerian (2600-2100 B.C.) and Egyptian civilisations (~1500 B.C.). The use of garlic as a medicinal herb is recorded in the oldest preserved medical book, The Egyptian *Codex Ebers* (Ebers Papyrus).[1] Several early civilisations came to similar conclusions regarding the therapeutic properties of garlic. The ancient civilisations of India, China, Greece, Rome and Egypt used it extensively. Garlic use was common among the working class as an agent that could increase endurance, prevent abdominal complications, and enhance the cardiovascular and respiratory systems. In ancient Egypt garlic was given to labourers working on the pyramids, it was thought to enable workers to work harder and longer hours. Greek athletes are reported to have ingested garlic before competing in the Olympics making it the first recorded "performance enhancer" in the history of sport.[1]

The use of garlic as a culinary and medicinal substance continues to this day. Contemporarily, an increased average life expectancy has unearthed a new set of health issues that are age-related. There has been questions on the over reliance of synthetic medicines, as opposed to herbal medicines, in addressing modern medical concerns. Several studies have shown that a shift to a Mediterranean diet reduces the risk of several age-related chronic diseases.[2] Garlic is one of the plants that is part of the Mediterranean diet and has received resurgent attention in research circles. Of particular interest to modern therapies, garlic is claimed to offer protection against cancer, cardiovascular disease, platelet aggregation, thrombosis, diseases associated with cerebral aging, arthritis, cataract formation; and can rejuvenate skin, improve cardiovascular circulation and increase energy levels.[3] The biological activity of garlic has been attributed to a group of structurally related organo-sulfur compounds found or generated within the clove under different conditions.

1.3 The Chemistry of Garlic

Fresh garlic contains mainly water with the bulk of the dry weight being fructose-containing carbohydrates (Table 1).[3] It also contains protein, fat, fibre, 17 amino acids, at least 33 sulfur containing compounds, the elements: germanium (14 µg/100 g), calcium (50–90 µ g/100 g), copper (0.02–0.03 µg/100 g), iron (2.8–3.9 µg/100 g), potassium (100–120 µg/100 g), magnesium (43–77 µg/100 g), chromium (0.3–0.5 mg/100 g), manganese (0.2–0.6 mg/100 g), boron (0.3–0.6 mg/100 g), barium (0.2–1 mg/100 g), aluminium (0.5–1 mg/100 g), sodium (10–22 mg/100 g), phosphorus (390–460 mg/100 g), zinc (1.8–3.1 mg/100 g) and selenium (15–35 µg/100 g). The fresh garlic clove contains various vitamins, namely thiamine (0.25 mg/100 g), riboflavin (0.08 mg/100 g), vitamin C (5 mg/100 g), nicotinic acid (0.5 mg/100 g) and retinal (15 µg/100 g).[4] The medicinal properties and biological properties of garlic are attributed to the sulfur-rich compounds present or generated when the clove is damaged.

Table 1: General composition of Garlic, [a]excluding protein and inorganic sulfate.[3]

Component	Amount (fresh weight, %)
Water	62-68
Carbohydrates (mainly fructose)	26-30
Protein	1.5-2.1
Amino acids: common	1-1.5
Amino acids: cysteine sulfoxides	0.6-1.9
γ-Glutamylcysteines	0.5-1.6
Lipids	0.1-0.2
Fibre	1.5
Total sulfur compounds [a]	1.1-3
Sulfur	0.23-0.37
Nitrogen	0.6-1.3
Minerals	0.7
Vitamins	0.015
Saponins	0.04-0.11
Total oil-soluble compounds	0.15 (whole)-0.7 (cut)
Total water-soluble compounds	97

The earliest chemical studies on garlic were by the German chemist Wertheim in 1844, who isolated diallyl (from *Allium*) disulfide from garlic oil. About five decades later in 1892, Semmler isolated 60 % diallyl disulfide, 20 % diallyl trisulfide and a minor component of diallyl tetrasulfide by fractional distillation of garlic oil. In 1944 Cavallito reported isolation of an odiferous extract (with antibacterial activity), which was coined allicin, by stirring freshly ground garlic clove in 95 % ethanol at 10 °C.[5]
The parent sulfur compound found in intact garlic clove is alliin (*S*-allylcysteine sulfoxide).[6] For years it remained a mystery as to how alliin was transformed to allicin upon damaging of the clove. In 1948 Stoll and Seeback reported that garlic cloves contain an enzyme alliinase which is housed in a different compartment to alliin and converts alliin into allicin when the clove is damaged (Scheme 1).[7&8] In the first step alliinase catalyses the decomposition of alliin to 2-propenesulfenic acid, while in a subsequent reaction two molecules of propenesulfenic acid self-condense to form allicin.

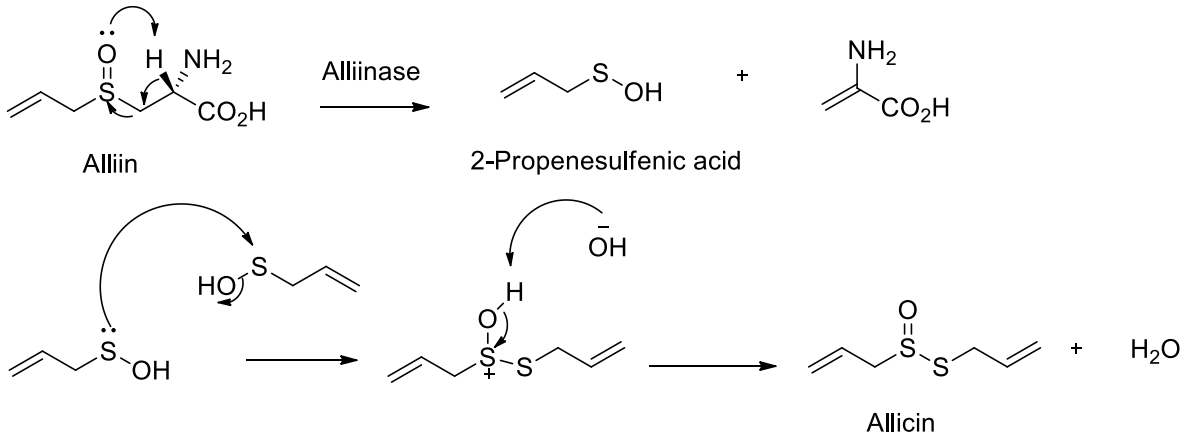

Scheme 1: The conversion of Alliin to Allicin by the action of the enzyme allinase

Allicin is an odoriferous, unstable thiosulfinate that is slightly soluble in water (2.5 % at 10 °C).[5] It degrades to give various sulfur compounds that are the consitiuents of crushed garlic preparations (the major organosulfides are listed in Fig 1). Allicin is easily transformed into oil-soluble organosulfides mainly diallyl disulfide and to a lesser extent diallyl sulfide and diallyl trisulfide. The relative amounts of the second-generation organosulfides present in a garlic preparation depends on the age and method of preparation of the garlic.[6]

Under certain conditions allicin can be transformed into vinyl dithiin or *E* and *Z* ajoene.[8] Vinyl diithiin was first observed from GC-MS analyses of the allicin fraction of a garlic extract.[8] *(E* and Z)-4,5,9-trithiadodeca-1,6,11-triene-9-oxide (Ajoene, **1**) was first reported in the 1980s following the work of Block and Apitz-Castro who elucidated its structure.[9]

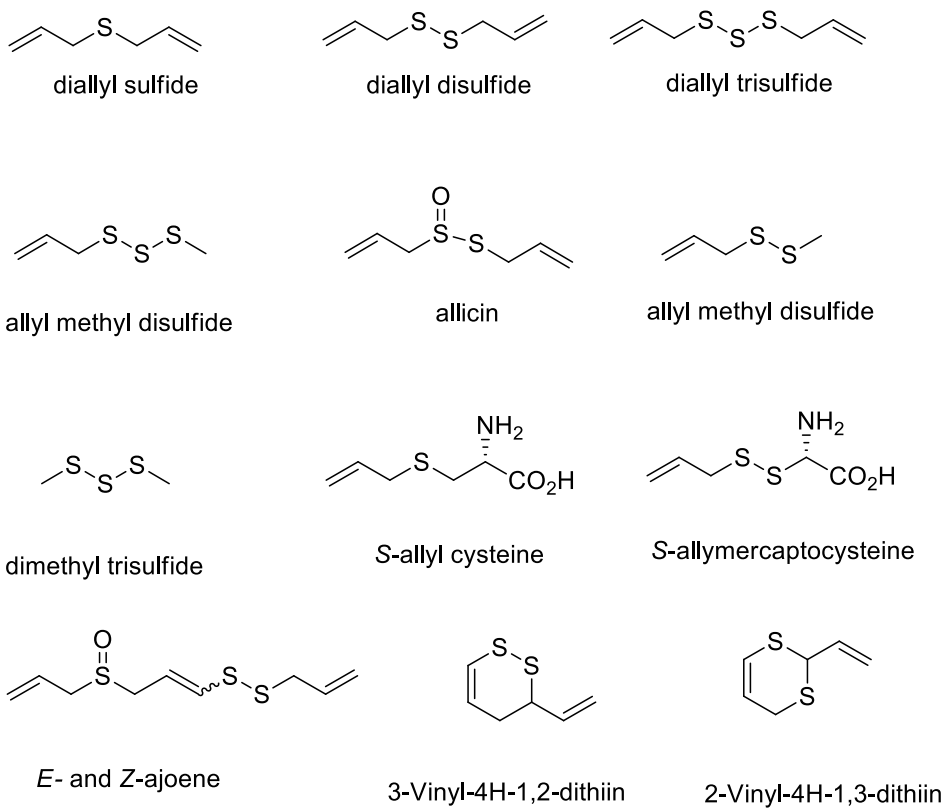

Figure 1: The major organosulfides found in crushed garlic

1.4 Ajoene

Ajoene, **1**, (Spanish for garlic = Ajo) is a rearrangement product of allicin. It is an organosulfide comprised of an allylic sulfoxide and an interesting vinyl disulfide functionality. It was Block and Apitz-Castro who first proposed the mechanism by which allicin degrades to ajoene (Scheme 2).[10]

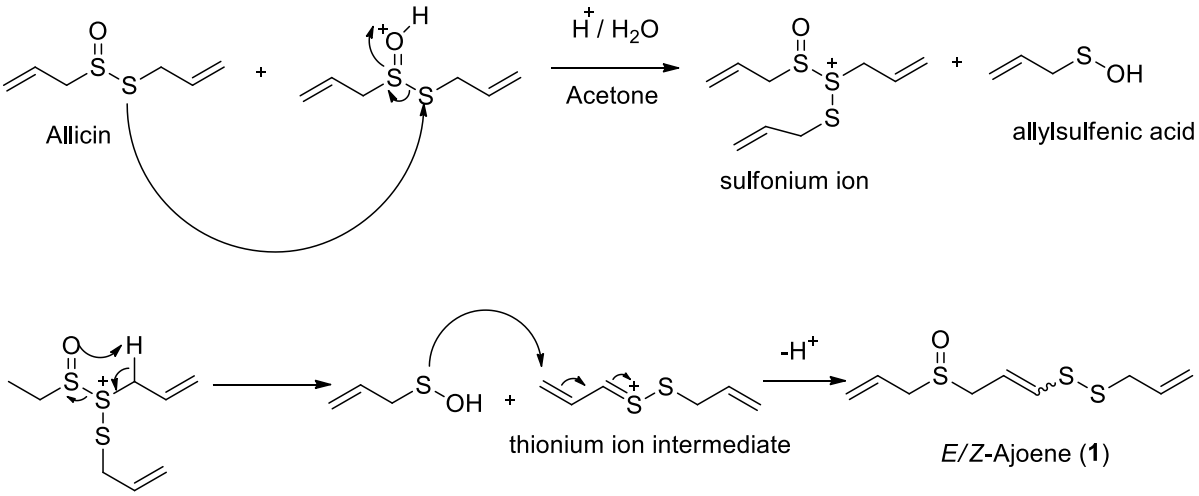

Scheme 2: Degradation of Allicin to Ajoene

The degradation of allicin to ajoene according to the proposed mechanism commences with *S*-thioalkylation of allicin. In the second step allylsulfenic acid is lost via a Cope-type elimination to give a thionium intermediate. In the final step allylsufenic acid re-adds to the thionium intermediate to give ajoene (**1**). In fresh garlic preparations the *Z*-ajoene isomer is reported to be present in about double the abundance of the *E*-isomer.[11] Block and Apitz-Castro reported the biomimetic chemical synthesis of ajoene, which involved refluxing a solution of allicin in an acetone-water (3:2) suspension.[10] The produced material, which was identical to the biological sample, was obtained via 4 h of centrifugation, then extraction using methylene chloride (DCM) and then the DCM concentrate was purified by flash chromatography. Ajoene (**1**) is reportedly obtained in about 34 % yield as a mixture of *E* and *Z* isomers (4: 1).

The early work by Block and co-workers in the 1980s demonstrated ajoene's ability to inhibit platelet aggregation, and since then there has been an increasing body of evidence reported on the biological activity of ajoene by several research groups in the past three decades. Overall ajoene has been reported to have antimicrobial, antiobesity, antifungal and anticancer activities.

1.5 The Biological Activity of Ajoene

1.5.1 Anti-Thrombotic Activity

Thrombosis is the formation of a blood clot in a blood vessel, obstructing circulatory blood flow. A thrombus (blood clot) can obstruct blood flow to an organ causing severe health complications. Physiologically platelet aggregation precedes the formation of a thrombus. Ajoene has been shown to inhibit platelet aggregation thus making it a potent thrombotic agent.

In vitro studies show that ajoene can reversibly inhibit platelet aggregation and activation induced by known agonists.[12] Ajoene was shown to synergistically potentiate the anti-aggregation properties (on human platelets) of the drugs prostacyclin, forskolin, indomethacin and dypiridamole.[13] The work of Apitz-Castro has shown that ajoene can prevent thrombus formation under highly thrombogenic conditions. Under *in vivo* flow conditions (mimicking small to medium blood vessel sizes) ajoene prevented thrombus formation induced by severe vascular damage.[12&14] Regarding the mechanism by which ajoene inhibits platelet aggregation there has been several suggestions.[15&16]

One of the suggestions was that ajoene interacts with a hemoprotein implicated in platelet aggregation. Using spectral measurement it was demonstrated that ajoene interacted cooperatively with the hemoprotein. The interaction of ajoene with the hemoprotein modified its binding to ligands regarded to be physiologically relevant effectors of platelet aggregation.[15] Studies have

shown that ajoene indirectly inhibits the synthesis of thromboxane A2 (a platelet activator) by strongly inhibiting the arachidonic pathway.[16]

1.5.2 Anti-Microbial Activity

Ajoene is a potent inhibitor of various pathogenic microbes of the protozoa, fungal and bacterial families, for which it has been shown that ajoene inhibits the growth of various Gram-positive and Gram-negative bacteria. The ajoene Minimum Inhibitory Concentration (MIC) was found to be 5 µg/mL against the gram-positive bacteria: *Bacillus cereus*, *Bacillus subtilis*, *Mycobacterium smegmatis* and *Streptomyces griseus*. Against the gram-negative bacteria, *Escherichia coli*, *Klebsiella pneumoniae* and *Xanthomonas maltophilia*, the MICs were found to be between 100 - 160 µg/mL.[17]

At concentrations below 20 µg/mL, ajoene inhibits the growth of yeast.[17] When fractions of garlic extract were studied for antifungal activity, the ajoene fraction was found to exhibit the strongest antifungal activity.[18] The growth of both the fungi species *Aspergillus niger* and *Candida albicans* was inhibited by ajoene at concentrations below 20 ug/ml.[18] Ajoene also inhibited the growth of the human fungal pathogen *Paracoccidioides brasiliensis* by disrupting the integrity of the fungi's cytoplasmic membrane.[19] In botany, ajoene inhibited the germination of plant pathogenic fungal spores.[20]

Ajoene has also been shown to inhibit phosphatidyl choline synthesis in trypanosomal pathogens, ajoene inhibited the proliferation of *Trypanosoma cruzi*, the causative agent of Chagas' disease.[21] It has been suggested that the antimicrobial activity of ajoene and similar compounds is dependent on the presence of the disulfide bond.

1.5.3 Anti-Obesity Activity

Obesity is a chronic disease that is increasing alarmingly worldwide. It is linked with various cardiovascular disorders and is a major risk factor for type 2 diabetes. It is characterised by excessive fat accumulation that alters health and increases mortality.[22] At a cellular level obesity is characterised by an increase in the number and size of adipocytes (fat storage cells). A key stage in the life-cycle of adipocytes is the differentiation of pre-adipocytes (in adipose tissue) to adipocytes. Thus treatments that can regulate the number and size of adipocytes are sought after. Recently it was reported that ajoene induces apoptosis in adipocytes.[23] At a concentration of 200 µM, ajoene decreased the cell viability of adipocytes by approximately 50 %.[23] In another study it was shown that linoleic acid had a synergistic effect on ajoene-induced adipocyte apoptosis.[24] The effect of ajoene on adipose tissue mass is a relatively new field and the molecular mechanisms are still being determined.[23]

The antitumor effects of garlic have been documented from as early as the ancient Egyptian civilisations. Hippocrates widely regarded as the father of medicine, used garlic to treat abdominal tumors.[1] The anti-carcinogenic effect of garlic has been attributed to allicin, thioallyl constituents and their derivatives found within the clove. From herein this review will focus on ajoene and its anti-cancer properties.

1.6 Cancer Overview

1.6.1 Cancer

Cancer is a group of diseases characterized by uncontrolled growth and spread (invasion and metastasis) of abnormal cells.[25] Cancer is the second leading cause of death in the first world, and a similar picture is also beginning to emerge in developing countries.[25] Approximately 10 million new cases of cancer are diagnosed each year.[25a] In 2012 about 14 million new cancer cases and approximately 8.2 million cancer fatalities were reported (WHO).[25b]

1.6.2 Treatment of Cancer

Current cancer chemotherapies target different stages in the cell-cycle. Apoptosis (programmed cell death) plays a key role in normal cell physiology. In cancerous cells there is a dysregulation of apoptosis. Chemotherapeutics work by targeting fast-dividing cells and inducing apoptosis. Chemopreventive drugs are classified as follows[26]:

1. **Akylating Agents—** This class of compounds covalently links to amino, carboxyl, sulfhydryl, and phosphate groups of biologically important molecules. The resulting effect being an impaired cellular function. An example is cisplatin.
2. **Antimetabolites—** These are structural analogues of metabolites involved in deoxyribonucleic acid (DNA) or ribonucleic acid (RNA) synthesis. Antimetabolites induce their cytotoxity by competing with natural metabolites for key active sites on enzymes or incorporation into DNA or RNA, thus impairing DNA or RNA synthesis. Cytarabine and fludarabine are examples.
3. **Natural Products —**Several antitumor compounds have been isolated from plants, fungi and bacteria.

   a) Antitumor antibiotics

   These are antibiotics produced by bacteria. An example is Bleomycin, its mode of action is through insertion into DNA strands resulting in the release of reactive oxidative species (ROS).

   b) Anthracyclines

   Anthracyclines are a class of structurally similar compounds which are produced by the fungus *Streptomyces percetus var caesius*. Anthracyclines have several modes of action most notably

their ability to intercalate between DNA base pairs and inhibition of DNA topoisomerases I and II. Doxorubicin is an example of this class of drug.

c) Podophyllotoxins

These are semisynthetic analogs of compounds naturally occurring in the roots of the American plant Mayapple (Podophyllum peltatum). These compounds work by inhibiting topoisomerase II. The two common podophyllotoxins are etoposide and teniposide.

d) Vinca alkaloids

Class of compounds derived from the periwinkle *Catharanthus roseus.* Vinca alkaloids work by binding to tubulin preventing formation of microtubules an essential component for cell division.

e) Taxanes

Are compounds derived from the needles of yew plants (*Taxus*), characteristic of this class is the diterpene backbone. Taxanes promote microtubule assembly and stability causing cell arrest in the mitotic stage of the cell cycle. Docetaxel is an example of a well-established mitotoxic taxane.

f) Camptothecin analogs

These drugs are semisynthetic analogs of camptothecin, an alkaloid isolated from the Chinese tree *Camptotheca acuminate*. Camptothecin analogs inhibit topoisomerase I and interrupt the elongation phase of DNA replication. Irinotecan and topotecan are semisynthetic camptothecin analogs.

Despite the progress that has been made in treating cancer over the last three decades, cancer incidence is still on the rise, cancer cases are expected to rise from 14 million in 2012 to about 24 million within two decades.[25] The genetic instability and fast-mutating nature of cancerous cells tend to leave most drugs inadequate after a few cycles of treatment. This long term ineffectiveness coupled with the fact that most chemotherapies have severe side effects, has kept the search for more anti-cancer agents a focal point. The design of anti-cancer agents requires the understanding of cell physiology and how cancerous cells evade apoptosis.

1.6.3 Eukaryote Cell Cycle

The cell cycle comprises of five phases: The resting phase G_0, Gap 1 (G_1), Synthesis (S), Gap 2 (G_2) and Mitosis (M). In the G_0 phase the cell is in a dormant state or resting state and no growth or multiplication occurs. Cells in the next stage of the cycle G_1, produce mRNA and participate in the physiological function characteristic of the tissue in which they are found. In G_1 the cell is actively

growing in size and preparing to copy its DNA. The next phase is S, where the cell makes a copy of its DNA. Once the cell has made a copy of its chromosomes, it undergoes a second growth phase (G_2), in which the cell prepares for mitosis. Finally the cell divides and forms two daughter cells (each containing a full set of chromosomes) during the M phase. The daughter cells can enter the cycle again via G_1 or enter a dormant state G_0. Progression through the different phases is a highly regulated process.[27]

Cells have developed a series of cell-cycle checkpoints, which are regulatory pathways that control the order and timing of cell cycle transitions and ensure that critical events such as DNA replication and chromosome segregation are completed with high fidelity.[28] Cell check point loss has been implicated in genomic instability and progression to cancer.[28] Check points are governed by a group of proteins known as cyclins and enzymes called cyclin dependent kinases (CDKs). Cell progression from one phase to the other is promoted by the binding of cyclin to its associated kinase thereby activating the enzyme.

To progress from G_1 to the S phase there has to be a favourable balance between stimulatory versus inhibitory signals towards cell growth. When the balance is favourable towards cell growth and multiplication, there is an increase in cyclin D which in turn binds to CDK4 and CDK6 (Figure 2). Once the cyclin D-CDK4/6 complex is formed it phosphorylates a growth-inhibitory factor known as retinoblastoma protein (pRb). In its hypophosphorylated active state pRb binds to the transcription factor E2F but once phosphorylated pRb can no longer bind to the transcription factor.

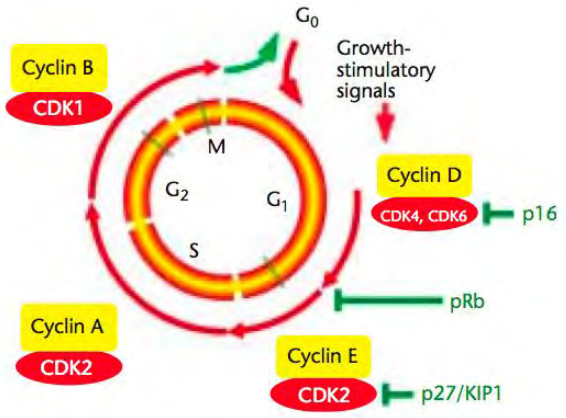

Figure 2: The cell cycle and critical regulators. [30]

E2F is then free to bind to certain parts of DNA, inducing transcription of several genes that code for proteins capable of taking the cell through to the S phase. One of these proteins is cyclin E. Once produced cyclin E binds to CDK2 and this complex is responsible for progression from G_1 to S phase. Several activated cyclin-CDK complexes are essential for progression through the cell cycle. Cyclin A-

CDK2 complex is required for the appropriate completion of DNA synthesis in the S phase. Entry into mitosis requires activation Cyclin B-CDK1 complex. Progression through the different stages of the cycle is blocked by proteins that inhibit activation of the different cyclin-CDK complexes. The inhibitory proteins p15 and p16 block the activity of the cyclin D-CDK complex (Figure 2).

As detailed above the cell-cycle is highly regulated, and progression through one phase of the cycle is characterised by an increase in a particular cyclin and activation of CDKs. CDK activation is down regulated by inhibitory proteins. When usually tightly regulated cell check points fail cancer is likely to result. In breast cancer over production of cyclin D and E results in overactive cyclin-CDK complexes.[27] The gene that codes for the inhibitory protein p16 is lost in skin melanoma.[28] In 90 % of all cancers there is oncogenic alteration of cyclins, CDKs and other components of the pRB pathway.[27]

1.6.4 Apoptosis

Apoptosis is an energy-dependent organised cell death that involves the activation of a group of cysteine proteases known as caspases.[29] Apoptosis occurs normally during development and ageing as a homeostatic mechanism for the cell populations in tissues and also helps the body rid itself of cancerous cells with damaged DNA. The body uses apoptosis as part of its defence mechanism, as an immunological response and in response to cell damage by disease or noxious substances.[29] The two main molecular pathways leading to apoptosis are the intrinsic (mitochondrial) and extrinsic (death receptor) pathway. The two pathways are linked and molecules in one pathway can influence the other.

There is a third pathway that uses T-cell mediated cytotoxicity and perforin-granzyme-dependent demise of the cell.[29] Figure 3 summarises the apoptotic events involved in each pathway. The two main pathways are intrinsic and extrinsic as well as a perforin/granzyme pathway. Each pathway initiates in response to some stimuli and following a set of energy-dependent molecular events activates an initiator (caspase 8, 9, 10). The major convergent point of the caspase-dependent pathways is at caspase 3 activation. Once caspase 3 is activated degradation of cellular proteins essential for cell survival starts and apoptosis is inevitable.

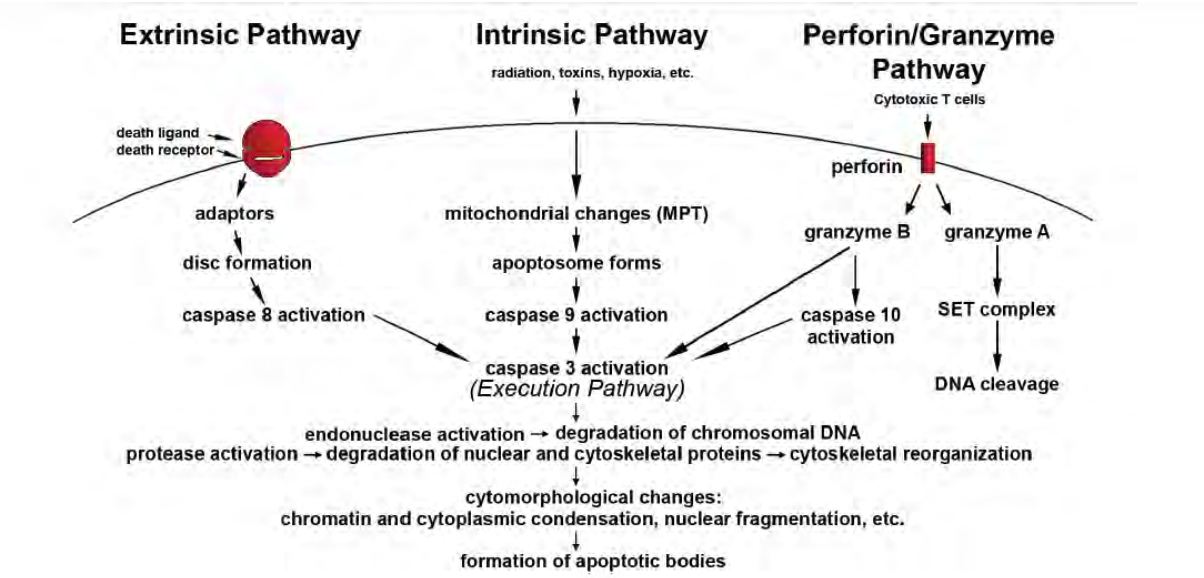

Figure 3: Schematic representation of the apoptotic pathways.[29]

The extrinsic pathway (Figure 3) is activated via extracellular receptor-mediated interactions that result from cues such as growth factor withdrawal and matrix detachment.[30] In the extrinsic pathway extracellular ligands (death ligands) bind to tumor necrosis factor receptors (TNF-R, death receptors) on the surface of the plasma membrane (Figure 3). An example of a death receptor is FAS and the death ligand that binds to it FASL. The binding of a death ligand to its corresponding receptor results in a cascade of events that lead to the activation of caspases and cleavage of proteins essential for cell survival.

In the intrinsic pathway (Figure 3) apoptosis occurs in response to intracellular signals such as DNA damage or oxidative stress. The signals that lead to intrinsic pathway may be due to toxins, hypoxia, viral infection, hyperthermia or free radicals. All these stimuli converge at the mitochondria, causing changes in the inner mitochondrial membrane. This results in opening of the mitochondrial permeability transition (MPT) pore.[31] Loss of mitochondrial transmembrane potential results in the release of pro-apoptosis proteins like cytochrome c into the cytosol. Cytochrome c and other proteins released from the mitochondria activate the caspase-dependent mitochondrial pathway. Cytochrome c binds and activates Apaf-1 forming a complex known as an apoptosome, which then recruits and activates procaspase 9. Activation of procaspase 9 leads to caspase 9 activation. The caspases set about destroying the cell's proteins leading to cell destruction.

Cytotoxic lymphocytes (CTL) induce their cytotoxicity mainly via the extrinsic pathway. However, through a novel mechanism CTL can exert their cytotoxicity on tumor cells and virus infected cells via secretion of perforin (a transmembrane pore-forming molecule).[29] CTL then releases (by exocytosis)

cytoplasmic granules including some structurally related proteases (granzymes). The perforin-granzyme induced apoptosis strongly activates caspases but is also capable of inducing apoptosis via a caspase independent pathway (Figure 3).[29]

Caspases have a fatal effect on cells and are thus regulated to ensure apoptosis does not occur untimely. The Bcl-2 family of proteins regulates apoptosis. Bcl-2 proteins can either be pro-apoptotic (e.g. Bad and Bax) or anti-apoptotic (e.g. Bcl-2 and Bcl-X). In response to apoptotic signals Bax and other pro-apoptotic Bcl-2 family proteins translocate to the mitochondrial membrane changing its permeability thus enabling cytochrome c release. The anti-apoptotic Bcl-2 family proteins counter these effects. A defect in the Bcl-2 family of protein's regulation system can inhibit apoptosis resulting in carcinogenesis. The genes coding for the apoptosis suppressors Bcl-2 and Bcl-X are known to be overexpressed in several tumour types.[27]

1.7 Anti-cancer Activity of Ajoene

1.7.1 Anti-mutagenic

The first aspect of ajoene's anti-cancer activity concerns its ability to prevent carcinogenesis. Consumption of garlic has been shown to reduce the chances of formation of several cancers, which has been attributed to the organosulfides present in the clove.[31] Ajoene has been shown to inhibit mutagenesis, initiated by the mutagens benzo[a]pyrene and 4-nitro-1,2-phenylediamine on *S. typhimurium*, in a dose-dependent manner.[32] The mechanisms as to how ajoene inhibits mutagenesis are not fully understood. It has been proposed that it could proceed via inhibition of cytochrome P450-dependent monooxygenases, which are responsible for carcinogen activation. It has also been suggested that the mechanism involves the induction of phase II detoxification enzymes, which are responsible for accelerated carcinogen detoxification.[32]

1.7.2 Anti-tumour

Ajoene has been shown to inhibit cell proliferation in a number of malignant cell-lines including mammary, bladder, colorectal, hepatic, nasopharyngeal, gastric, prostrate, lung, pancreatic, lymphoma, leukemia and skin with an IC_{50} range of 5 - 41 μM.[33] Scharfenberg and co-workers were the first to show the cytotoxicity of ajoene, which was demonstrated on a tumourgenic lymphoid cell line derived from a Burkitt lymphoma (BJA-B), with ajoene exhibiting comparably less cytotoxicity on the non-tumourgenic control cell line (baby hampster kidney BHK_{21}) and human primary fibroblasts.[34]

Scharfenberg's findings on ajoene's cytotoxicity and selectivity have been substantiated in several other publications. In the work by Dirsch and co-workers ajoene induced apoptosis in human acute

myeloid leukemia cells (HL60), as well as in peripheral blood mononuclear cells (PBMC) isolated from a patient with a chronic myelogenous leukemia.[33a] Importantly this study showed ajoene was target specific, as quiescent and proliferating peripheral mononuclear blood cells isolated from healthy donors were not affected by ajoene treatment.[33a]

In subsequent work ajoene's selectivity was demonstrated by Li and co-workers who showed that *Z*-ajoene has anti-proliferative activity against various human cancer cell lines (with IC_{50} values in the range 5.2 µM-26 µM) and to a lower extent against normal marsupial kidney cells (PtK2).[33b] In an experiment to evaluate the cytotoxic effects of ajoene, two tumourgenic cell lines were chosen promyeloleukemic (HL60) and narsopharyngeal carcinoma (KB), and one normal marsupial kidney cell line (PtK2).The cells were incubated with ajoene (1-20 µM) and cell viability measured using a MTT-based colorimetric assay. Figure 4 shows the gradual decrease of cell viability with increasing concentration of ajoene. HL60 cells were the most sensitive to ajoene cytotoxicity, with only 10 % of the cells surviving 48 hours of incubation with 20 µM ajoene, while the KB cells were less responsive than the HL60 cells with 30 % of the cells surviving 20 µM ajoene treatment (Figure 4). The PtK2 cells were more resistant to ajoene cytotoxicity, with 75 % of the cell fraction viable after a 48 hr incubation period. These results demonstrate ajoene's specificity towards tumourgenic cells.

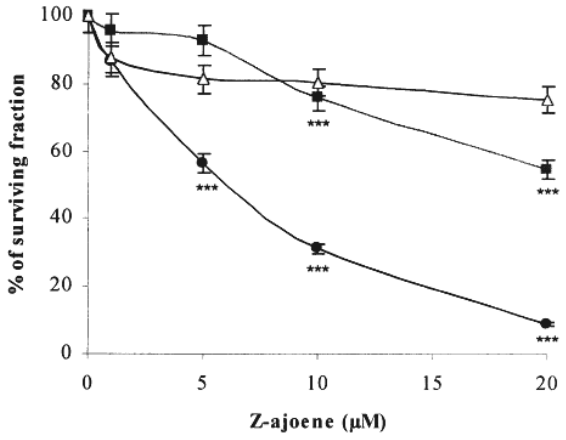

Figure 4: The effects of Z-ajoene on cell viability of; HL60-●-, KB -■-, and PtK2-Δ-. Cells were exposed to increasing concentrations of Z-ajoene (1-20 uM) for 48 hours.[33b]

In vivo ajoene has been found to be effective at treating skin carcinomas both in rodents and in humans.[33b&c] In the study by Li and co-workers Kunming mice were inoculated with transplanted tumours: hepatorcarcinoma 22 and sarcoma 180 (S180). After inoculation (24 h later) the mice were treated with a specific concentration of *Z*-ajoene (2, 4 or 8 mg/kg) via intraperitoneal (i.p.) injection

every day for four weeks. Tumour growth inhibition was measured by weighing of the excised tumours. Compared to untreated mice, tumour growth was inhibited by 10 % and 32 % in S180 implanted mice treated with 4 and 8 mg/kg ajoene respectively. H22 transplanted mice that received 2 and 4 mg/kg of ajoene every day reached 34 % and 42 % tumour inhibition. The results showed that ajoene treatment retards tumour growth. In a similar mouse-model study, ajoene was found to inhibit subcutaneous tumour growth in mice inoculated with B16/BL6 melanoma cells and also reduce the occurrence of metastases in the lung by about 90 % compared to untreated mice.[33c]

Topical application of ajoene in patients with basal cell carcinoma (BCC) resulted in the reduction of tumour size in 81 % of the patients.[35] In this study by Tilli and co-workers, a group of 21 patients with histologically proven BCC and tumor sizes of maximum diameter 2 cm were selected. The carcinomas were treated twice a day by topical application of a 0.4 % ajoene cream (400 mg ajoene, 0.3 ml polysorbate 80, and 0.3 ml sorbitonoleate in 100 ml 1% carbomeric gel). After six months of treatment tumour sizes were measured the results are shown in Figure 5. In 17 of the patients ajoene treatment reduced the tumour size, while in 3 patients the tumour size increased and in 1 of the patients the tumour size was the same as before treatment (Figure 5).[35]

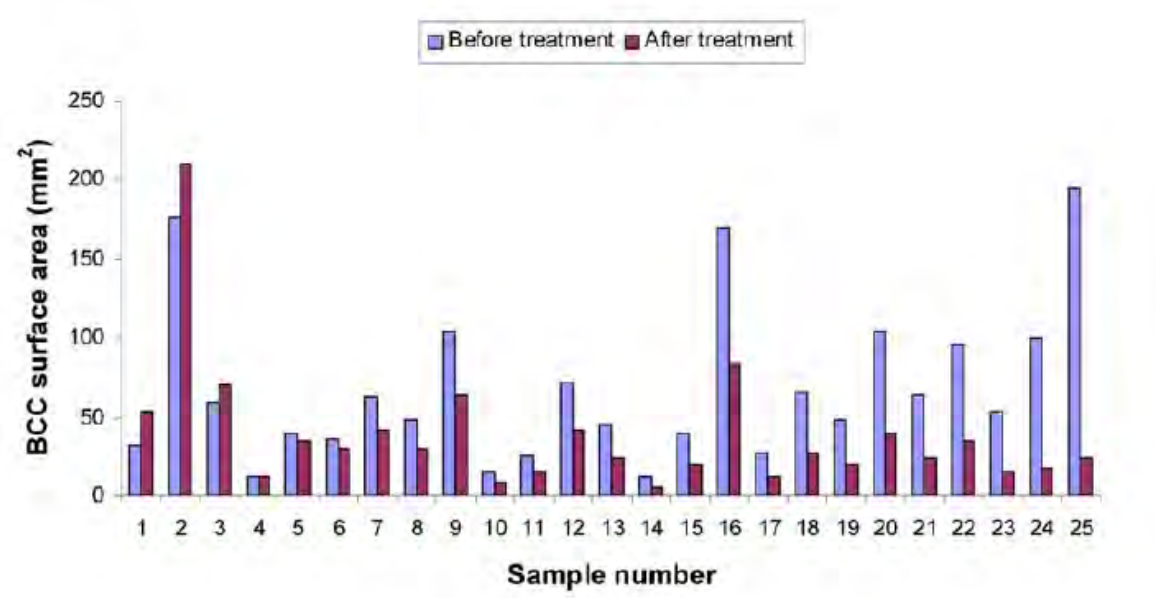

Figure 5: Effect of ajoene on tumour size after topical application in the individual patients.[35]

1.7.3 Chemosensitization

One of the major problems in cancer chemotherapy is the development of drug resistance. Chemosensitization is a strategy used to counteract tumour cell's resistance to a drug, such that when administered with the chemosentisization agent the drug becomes effective again. Tumour cells have several mechanisms by which they become resistant to chemotherapy, which may

include: increased drug efflux and decreased drug influx, drug inactivation, alterations in drug target, processing of drug-induced damage, and evasion of apoptosis (Figure 6).[36] Increased drug efflux occurs due to the overexpression of resistant drug efflux transporters (for example MDR1/Pgp and BCRP MRPs). Similarly certain intracellular molecules can inactivate drugs such as high levels of the thiol glutathione, which is known to inactivate platinum drugs. The third method by which cells can become resistant to chemotherapy is the up-regulation of the survival signal with inhibition of cell death. This can be through the overexpression of growth factors. As described earlier, the over-expression of anti-apoptotic proteins (ie Bcl-2) can prevent cell death, and lead to drug resistance,. These resistance modifications can lead to the development of drug-resistant cancer cells (Figure 6). A successful chemonsensitization agent targets and supresses one or more of the resistance mechanisms making drug-resistant cancer cells more susceptible to therapy.[36]

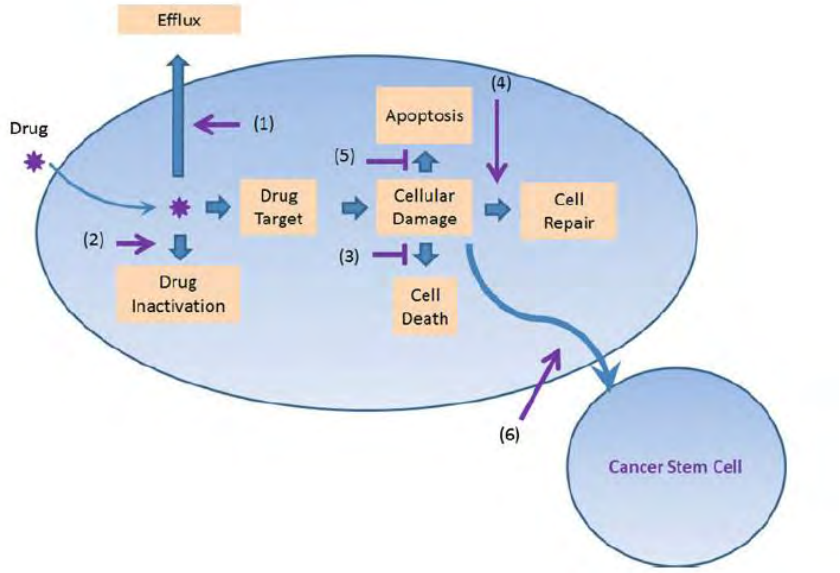

Figure 6: Overview of proposed mechanisms of drug resistance to cancer chemotherapy. (1) Over- expression of a transporter that can efflux the drug, (2) inactivation of the drug by an increased concentration of certain intracellular molecules, (3) up-regulation of survival signal and inhibition of cell death, (4) activation of cellular repair pathways, (5) up-regulation of anti-apoptotic proteins and factors, (6) development of resistant cancer stem cells.[36]

In 2004 Hassan reported that ajoene increases the susceptibility of drug-resistant acute myeloid leukemia (AML) cells towards fludarabine and cytarabine (leukemia drugs).[37] While ajoene did not induce apoptosis on its own, in combination with cytarabine or fludarabine ajoene enhanced the drugs' activity. The mode of chemosensitization by ajoene is suggested to occur through targeting the anti-apoptotic resistance mechanism. This was confirmed by reduction in the concentration of

the anti-apototic protein Bcl-2 and activation of capase 3 in ajoene-treated cells.[37] Hassan's results open a new interesting field of ajoene as a chemosensitization agent in cancer treatment, which as yet has not been exploited chemically.

1.8 Signalling Pathways

In the 1990s Dirsch and co-workers showed that ajoene induces apoptosis in human promyeloleukemic cells (HL-60) with the generation of intracellular reactive oxidative species (ROS).[33a] A dose- and time-dependent increase in intracellular peroxide was observed when HL-60 cells were treated with ajoene. The peroxide production was observed using flow-cytometry and was evident from as early as 5 min after treatment with ajoene. NF-kB is a factor that has been shown to be involved in inducing apoptosis in some cells and also to be activated during oxidative stress.[33a] In the above study Dirsch and co-workers were able to show that there was activation of NF-kB when HL-60 cells were subjected to ajoene treatment. Interestingly, when cells were pre-incubated with the anti-oxidative *N*-acetylcysteine prior to ajoene treatment, there was significant decrease in ROS production and in NF-kB activation. These results showed that ajoene induces apoptosis in HL-60 cells using a mechanism that involves ROS production and activation of the transcription factor NF-kB.[29 &33a]

In a follow up study, Dirsch showed that in the HL-60 cell-line ajoene-induced apoptosis was mitochondrial dependent and involved the caspase cascade.[33d] Using a fluorometric DEVD-cleavage assay caspase-like activity could be detected from as early as 4 h after cell exposure to ajoene. This caspase-like activity was confirmed following the cleavage of poly(ADP-ribose)polymerase (PARP). The PARP protein is a nuclear protein involved in DNA repair, and is a good marker of caspase activity during apoptosis. The time-dependent cleavage of PARP and appearance of the typical 85-kDA fragment after HL-60 cells were treated with ajoene is shown in Figure 7a.

Interestingly, the apoptosis induction did not require activation of the death-receptor pathway, as ajoene induced apoptosis in cloned HL-60 cells devoid of CD95 receptors. Several key chemotherapeutic drugs have been shown to express their cytotoxicity by involving the CD95 receptor system to evoke the apoptotic signal.[33] An effort was made to investigate whether the apoptotic pathway depended on caspase activity. When cells were pre-incubated with zVAD-fmk (broad spectrum caspase inhibitor) prior to ajoene treatment, apoptosis was inhibited. The reliance of ajoene-induced apoptosis on caspase activation was measured by DNA analysis using flow cytometry. Compared to cells treated with ajoene alone (Figure 7b, middle panel) the DNA content

in zVAD-fmk pre-treated cells remained intact (Figure 7b, right panel). This result showed that ajoene-induced apoptosis is caspase dependent.

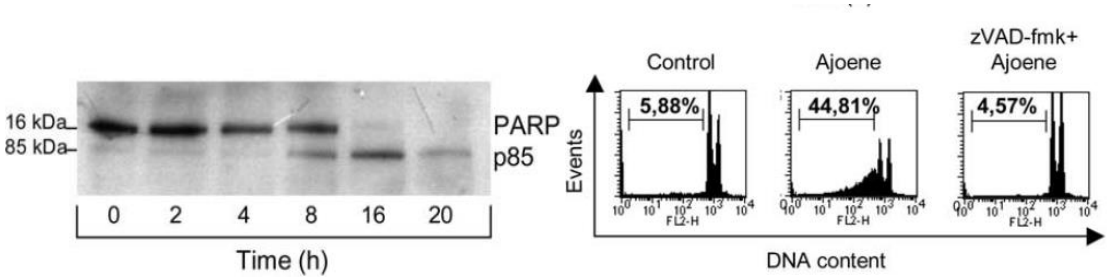

a) b)

Figure 7: Ajoene-induced apoptosis in HL-60 cells is caspase dependent. a) Caspase like time dependant cleavage of PARP; b) the caspase inhibitor zVAD-fmk inhibits ajoene-mediated apoptosis.[33d]

An integral part of apoptotic pathways that act independently of the death receptors is mitochondrial membrane permeabilization (MMP, see 1.5.4). Dirsch *et. al.* showed that ajoene induced MMP and that there was a time dependent release of cytochrome c into the cytosol when HL-60 cells were treated with ajoene (Figure 8a).

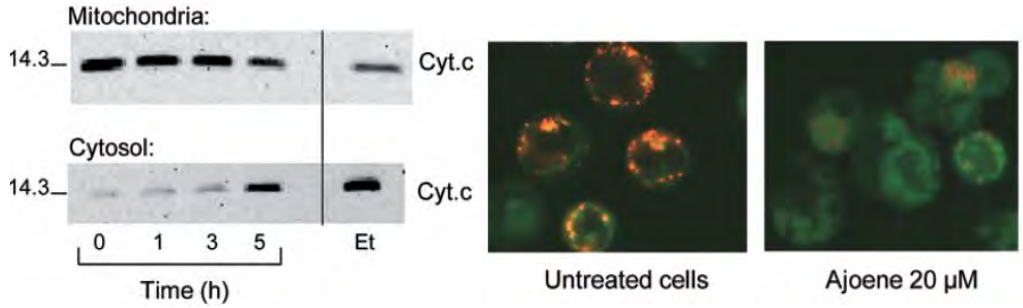

a) b)

Figure 8: a) HL-60 cells treated with 20 µM ajoene showed timely release of cytochrome c into the cytosol. b) HL-60 cells showing localisation of red fluorochrome JC-1 in the mitochondria (Left panel) and ajoene treated cells showing the green monomer fluorescence typical of membrane potential loss (right panel).

Evidence of change in membrane potential was monitored by use of the fluorochrome JC-1, which forms red aggregates or green monomers depending on the mitochondrial membrane potential. Untreated cells predominantly show localisation of a red fluorescence indicating an intact membrane (Figure 8b left panel). As early as 4 hours after exposure to ajoene there was significantly less red fluorescence (Figure 8b right panel). After 8 hours the green fluorescence typical of a loss of membrane potential could be observed using confocal microscopy.

Independently Li *et. al.* confirmed Dirsch's findings regarding the mechanism involving mitochondrial and caspase cascade activation. Li *et. al*. went on to show that *Z*-ajoene-induced apoptosis involves cleavage of the anti-apoptotic Bcl-2 protein. The evidence seems to suggest that the intrinsic mechanism is the pathway by which ajoene induces apoptosis in cancer cells.

1.9 Mode of Action and Drug Targets of Ajoene

Although the anti-cancer activity of ajoene has been linked to the mitochondrial-dependent apoptosis pathway, the upstream drug targets and mode of action are still to be elucidated. Ajoene and related organosulfides have been shown to induce cell-cycle arrest in the G_2/M phase of the cell cycle,[33b,38] and there have been suggestions that the activity of garlic organosulfides resides in the thiol oxidising disulfide bond. In the case of ajoene the disulfide bond is further activated by the presence of an adjacent vinyl group.

Disulfides can act as oxidising agents by thiolating cysteine residues of proteins to form mixed disulfides which lead to the disruption of normal protein function and eventual cell death.[39] In this regard ajoene has been reported to be an inhibitor of thiol-containing enzymes: gastric lipase, human glutathione reductase (GR) and *T. cruizi* trypanothione reductase.[40] Gallwitz and co-workers showed by crystal structure analysis that inhibition of GR by ajoene resulted in the formation of a covalent bond between ajoene and a cysteine residue (position Cys-58) in the enzyme active site. The [CH_2=CH-CH_2-SO-CH_2-CH=CH-S] ajoene moiety was incorporated into this newly formed disulfide (Scheme 3 (i)). The incorporated ajoene moiety formed a hydrogen bond between the oxygen of the sulfoxide and the N-H of alanine-34 in the near vicinity. This interaction was reported to highlight the possible biological significance of the sulfoxide, forming important hydrogen bonds within the target site. The mixed disulfide formed seems to suggest that the cysteine thiol adds nucleophilically and regioselectively onto the vinyl sulfur of ajoene with the allyl thiol as the leaving group (Scheme 3 (i)).[40]

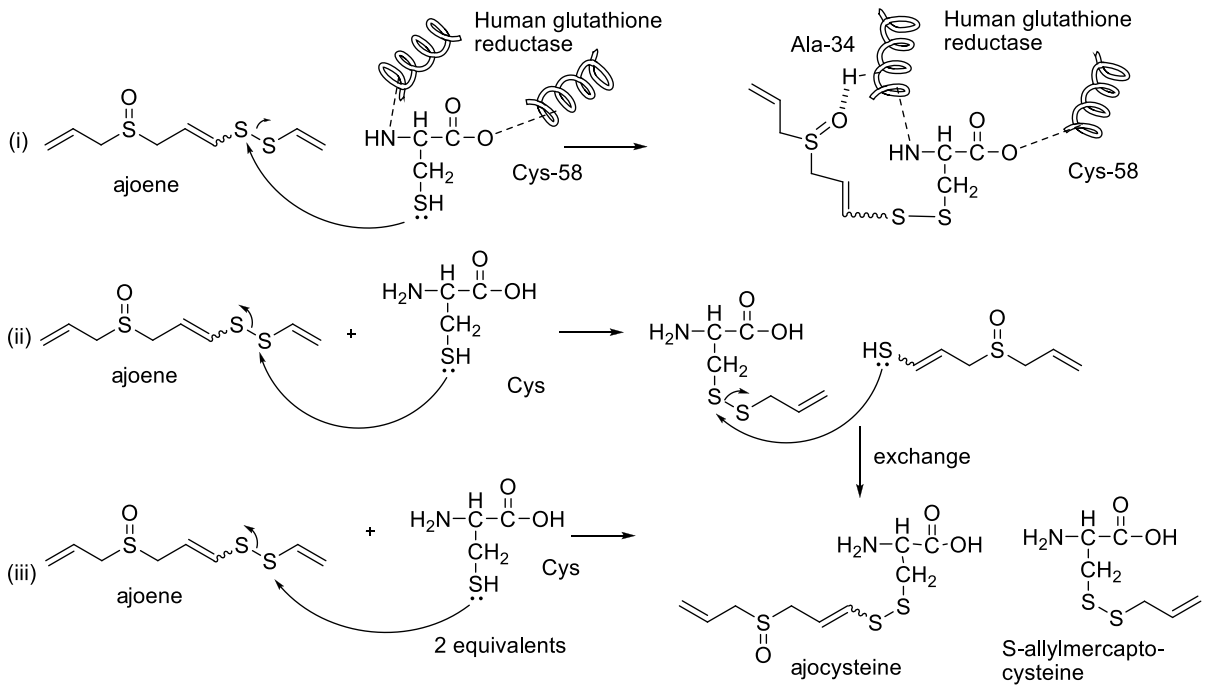

Scheme 3: (i) Reaction of ajoene with cysteine residue on GR;[40] (ii) Reaction of ajoene in a cell free environment (i.e. in solution) with 1 equivalent of cysteine;[41] (iii) When ajoene reacts with 2 equivalents of cysteine in-solution two products are formed.[41] Adapted and modified from [47].

This result is mechanistically counter-intuitive as the vinyl-S anion is the more stable leaving group, which would indicate that a nucleophilic attack on the allyl-S of the disulfide would be more favoured. Importantly a cell-free (in-solution) model reaction of ajoene with cysteine by Lawson and Wang was found to form *S*-allylmercapto-cysteine as the main product (Scheme 3 (ii)), indeed showing that the favoured nucleophilic attack occurs on the allyl-S.[41] Previously, we have also verified this finding in our labs by heating ajoene and cysteine together in ethanol in which the major product isolated was the *S*-allylmercapto-cysteine. In a report by Lawson *et al* they showed that when 2 equivalents of cysteine were reacted with 1 equivalent of ajoene both ajocysteine (3-((3-(allylsulfinyl)prop-1-enyl)disulfanyl)-2-aminopropanoic acid) and *S*-allylmercapto-cysteine were isolated (Scheme 3 (iii)),[41] suggesting that the formation of ajocysteine might occur as a secondary reaction. Mechanistically, the ajocysteine is best described as a secondary product that results from the primary product (*S*-allylmercapto-cysteine) undergoing a disulfide exchange with the vinylic-S of ajoene (Scheme 3). Overall, the mode of action suggestion here is that ajoene thiolates cysteine residues resulting in altered enzyme function that ultimately results in cell death.

The diverse biological activity ajoene tends to suggest that there might be multiple drug targets, there is evidence linking ajoene's biological activity with its ability to interact and modify proteins e.g. β-tubulin and $\alpha_4\beta_1$ integrin.[33b&d] In a study to investigate whether ajoene affected microtubule

assembly, PtK2 cells incubated with *Z*-ajoene underwent a twofold increase in cells blocked in mitosis phase compared to untreated cells.[33b] The microtubule assembly is highly governed in the cell and its integrity determines whether cells undergo replication. The microtubule cytoskeleton in untreated Ptk2 cells was healthy and intact whilst there was a dose dependent degradation of the cytoskeleton in ajoene treated cells as observed using indirect immunofluorescence technique.[33b] Ajoene induced microtubule or tubule disassembly pointing to a possible drug target for this compound.[33b]

1.10 Summary

In summary garlic has been used as a culinary and therapeutic agent for over 5000 years. The therapeutic effects of garlic have been attributed to the several organosulfides found within the clove. When garlic is macerated allicin, an unstable thiosulfinate, is generated which in turn degrades to form several organosulfides. Pertaining to this thesis ajoene is one of the more stable degradation products from allicin. Ajoene is reported to possess a range of biological activities to include antimicrobial, antifungal, antiobesity and anticancer. Regarding its anti-cancer properties there is strong evidence suggesting that ajoene induces apoptosis in cancer cells via the intrinsic pathway. The drug targets and mode of action of ajoene are not yet fully defined, but there is evidence of ajoene possibly thiolating proteins through mixed disulfide formation at susceptible cysteine residues. Several studies have shown ajoene's ability to induce cell arrest in the G_2/M phase and there is evidence that this might be due to ajoene's ability to thiolate b-tubulin and to cause microtubule disassembly. The work in this thesis was directed towards the Structure-activity Relationships (SAR) study of ajoene analogues.

Chapter 2: Synthetic aspects of ajoene and its analogues

2.1 Introduction

The only reported synthesis of ajoene is the biomimetic synthesis by Professor Eric Block.[9] Ajoene can also be obtained from organic extracts of crushed garlic but the yield of ajoene from this method is low and the procedure is cumbersome.[11] This chapter addresses the synthetic aspects of ajoene (regarding Block's biomimetic synthesis) and the UCT (University of Cape Town) synthesis which was developed to access ajoene analogues.

2.2 Block's Biomimetic Synthesis

In the 1980's Block developed a synthetic route to ajoene that mimics the way that it is made in nature, by heating allicin in an acetone-water (3: 2) solution. The allicin had been prepared beforehand in high yield by the mono-oxidation of commercially available diallyl disulfide using peracetic acid (Scheme 4 (i)).

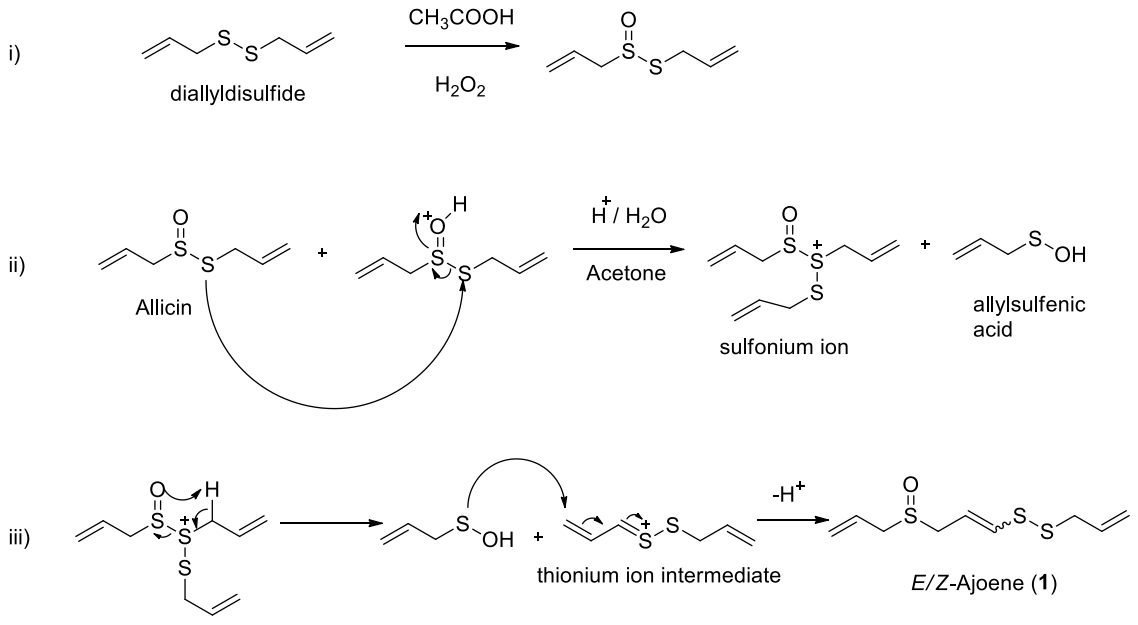

Scheme 4: Block's biomimetic synthesis of ajoene from allicin.

Mechanistically, the conversion of allicin to ajoene commences with the acid-catalysed self *S*-thioalkylation of allicin yielding a sulfonium ion intermediate and allylsulfenic acid (Scheme 4 (ii)). In the next step the sulfonium ion eliminates a molecule of allylsulfenic acid in a Cope-type elimination to give a thionium ion intermediate. Allylsulfenic acid then adds to this thionium intermediate via a Michael addition to give ajoene as mixture of *E* and *Z*-isomers (Scheme 4 (iii)).

Block's biomimetic synthesis is reported to only produce ajoene in a low yield of 34 %, although the Hunter lab has never been able to reproduce this yield and typically only achieve around 4% yield. The other drawback of Block's synthesis is that it does not allow for variability in the starting material as the mechanism demands the presence of an allyl group in the thiosulfinate starting material. As can be seen from Scheme 4 above, inevitably an allyl group ends up on the disulfide side of the molecule. Thus using this method ajoene analogues containing the sulfoxide and vinyl disulfide pharmacophore but with a non-allyl R_2 (Figure 9) group cannot be accessed.

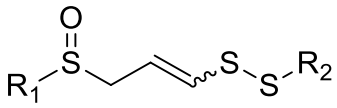

Figure 9: The general structure of ajoene analogues.

A synthetic route to ajoene analogues with variable end groups (R_1 and R_2) was developed in our group a few years ago and several analogues have been accessed as described below.[42]

2.3 University of Cape Town Synthesis

Our group has developed a concise four-step synthetic sequence to ajoene analogues, Scheme 5. This route allows access to a broad range of terminally substituted analogues.

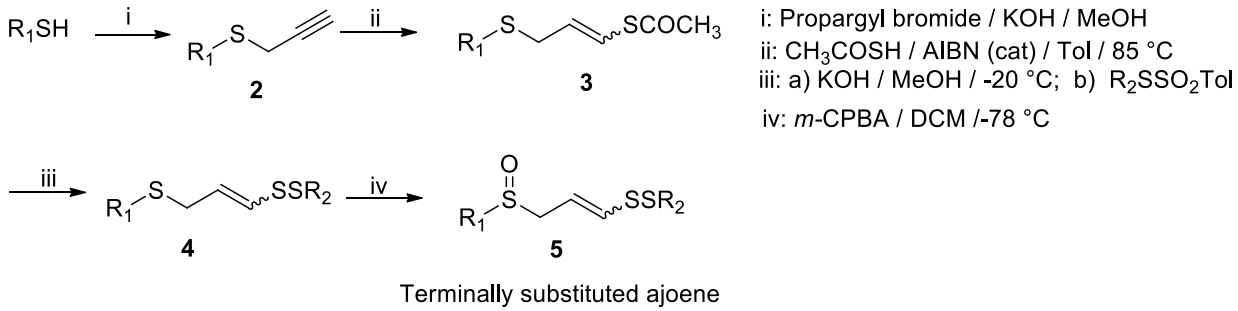

Scheme 5: University of Cape Town synthesis of substituted ajoenes.

2.3.1 Step 1: Propargylation

The first step of the synthesis is the propargylation of a thiol, the latter either commercially available or accessed via thiourea chemistry. Using thiourea chemistry a variety of thiols can be accessed, via refluxing thiourea with the relevant akyl halide (R_1X) in acetonitrile to form an isothiouronium salt. When the isothiouronium salt is subjected to potassium hydroxide (KOH) at low temperature, hydrolysis occurs releasing an alkylated thiol and urea (Scheme 6 step i). Owing to the odiferous nature of thiols it is more practical to avoid their isolation and thus the thiol is propargylated in situ using propargyl bromide to yield the desired propargyl thioether, **2** (Scheme 6 step ii). **2** can be

isolated via an extractive work-up, which is followed by distillation or column chromatography, depending on the nature of the R_1 group.

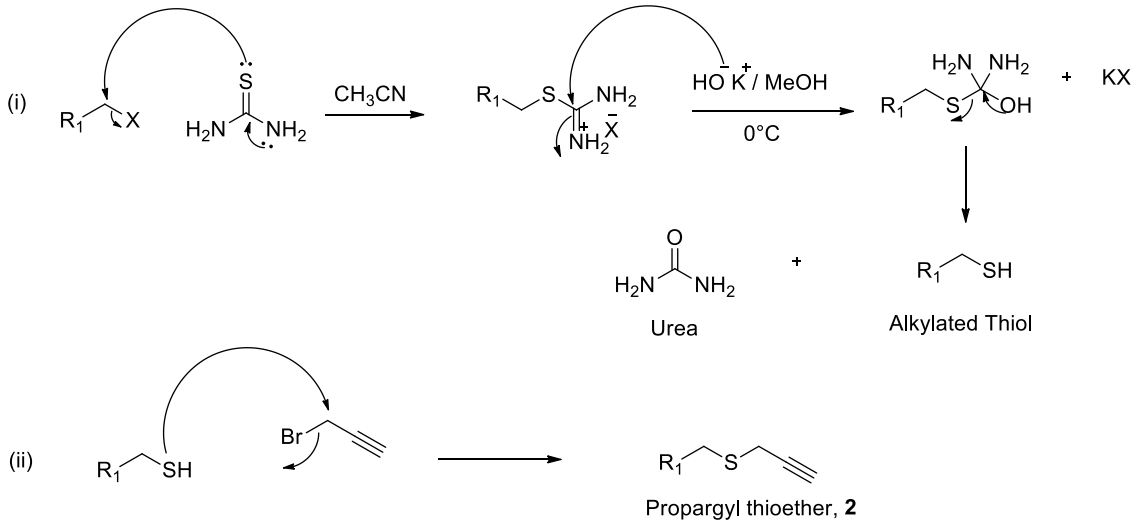

Scheme 6: Preparation of propargyl thioether, **2**.

2.3.2 Step 2: Radical addition

Having obtained the desired propargyl thioether **2** the next step is the key regioselective addition of thiolacetic acid to **2**, via radical addition to the terminus of **2**, using ACCN (1,1`-azobis(cyclohexane-1-carbonitrile)) as a radical initiator, to form vinyl thioacetate **3**. As the *Z*: *E* ratio is determined in this step the radical addition reaction became the key of the synthetic route. This reaction was studied by Kampmeier and Chen in the 1960s, in which they showed that the radical addition of thiolacetic acid to 1-hexyne occurs regioselectively and with some level of stereoselectivity.[43] Interestingly they reported that the favoured stereo-isomer was the *Z*-isomer. Since the *Z*-isomer of ajoene is reported to be more biologically active than the *E*-isomer a synthetic route that favours *Z*-selectivity is desirable for ajoene analogues.

The radical addition mechanism presumably follows the classical initiation, propagation and termination sequence typical of radical reactions, Scheme 7.

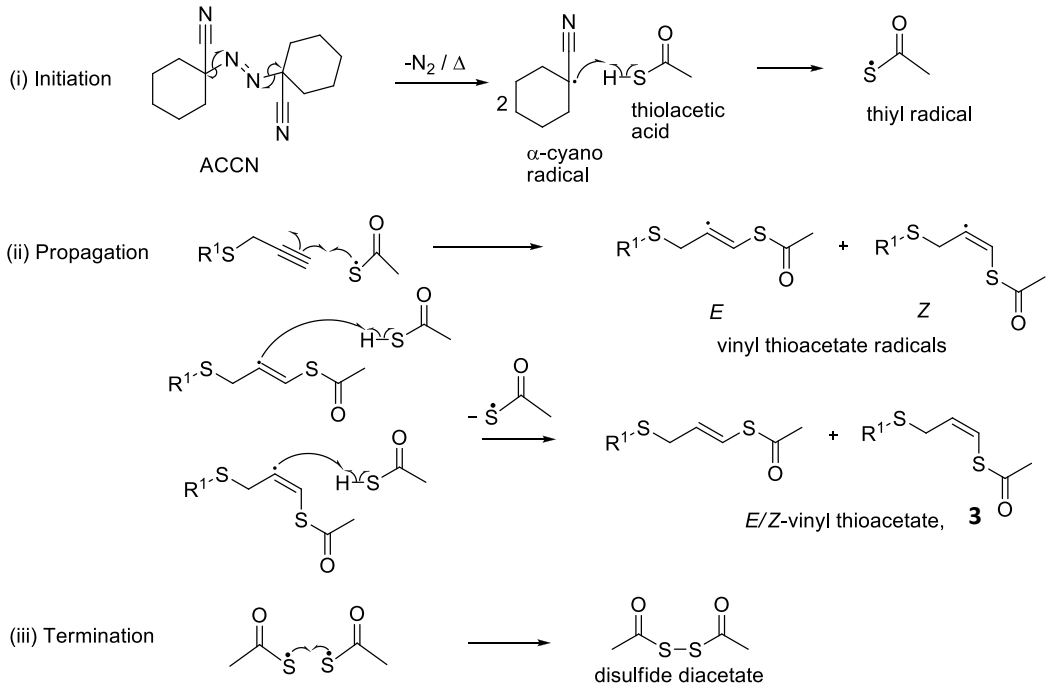

Scheme 7: Radical addition mechanism: (i) initiation, (ii) propagation and termination.

At about 85 °C the radical inititator 1,1'-azobis(cyclohexanecarbonitrile) undergoes homolytic cleavage that is entropically favoured, to give α-cyano radicals with the release of nitrogen gas (initiation). The α-cyano radical then abstracts a proton from thiolacetic acid to form a thiyl radical. The propagation step involves the regioselective addition of the thiyl radical to the terminus of the propagyl thioether forming a vinyl thioacetate radical, which abstracts a hydrogen from thiolacetic acid to regenerate the thiyl radical. The reaction is terminated when two thiyl radicals dimerise to form disulfide diacetate. The vinyl thioacetate, **3** is obtained as a mixture of *E*- and *Z*-isomers in the ratio 2: 3 respectively. The stereoselectivity could be explained on the basis that there is an equilibrium between the *E*- and *Z*- vinyl thioacetate radicals such that they interconvert. During the subsequent hydrogen abstraction from thiolacetic acid the *Z*- vinyl thioacetate reacts faster as there is less steric interference with the approaching thiol acetic, whereas in the *E*-vinyl thioacetate there is a clash with the thioacetate substituent. Thus the *Z*-isomer is preferred kinetically.

2.3.3 Sulfenylating agent

The "right hand side" (-SR_2 in Figure 9) of the ajoene analogue is built from a thiosulfonate sulfenylating agent (see Scheme 8) that acts as a soft nucleophile towards enethiolate anion. The thiosulfonate agent is made beforehand by reacting an appropriate alkyl halide with potassium thiotosylate (Scheme 8), in which R_2 group of each specific analogue is embedded in the akyl halide of choice.

The thiosulfonate $S(SO_2)R$ grouping is structurally analogous to an O-sulfonate ester (e.g. tosylate). However, where the O-sulfonate ester makes the adjacent carbon susceptible to S_N2 nucleophilic attack, the thiosulfonate provides an electrophilic attack site for soft nucleophiles.

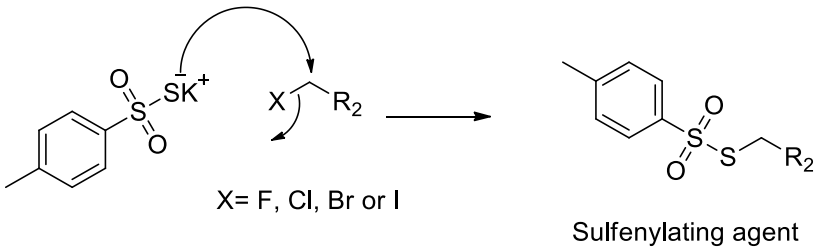

Scheme 8: Synthesis of the sulfenylating agent.

2.3.4 Step 3: *S*-Sulfenation step

With the two sides of the ajoene analogue in hand the next step involves coupling the two ends via a thiol deprotection and sulfenylation. This was achieved by deprotecting the vinyl acetate **3** to its enethiolate using KOH at – 40 ° C and then sulfenylating at low temperature. The deprotection step was carried out at a low temperature to avoid geometrical isomerisation of the *Z*-enethiolate to its thermodynamically more stable *E*-isomer. The sulfenylation occurs on the basis of Hard Soft Acid-base theory (HSAB) with the soft enethiolate sulfur attacking the soft electrophilic divalent sulphur of the sulfenating agent (Scheme 9).

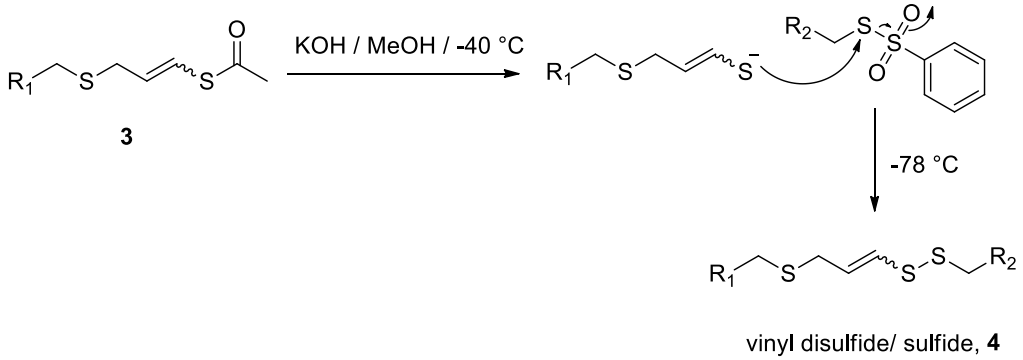

Scheme 9: *S*-Sulfenylation step

2.3.5 Step 4: Oxidation

Having obtained the vinyl disulfide/ sulfide **4**, the next step was the chemoselective oxidation of the sulfide in the presence of the double bond and the vinyl disulfide. This is achieved by using 1.1 equivalents *m*-CPBA (meta-chloroperoxybenzoic acid) with the temperature kept below – 60 ° C. The

more nucleophilic sulfide undergoes oxidation to the sulfoxide and importantly both the disulfide and the alkene are left intact, Scheme 10.

Scheme 10: Oxidation of vinyl disulfide/ sulfide to target ajoene **5**

2.3.6 Summary

The UCT synthesis described above is a versatile route for producing terminally substituted ajoenes. Several ajoene analogues have been synthesized in our group and analogues relevant to this thesis will be discussed in section 2.4. It has been noted that some analogues could be separated into *E*- and *Z*-isomers, although in other cases the analogues could not be separated and were tested as an E/Z-mixture. Furthermore the parent ajoene could not be accessed via this synthetic route, in which it was postulated that radical addition to the allyl group occurred during the radical addition step via a 5-exo- or 6-endo-trig process.[42] Recently Han *et. al.* reported the synthesis of ajoene using a modified University of Cape Town Synthesis, although the details were not provided.[44]

2.4 Structure-Activity Relationships of Ajoene analogues

Several ajoene analogues have been synthesized by previous researchers using the UCT synthesis (2.3) and in an SAR study several of these analogues were evaluated for their anti-proliferation effect (measured using the MTT proliferation assay) on the oesophageal cell line WHCO1, the results are summarised in Table 2.[45]

Initially the focus was to vary the R_1 end group whilst retaining the sulfoxide/disulfide core and retaining R_2 as an allyl like in the parent ajoene (Table 2, **5a**-**g**). It was noted that analogues containing an R_1 aromatic group had increased activity when compared to ajoene and on this basis the R_1 end group was optimised to a *p*-methoxybenzyl group. Having identified the *p*-methoxybenzyl as the lead R_1 terminal, attention was turned to the R_2 substituent. Similarly it turned out that aromatic substituents increased the activity of analogues (**5h**-**j** and **6a**) and the *p*-methoxybenzyl substituent returned the most activity. From this SAR study a lead compound in which the terminal groups were substituted for *p*-methoxybenzyl, **6a**, was identified with an IC_{50} of 2.1 ± 0.4 µM, which is about 12-fold more active than *Z*-ajoene. The IC_{50} value of **6a** is within the same range as the *in*

vitro IC_{50} obtained for the oesophageal cancer clinical drugs cisplatin and 5-fluorouracil, which were found to have an IC_{50} of 9.2 µM and 7.9 µM respectively on the same cell line.[45]

Table 2: Structure-activity study of ajoene analogues on the proliferation of the oesophageal cancer cell line WHCO1

Compound no.	**Isomer**	Terminally substituted ajoene, **5**		**IC_{50} ± SD (µM)**
		R_1	**R_2**	
ajoene	*Z*	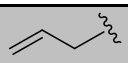	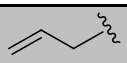	25.0 ± 2.8
	E			30.0 ± 7.8
5a	*Z*	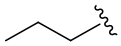	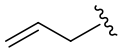	23.0 ± 4.2
	E			37.0 ± 4.5
5b	*E*/*Z*		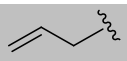	23.0 ± 6.7
5c	*Z*	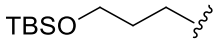	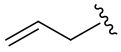	38.0 ± 5.9
	E			27.0 ± 5.6
5d	*Z*	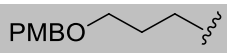	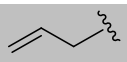	21.0 ± 0.6
	E			18.0 ± 5.7
5e	*Z*	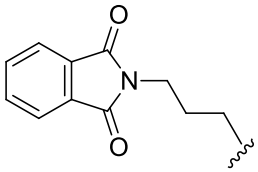	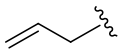	33.0 ± 1.4
	E			68.0 ± 1.5
5f	*E*/*Z*	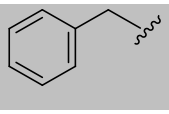	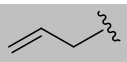	8.9 ± 1.2
5g	*E*/*Z*	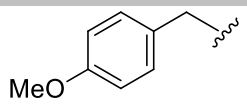	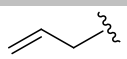	7.4 ± 0.7
5h	*Z*	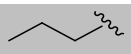	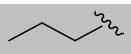	18.0 ± 4.1
	E			24.0 ± 2.8
5i	Z	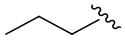		26.0 ± 7.5
	E			28.0 ± 7.2
5j	*E*/*Z*	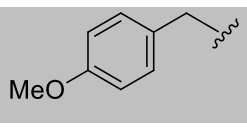	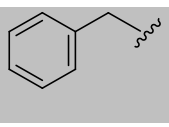	3.1 ± 1.1
5k	*E*/*Z*	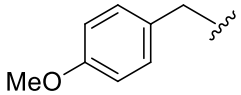	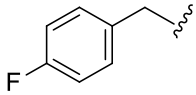	16.0 ± 1.1

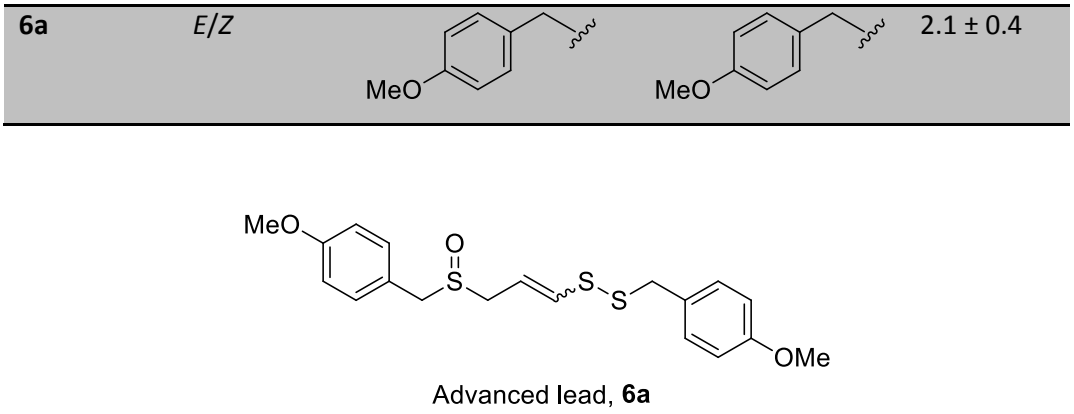

Figure 10: The advanced lead as identified by SAR study.

The initial part of the SAR study thus had established that the terminal end-groups (R_1 and R_2) are non-essential for retention of anti-proliferation activity against WHCO1 cells and therefore the next part of the structure-relationships analysis now focused on the importance of the vinyl disulfide and sulfoxide groups. For this purpose several structural analogues (**6b**-**6f**) of the lead **6a** were synthesized. The MTT assay (Table 3) was used to measure the WHCO1 anti-proliferation activity of the compounds.[45]

Analogues retaining the disulfide **6a** (2.1 μM), **6b** (0.7μM) and **6f** (16 μM) demonstrated anti-proliferation activity whilst those in which the disulfide was removed **6c, *Z*-6d** and ***E*-6d** were found to be inactive. In compound **6f**, where the vinyl double was removed, activity dropped by about 8-fold compared to **6a**. From these observations it was hypothesized that the pharmacophore resides within the disulfide bond and that the vinyl group labilises the disulfide pharmacophore.

Compound **6e**, in which both the vinyl double bond and sulfoxide group were absent, was not active and when the sulfoxide was installed in conjunction with a non-vinylic disulfide in **6f** moderate activity was restored. This suggests that the sulfoxide has a synergistic effect on the disulfide pharmacophore and might be essential for retention of activity when the vinyl bond is removed.[45] A major part of the work in this current thesis was directed at clarifying this result and probing the importance of the vinyl double bond.

Table 3: Structureeactivity pharmacophore analysis of ***E/Z*-6a** regarding inhibition of WHCO1 cell proliferation.[45]

Compound no	Structure	WHCO1 IC_{50} ± SD (µM)
6b	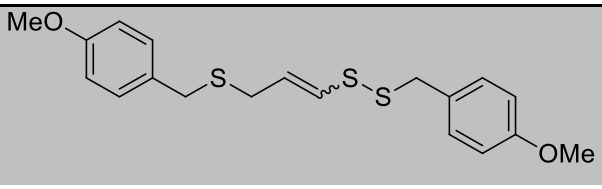	0.7 ± 0.3
E/Z-6a	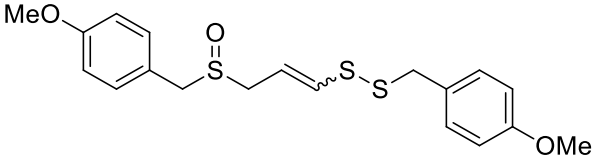	2.1 ± 0.4
***E/Z*-6c**	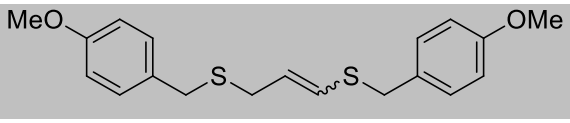	> 200
***Z*-6d**	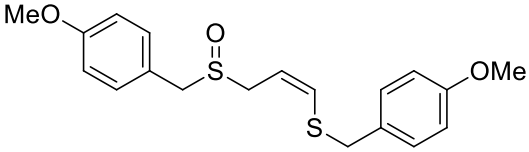	> 200
***E*-6d**	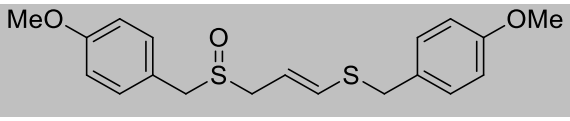	> 200
6e	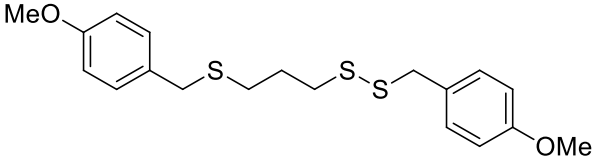	> 200
6f	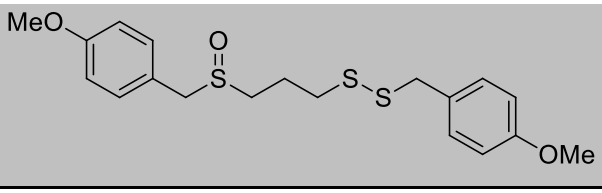	16 ± 3.7

2.4.1 *In vivo* and Metabolic Studies on Ajoene Analogue 6a

Owing to its impressive *in vitro* results **6a** was chosen as a candidate for an *in vivo* evaluation. A nude mouse model was used to evaluate the antitumor properties, but due to its high lipophilicity **6a** could not be administered as an oral dose and so it was delivered via an intralipid vehicle through intraperitoneal injection.[46] Mice were inoculated with WHCO1 cells (2.5 X 10^6 cells) delivered via subcutaneous injection and the tumours were allowed to develop for 3 days. Thereafter, mice were treated with either **6a** in intralipid, or intralipid alone (control) for 4 weeks. At the end of the

experiment, the mice were killed and the tumours were removed and weighed. Treatment with **6a** was found to have no effect on tumour growth as treated mice did not exhibit reduced tumour sizes.[46] Lead **6a** was therefore highly effective *in vitro* at inducing apoptosis in cancer cells but failed to reduce tumour cell growth *in vivo*. It was thought that this failure may be due to either poor water solubility of **6a** or metabolic instability resulting in poor bioavailability.[46]

In order to follow up on the second hypothesis that **6a** may be metabolically unstable, a sample of the compound was sent to the Department of Pharmacology UCT for pharmacokinetic evaluation. **6a** was incubated in whole blood, plasma and red blood cell (RBC) fractions of mouse blood at 37 °C for 2 h. **6a** was found to be stable in plasma but the compound rapidly degraded in whole blood and RBC fractions (Figure 11). This implies that **6a** is interacting with RBCs in mouse blood and this causes rapid degradation of the compound ultimately reducing its bioavailability.

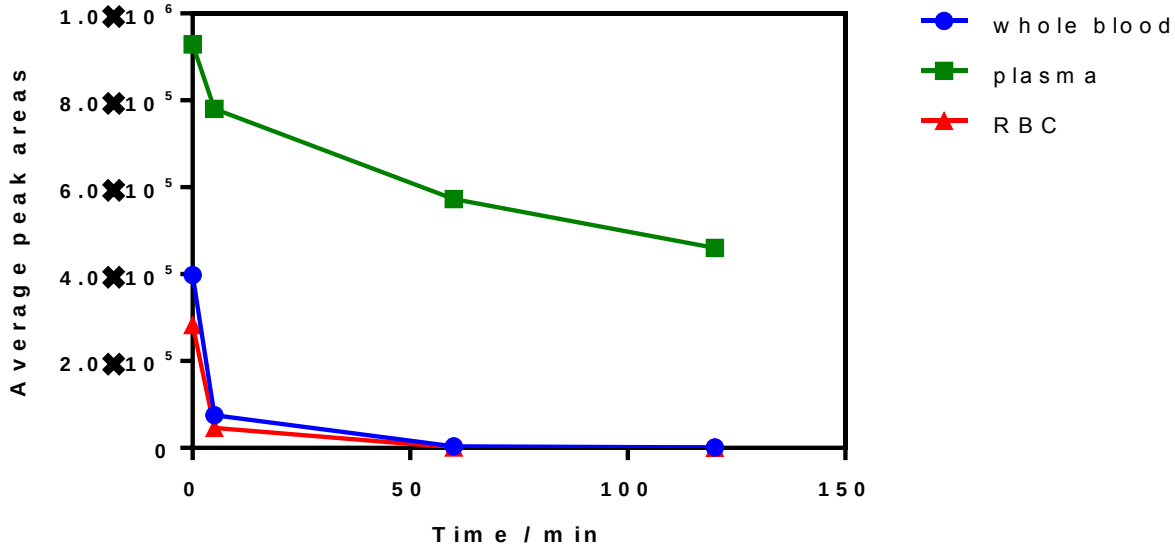

Figure 11: *In vitro* metabolic stability of **6a** in plasma, whole blood and red blood cell fractions.[47]

The result obtained is supported by a literature report by Lawson and Wang, in which they found the half-life of ajoene in whole blood to be less than 2 min while that of diallyl disulfide (DADS) was 60 min.[41] Both ajoene and DADS possess a disulfide bond, the difference being that in ajoene the disulfide is vinylic and this may be the source of metabolic instability.

Thus with the background of these results the work presented in this dissertation became part of a broader project with the aim to improve the water solubility and metabolic stability of the lead compound **6a**.

2.5 Water-Soluble and Metabolically-Stable Ajoene Analogues

2.5.1 Water-Soluble Ajoene Analogues

At the onset of the current project several analogues had been synthesized in our group by Mandla Mabunda with the aim of addressing the water solubility issues of lead **6a**. Four analogues, with groups of varying polarity for enhancing aqueous solubility (R) (Figure 12) were accessed using the UCT synthesis.

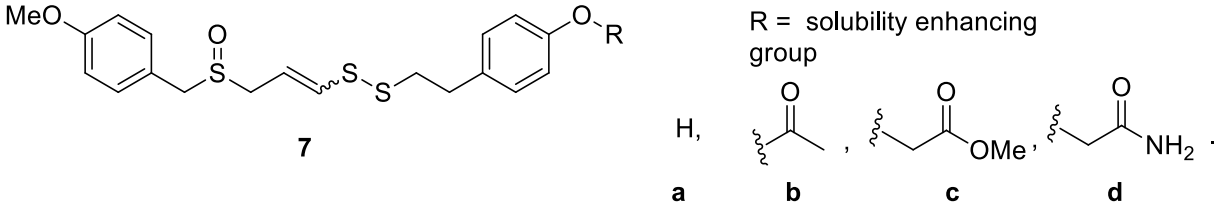

Figure 12: The structure of water soluble ajoene analogues.

The solubility of the analogues was assessed using a turbidimetric aqueous solubility assay and the results did indeed support improved aqueous solubility over that of the lead compound **6a**. The phenol, **7a**, and ester, **7c**, analogues were the most soluble in aqueous solvent.[47]

More importantly, coupled to the increase in water solubility, these analogues all demonstrated retention of anti-proliferation activity against the WHCO1 cell line, Table 4. This pleasing result demonstrated that it is possible to increase the solubility of analogues without compromising the potent anti-proliferative activity. The amide analogue, **7d**, was selected for an *in vivo* assessment, but again, this analogue was not found to reduce tumour growth, possibly due to the presence of the vinyl group rendering the compound metabolically unstable in blood.

Table 4: Water soluble ajoene analogues anti-proliferative activity against WHCO1 cells.

Compound Name	Structure	WHCO1 IC50 ± SD (μM)
Bis-PMB, 6	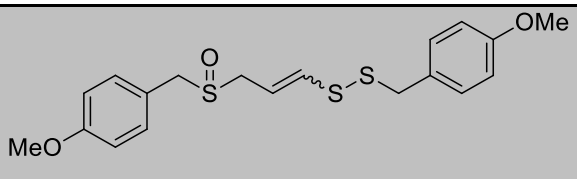	2.1 ± 0.4
7a	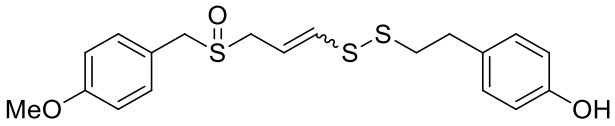	1.9 ± 0.8
7b	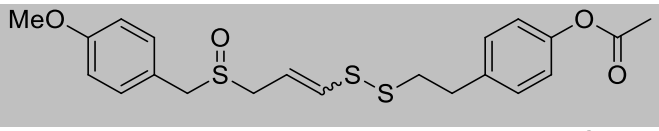	3.6 ± 0.04
7c	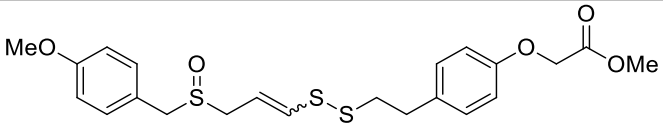	1.7 ± 0.9
7d	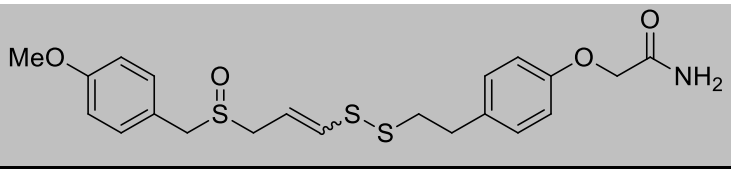	7.7 ± 1.7

2.5.2 Metabolically stable Ajoene analogues

Based on the SAR study of **6a** (2.4) it was determined that the disulfide is the pharmacophore in ajoene analogues and that the vinyl bond enhances the activity. We hypothesize that the vinyl double may render **6a** to be unstable in whole blood thereby preventing it from reaching the tumour and rendering the compound inactive when delivered by IP injection *in vivo*. The aim of this project was to synthesize the more water soluble ajoene analogues but lacking the vinyl group as a comparison with analogues **7a-d** the targets became **8a-d** as shown in Figure 13.

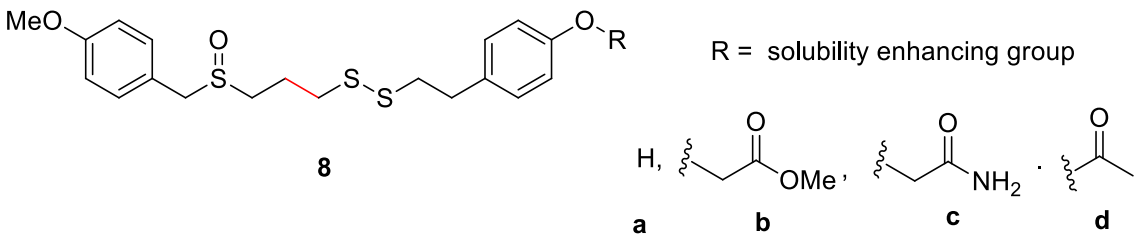

Figure 13: Structure of metabolically stable ajoene analogue targets.

This study aimed to address two questions:

1) Is the double bond essential for activity? And
2) Does its removal aid in increasing metabolic stability.

2.6 Objectives

Synthesize a small library of ajoene analogues lacking the vinyl double bond (dihydroajoenes, Figure 13).

Biologically evaluate this library of compounds.

Carry out a study towards synthesis of an ajoene-drug conjugate for chemosensitization evaluation.

Each of these objectives will be discussed in the next Chapter.

Chapter 3: Results and Discussion

3.1 Dihydroajoenes

3.1.1 Dihydroajoene Synthesis

At the onset of this project four analogues of ajoene with aqueous-solubility enhancing groups had been synthesized (Chapter 2, Table 3), and though very active *in vitro* we were soon to learn that the analogues were ineffective *in vivo.* Thus the synthesis of the dihydroajoenes (Figure 13) began with the aim of evaluating whether we could improve metabolic stability, by removing the vinyl bond, while retaining anti-cancer activity in these analogues.

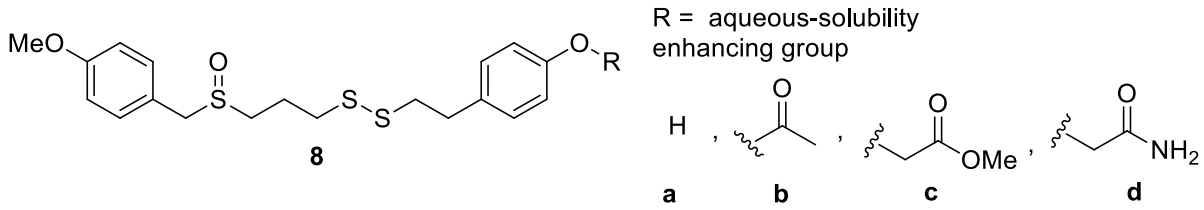

Figure 13: Structure of dihydroajoene targets

3.1.2 Synthetic Rationale

A retrosynthetic analysis of a synthetic route to the dihydroajoene core is shown in Scheme 11. The synthetic route is a divergent one with the different aqueous solubility enhancing groups (R) being installed at the end of the sequence. It was imagined that chemoselective oxidation of the coupled product, **13a**, would be possible at the anticipated more electron-dense benzyl sulfide to give the sulfoxide, **8a**. Using previously established methodology **13a** could be obtained in a two-step one-pot synthesis from the commercially available *p*-methoxybenzyl chloride, 1,3-propanedithiol and a previously prepared thiotosylate **11**, prepared via an S_N2 reaction between potassium thiotosylate and iodide **10**. In turn, **10** was envisaged to be made from the commercially available ester methyl 4-hydroxyphenylacetate by a two-step sequence of reduction followed by alcohol-halogen exchange (Appel Reaction).

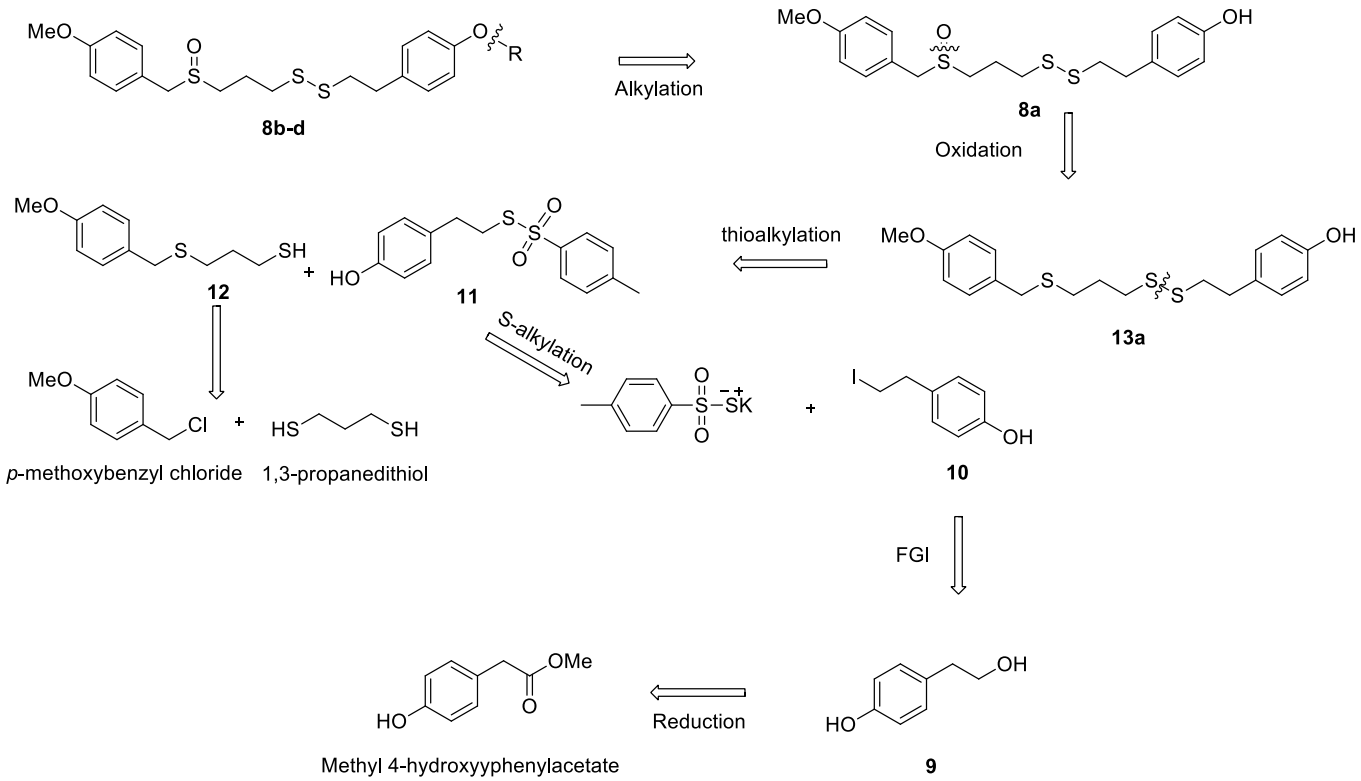

Scheme 11: Retrosynthetic analysis of the dihydroajoene synthesis.

3.1.3 Thiotosylate Sulfenating Agent, 11

The synthesis commenced with preparing the sulfenating agent for the disulfide end (right hand side) of the molecule. Starting from commercially available methyl 4-hydroxyphenylacetate previous work had shown that **11** could be obtained in relatively high yield over three steps. [47]

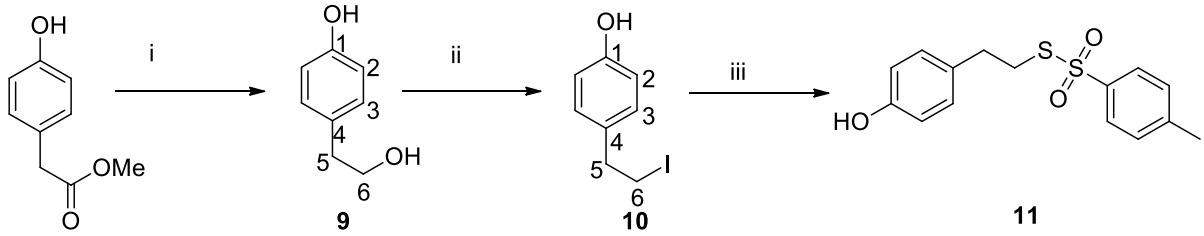

i) $LiAlH_4$/ THF / -78 °C ii) I_2,PPh_3, imidazole / THF iii) Potassium thiotosylate / DMF

Scheme 12: Synthetic route to sulfenating agent **11**

3.1.3.1 Alcohol, 9 [49]

Methyl 4-hydroxyphenylacetate was added to a stirring mixture of $LiAlH_4$ (2 equiv) in dry THF at – 78 °C and full conversion of the ester to the alcohol, **9**, was observed on TLC after 2 h, with **9** appearing as a more polar spot on the plate. The reaction was quenched at 0 °C using 1 M HCL to bring the pH

down to 3. After the reaction work-up and chromatography the solid residue was recrystallized from a minimum amount of EtOAc and hexane to give **9** as a white powder in 82 % yield.

The ^{1}H NMR spectrum of **9** revealed a broad singlet at 8.00 ppm corresponding to the phenolic hydrogen, an AA'BB' system at 6.74 (H-2) and 7.05 (H-3) corresponding to a *p*-disubstituted aromatic system and a broad singlet at 3.53 ppm corresponding to the newly formed hydroxyl group. The ^{13}C NMR spectrum confirmed reduction by virtue of the disappearance of the carbonyl resonance. Interestingly, C-2 (116.0) was more shielded than C-3 (130.8), which is explained by the mesomeric effect of the oxygen atom donating a lone pair of electrons into the π-system.

3.1.3.2 Iodide, 10 [50]

Having obtained the alcohol, **9**, in good yield the next step was conversion of the primary alcohol to its corresponding alkyl halide. Several methods can be used to achieve this transformation including activation to a sulfonate ester followed by displacement by tetrabutylammonium Iodide to afford the iodide; Lewis Acid activation with BF_3 in Et_2O; reaction with $SOCl_2$; the combination of P_4 and I_2. After careful consideration we decided to use triphenylphosphine and iodine to convert the primary alcohol into an iodide. This methodology tends to give rapid, clean conversion and the reaction can easily be followed on TLC. The reaction is very similar to the Appel reaction were triphenylphosphine and tetrahalomethanes (CCl_4, CBr_4) are used to convert primary or secondary alcohols into alkyl halides. The reaction was performed by dissolving I_2 (1.2 equiv) and PPh_3 (1.2 equiv) in dry THF and then adding the alcohol (1.0 equiv) and imidazole (1.2 equiv), the latter to neutralise the HI by-product formed. The reaction was allowed to proceed overnight at room temperature and the product **10** was isolated as a white powder in 91 % yield.

The synthesis of **10** was confirmed using ^{1}H and ^{13}C NMR spectroscopy. The ^{1}H NMR spectrum revealed the disappearance of the hydroxyl proton peak which was at 3.53 ppm previously in **9**, while the H-6 protons were now further upfield at 3.31 ppm due to the lower deshielding effect of iodine. The aromatic region showed a characteristic AA'BB' system (apparent doublets) at 6.78 (H-2) and 7.06 (H-3) still intact. Similarly the broad singlet at 4.87 ppm confirmed that the phenolic OH had been left intact, while the ^{13}C NMR spectrum showed C-6 shift upfield from 64.3 ppm to 6.2 ppm, confirming the change in functional group from the very electronegative second-period element oxygen to the fourth-period element and highly shielding iodine.

3.1.3.3 Phenolic Thiotosylate tether, 11

The thiotosylate sulfenylating agent **11** was obtained by stirring the iodide, **10**, with potassium thiotosylate (3.0 equiv) in DMF for 2 h (Scheme 13). Using column chromatography **11** was isolated as a golden-brown oil in 91 % yield.

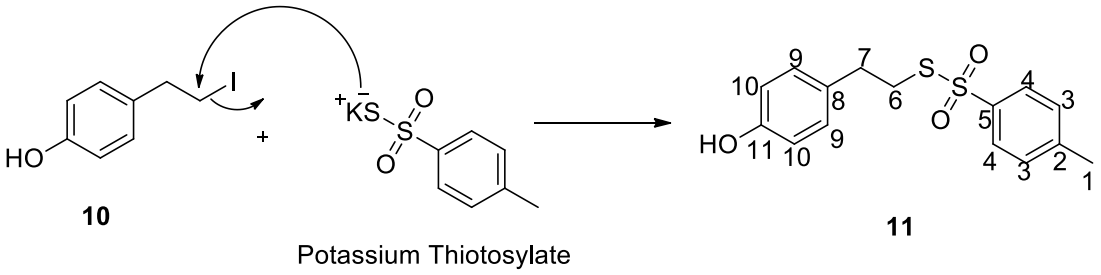

Scheme 13: Synthesis of phenolic thiotosylate tether **11**.

The product was fully characterised using IR, HRMS, ^{1}H and ^{13}C NMR spectroscopy. Its IR spectrum revealed the presence of a tosylate group (-RSO_2R-) at 1228 cm^{-1} and also an aromatic phenol (ArOH) at 3152 cm^{-1}. The ^{1}H NMR spectrum revealed a characteristic AA'BB' system (apparent doublets) at 6.74 ppm (H-10) and 6.95 ppm (H-9), and 7.34 ppm (H-3) and 7.81 ppm (H-4) for the aromatic hydrogens confirming the presence of two *p*-substituted aromatic rings. The distinctive methyl singlet (H-1) on the ring and a broad phenolic hydroxyl singlet were observed at 2.45 ppm and 3.38 ppm respectively. The two methylene protons H-6 and H-7 were observed as triplets integrating for two protons each at 2.83 ppm and 3.18 ppm respectively. The ^{13}C NMR spectrum revealed all the 8 aromatic carbon signals expected in the region 114 -155 ppm, while the methyl resonance could be observed upfield at 21.8 ppm and the two methylene carbons C-6 and C-7 observed at 34.4 ppm and 37.6 ppm respectively. The downfield shift of the C-6 methylene (6.4 ppm to 34.4 ppm) provided substantial evidence for the formation of a C-S bond. High-Resolution Mass Spectrometry confirmed the structure of **11**, with the dominant molecular ion being found at 309.0615 $[M+ H]^{+}$; $C_{15}H_{17}O_3S_2$ requires 309.0619.

3.1.4 Mono-PMB thiol, 12

3.1.4.1 Two-step, one-pot synthesis of coupled product 13a

With the thiotosylate, **11**, in hand attention was focused on obtaining the coupled product **13a**, which was envisaged could be obtained from a two-step, one-pot synthesis reaction involving the monoalkylation of 1,3-propanedithiol by *p*-methoxybenzyl chloride (*p*MBCl) followed by a second alkylation with the thiotosylate, **11**.

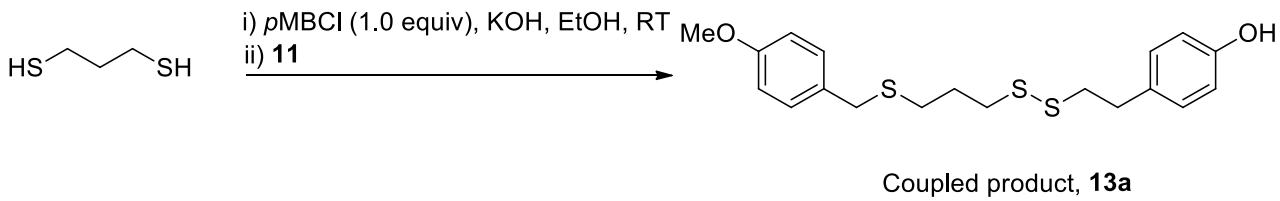

Coupled product, **13a**

Scheme 14: Two step, one-pot synthesis of coupled product **13a**

In the initial approach, 1,3-propanedithiol (1.1 equiv) and potassium hydroxide (1.3 equiv) were dissolved in degassed EtOH and stirred for 5 min at room temperature, and then *p*MBCl (1.0 equiv) dissolved in EtOH was added to the reaction dropwise via a syringe over 1 h. After stirring the reaction mixture for 2 h another 2 equivalents of KOH was added followed by thiotosylate **11** (1.0 equiv) dissolved in EtOH. After stirring for 3h the desired product **13a** was isolated in 47 % yield. This one-pot methodology was more desirable as it avoided isolation of the odiferous thiol **12**. However, several experiments revealed that the first step was sluggish and that inevitably alkylation occurred on both sulfurs of the dithiol to give the undesired di-*p*-methoxybenzylated bis-sulfide as a competing product. Several efforts to manipulate the reaction conditions to achieve mono *S*-alkylation resulted in even lower yields. At this point it was decided to optimise the two reactions independently, i.e. optimally synthesise and isolate the mono-sulfide and then experimentally find the optimal conditions for coupling the remaining thiol group into the thiotosylate **11**.

3.1.4.2 Mono-PMB thiol, 12

The studies carried out in 3.1.4.1 revealed that bis-alkylation of the 1,3-dithiol occurred, and in some instances the ratio of mono- : di-alkylated product was 1 : 1 (by TLC analysis). Furthermore, chromatography of the reaction residue was laborious as the product and by-product had a similar Rf on TLC (0.30 and 0.25 respectively in 1 % EtOAc: Hexane). Given these results it was decided to keep the concentration of *p*MBCl at one equivalent, with a slight excess of 1,3-propane dithiol (1.1 equiv) and also to try the alkylation at 0 °C in order to minimize formation of the di-alkylated product. Indeed this paid off as at 0 °C the formation of the di-alkylated product was minimised.

Thus, 1,3-propanedithiol (1.1 equiv) was dissolved in degassed methanol, KOH (1.3 equiv) was added to the reaction and the solution stirred for 5 min at 0 °C. This was followed by addition of a solution of *p*MBCl (1 equiv) in methanol which was slowly added to the reaction dropwise over 30 minutes. Using this optimised method the desired thiol **12** was isolated by column chromatography as a highly odoriferous lime-green coloured oil in 71 % yield.

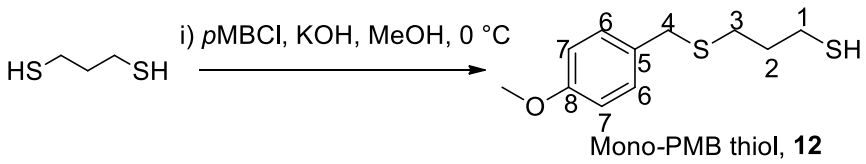

Scheme 15: Synthesis of Mono-PMB thiol **12**

12 is a new compound that was fully characterised using IR, MS, HSQC, ^{1}H and ^{13}C NMR spectroscopies. Its ^{1}H NMR spectrum revealed a diagnostic thiol triplet at 1.31 ppm, H-2 as a quintet at 1.84 ppm, H-3 as a triplet that coupled with H-2, H-4 as a singlet at 3.66 ppm and in the aromatic region an AA'BB' system (apparent doublets) at 6.84 (H-7) and 7.20 (H-6). The H-1 protons experienced coupling with the sulfhydryl hydrogen resulting in the appearance of H-1 as a quartet at 2.58 ppm. The ^{13}C NMR spectrum showed interesting features, with C-1 and C-3 observed upfield at 23.6 ppm and 29.7 ppm indicating a shielding effect by the neighbouring sulfurs, while the C-2 methylene was further downfield at 33.2 ppm. Also, the benzylic C-4 was observed at 35.8 ppm, again rather shielded for a substituted benzyl, due to the neighbouring sulfur. The methoxy signal was observed as expected at 55.4 ppm and all aromatic peaks (4) were found in the region 114.0-159.0 ppm. The methylene protons were all co-related to their respective carbons using HSQC.

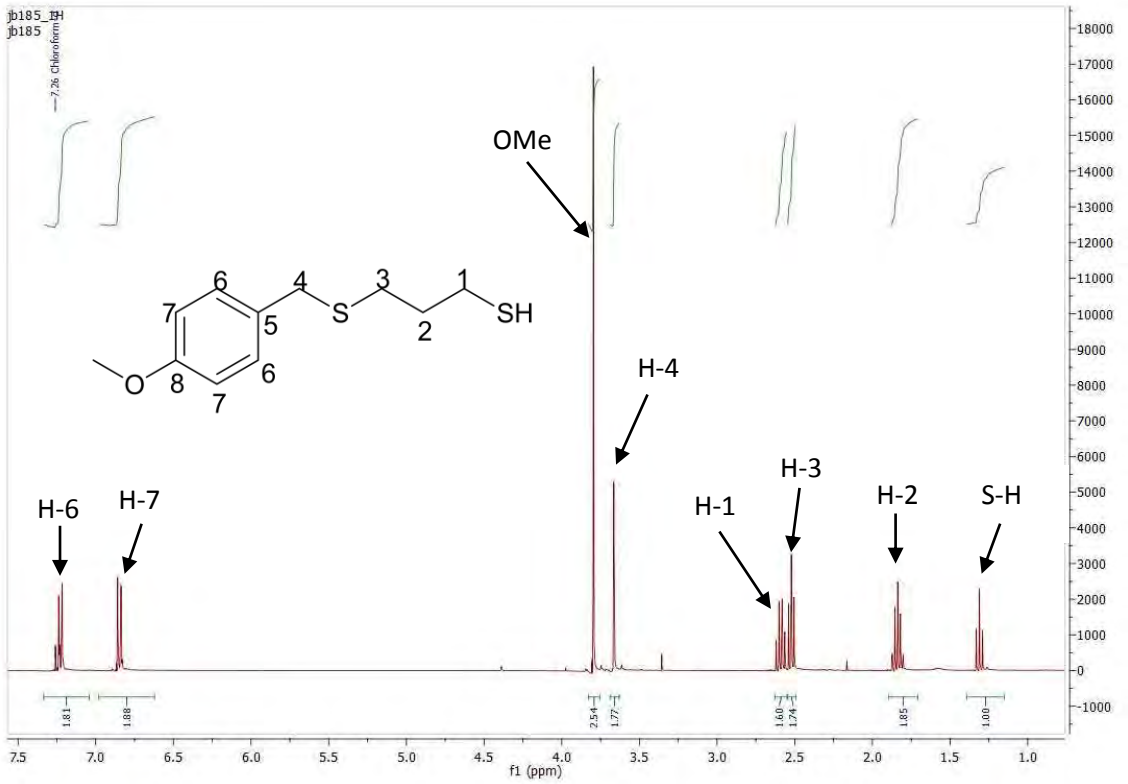

Figure 14: ^{1}H NMR Spectrum of **12**

3.1.5 Coupled product, 13a

Having obtained **12** in a decent yield, the next step was the disulfide formation step involving thiotosylate, **11**. Our initial approach mirrored the second step of the one-pot synthesis discussed in 3.1.4, which involved dissolving **12** (1.2 equiv) and KOH (2 equiv) in ethanol and then adding phenolic thiotosylate **11** (1 equiv) to the reaction at room temperature. The reaction was complete in 5 mins according to TLC, although the desired product **13a** was isolated in a poor yield of only 40 %. It was postulated once formed, that the product could be undergoing a secondary reaction presumably via disulfide exchange. Several conditions were explored experimentally to optimise the reaction outcome, which are summarised in Table 5.

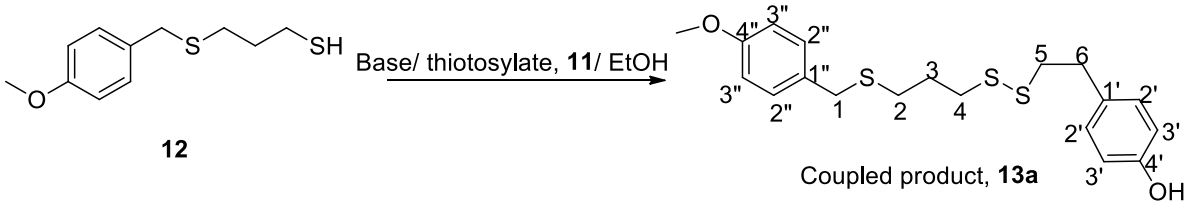

Scheme 16: Reaction to coupled intermediate **13a**

During the optimisation process it was noted that lower temperatures resulted in higher yields of **13a** (Table 5), with presumably the secondary reaction being much slower at these temperatures. Similarly the reaction yields improved drastically when the phenolic tosylate, **11**, was added in excess (Table 5, entry 6-8), and this supported the view that remaining thiol was reacting with the newly formed product, **13a**, to give secondary products. The reaction occurred rapidly using KOH, so the moderate base triethylamine was used instead which presumably reduced the ionicity of the phenoxide formed based on the change in cation from potassium to triethylammonium.

Table 5: Optimisation of reaction to coupled intermediate **13a**

Entry	Thiol, 12 (equiv)	Base	Tosylate 11 (equiv)	Temperature	Yield of 13a
1	1.2	KOH (2 equiv)	1	RT	40 %
2	1.2	KOH (2 equiv)	1	0 °C	40 %
3	1.2	KOH (2 equiv)	1	- 20 °C	~ 40 %
4	1.2	KOH (2 equiv)	1	- 78 °C	50 %
5	1	KOH (2 equiv)	1.2	-20 °C	24 %
6	1	KOH (2 equiv)	1.2	- 78 °C	60 %
7	1	NEt_3(2.5 equiv)	1.2	- 78 °C	60 %
8	1	NEt_3(1.5 equiv)	2.5	- 78 °C	88 %

From this study we found that the conditions involving excess of **11** (2.5 equiv), triethylamine (1.5 equiv) and a low temperature of – 78 °C gave an excellent yield of 88 % (entry 8) of **13a**.

13a is a new compound that was fully characterised using IR, HRMS, HSQC, ^{1}H and ^{13}C NMR spectroscopy. Its ^{1}H NMR spectrum revealed the presence of a double pair of apparent doublets in the aromatic region at 6.75 (H-3') and 7.05 ppm (H-2'), and 6.84 (H-3") and 7.22 ppm (H-2"), confirming the introduction of a second *p*-substituted-aromatic moiety. The distinctive methoxy and phenolic protons were observed as singlets at 3.79 and 4.77 ppm respectively, the methylene protons H-3, H-2, and H-4 were observed at 1.93, 2.51 and 2.73 ppm respectively, while H-5 and H-6 were observed as a broad singlet at 2.89 ppm which was unexpected, but may be explained as a pair of overlapping triplets that did not resolve well. Synthesis of **13a** was confirmed by High-Resolution Mass Spectrometry, in which the major molecular ion was found at 379.0860 $[M-H]^{+}$; $C_{19}H_{23}O_2S_3$ requires 379.0866. The biological evaluation of **13a** will be discussed in Chapter 4.

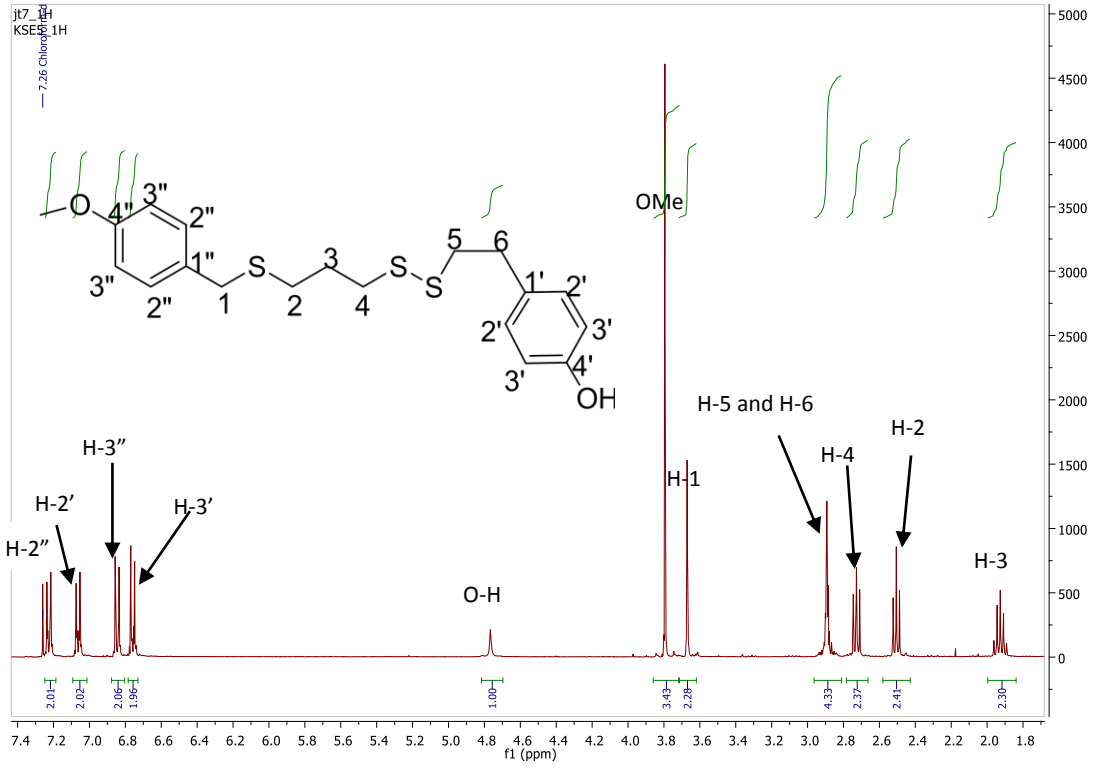

Figure 15: The ^{1}H NMR spectrum of **13a**

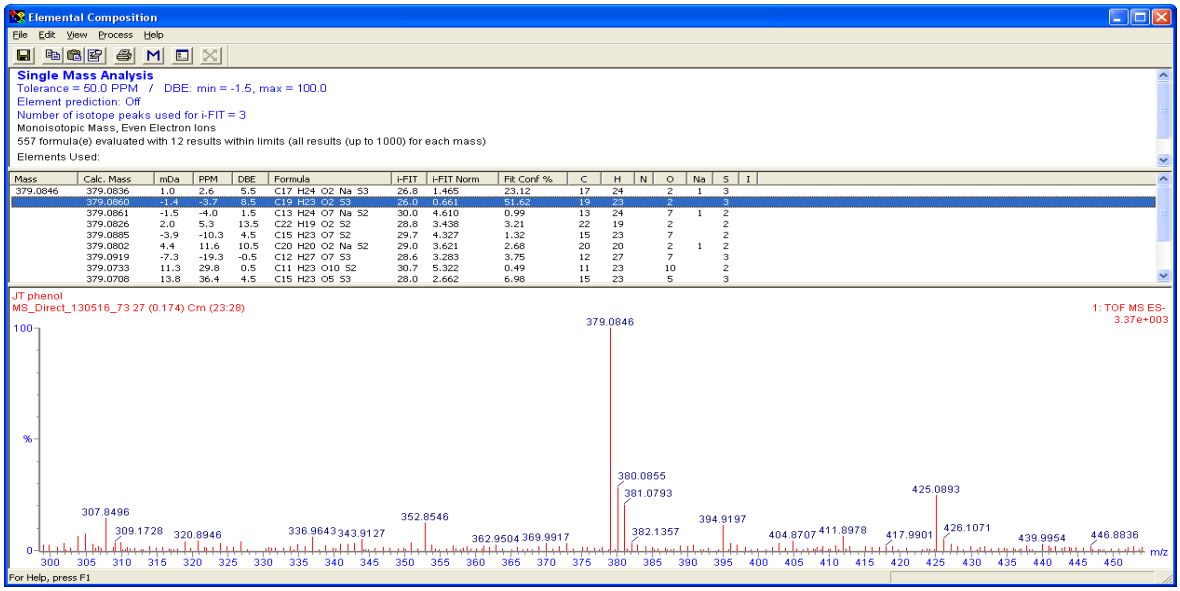

Figure 16: The HRMS of **13a**

3.2 Dihydroajoenes with water-solubility enhancing groups

As described in section 3.1.1 one of the objectives of this project was to synthesize ajoene analogues with water-solubility enhancing groups (WSGs) (see Figure 13).

We envisaged a divergent synthesis involving various alkylations of the phenol-sulfoxide **8a** to install the various WSGs as the last step (Scheme 11). Using this sequence, as described later, we could obtain the ester analogue **8c** relatively easily (see section 3.2.5). However, the two analogues, namely acetate, **8b**, and amide, **8d**, proved difficult to obtain. In the case of **8d** the product was obtained with an inseparable impurity so could not be used further. Due to these unexpected issues the synthetic sequence was altered such that derivatization of **13a** preceded the oxidation step (Scheme 17).

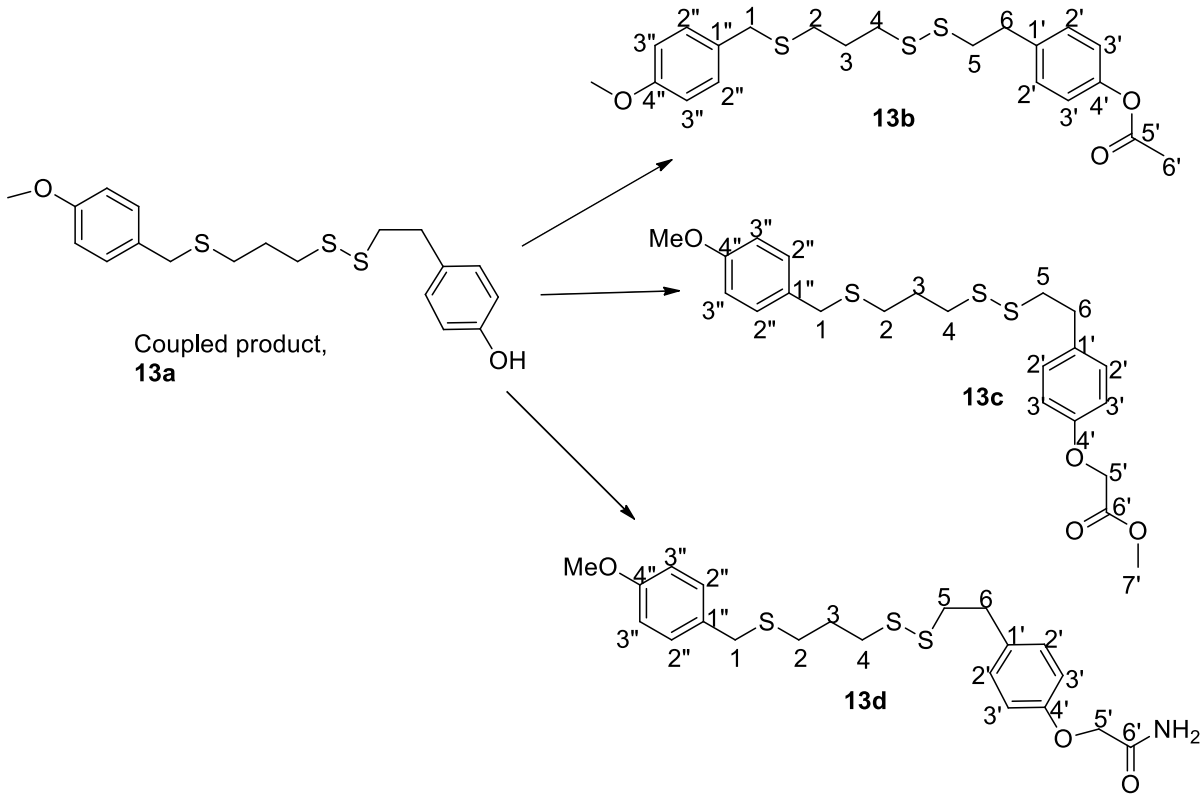

Scheme 17: Alkylation of the coupled product **13a**

3.2.1 Trisulfide-acetate 13b

The first derivative chosen was the acetate **13b** which could be easily prepared by a standard acetylation using acetyl chloride with triethylamine in dichloromethane (DCM) as solvent. The reaction was complete after only 1hr, and the less polar acetate **13b** was isolated as yellow oil in a modest yield of 64 %. As before, **13b** is a new compound that was fully characterised using IR, HRMS, HSQC, ^{1}H and ^{13}C NMR spectroscopy. Its IR spectrum gave a carbonyl absorption at 1750 cm^{-1}, while the ^{1}H NMR spectrum revealed a new methyl peak at 2.30 ppm corresponding to the acetyl methyl H-6', together with disappearance of the OH singlet which was at 4.77 ppm in **13a**. The ^{13}C NMR spectrum confirmed the presence of the acetyl group by virtue of a new ester carbonyl (C-5') at 169.5 ppm and a methyl C-6' at 21.1 ppm. All protons were correlated to their carbon assignments with the aid of HSQC and the synthesis final confirmation came from High-Resolution Mass Spectrometry (HRMS), with the molecular ion as 445.0933 $[M + Na]^{+}$; $C_{21}H_{26}NaO_3S_3$ requires 445.0942.

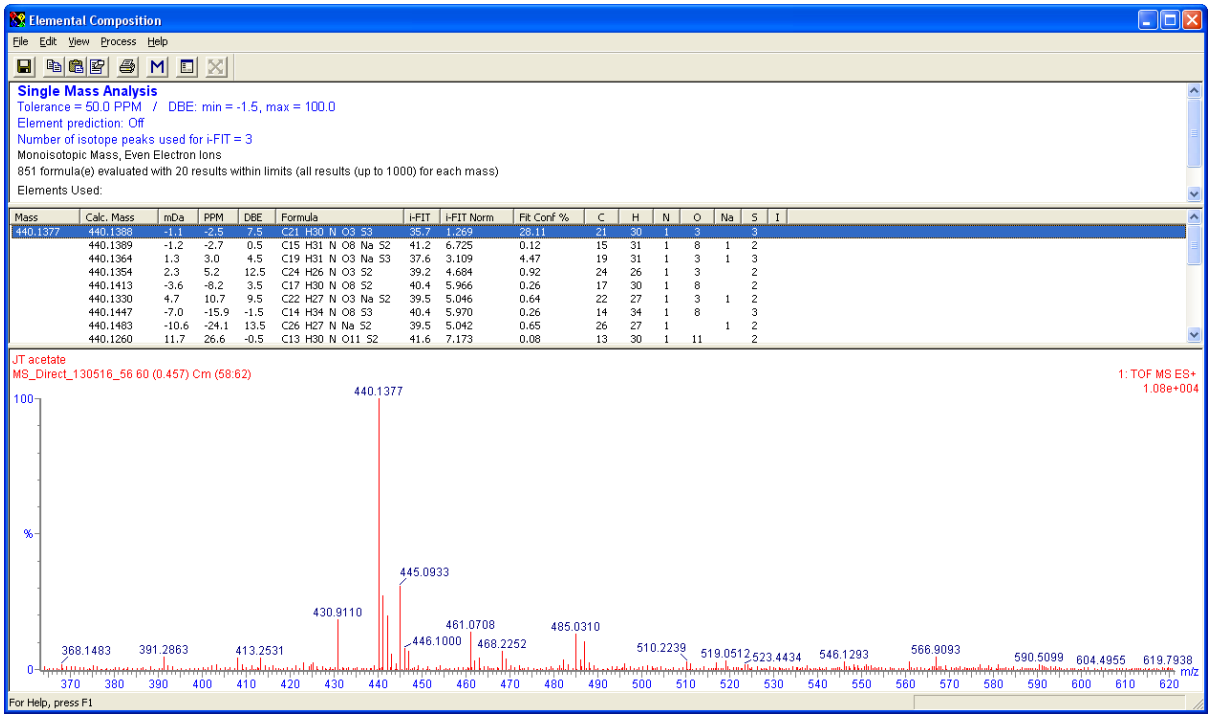

Figure 17: The HRMS of trisulfide-acetate **13b**

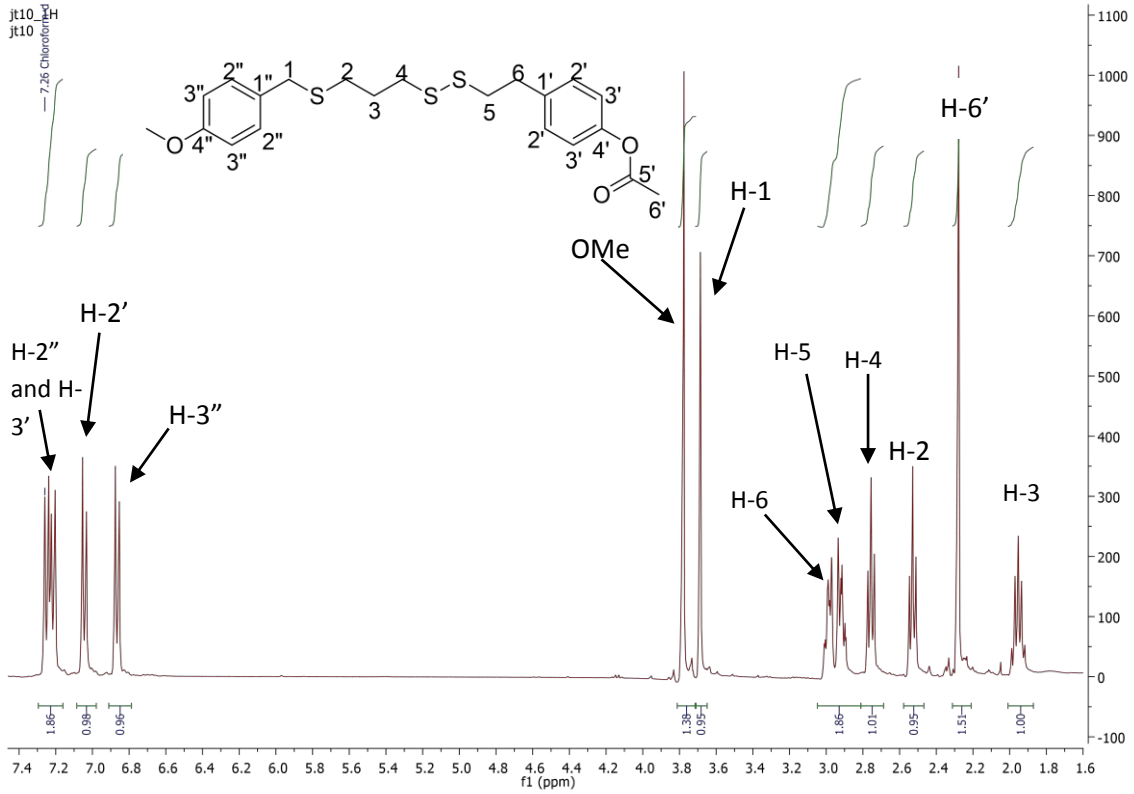

Figure 18: ^{1}H NMR spectrum of trisulfide-acetate **13b**

3.2.2 Trisulfide-ester 13c

For the next derivative, **13c**, involving alkylation with methyl 2-bromoacetate the base was changed to potassium carbonate (1.5 equiv) in dry acetonitrile, in order to promote the more difficult S_N2 reaction (compared to the S_NAc of the acetylation) via a more ionic phenoxide ion (K^+). The reaction mixture was stirred under N_2 at 45 °C overnight, and the desired trisulfide-ester, **13c**, was isolated as a dark-yellow oil in 78 % yield. **13c** is a new compound that was fully characterised using IR, HRMS, HSQC, ^{13}C and ^{1}H NMR spectroscopies. Its IR spectrum revealed an absorbance band at 1750 cm^{-1} corresponding to a carbonyl absorbance, confirming the presence of the ester carbonyl. The ^{1}H NMR spectrum of **13c** when compared to that of **13a** revealed distinctive new singlets for H-7' (Me) and H-5' (CH_2) at 3.79 and 4.61 ppm respectively. Similarly, the ^{13}C NMR spectrum also confirmed the introduction of the methoxycarbonylmethylene moiety , with the C-6' carbonyl observed at 169.7 ppm, and the C-7' and C-5' resonances at 52.5 ppm and 65.7 ppm respectively, the latter more deshielded by both oxygen and carbonyl groups. Finally, synthesis of **13c** was confirmed using High Resolution Mass Spectroscopy (HRMS), in which the major molecular ion was found at 475.1047 $[M+Na]^+$; $C_{22}H_{28}NaO_4S_3$ requires 475.1047. HRMS was used because combustion analysis generally does not give accurate enough results with oils.

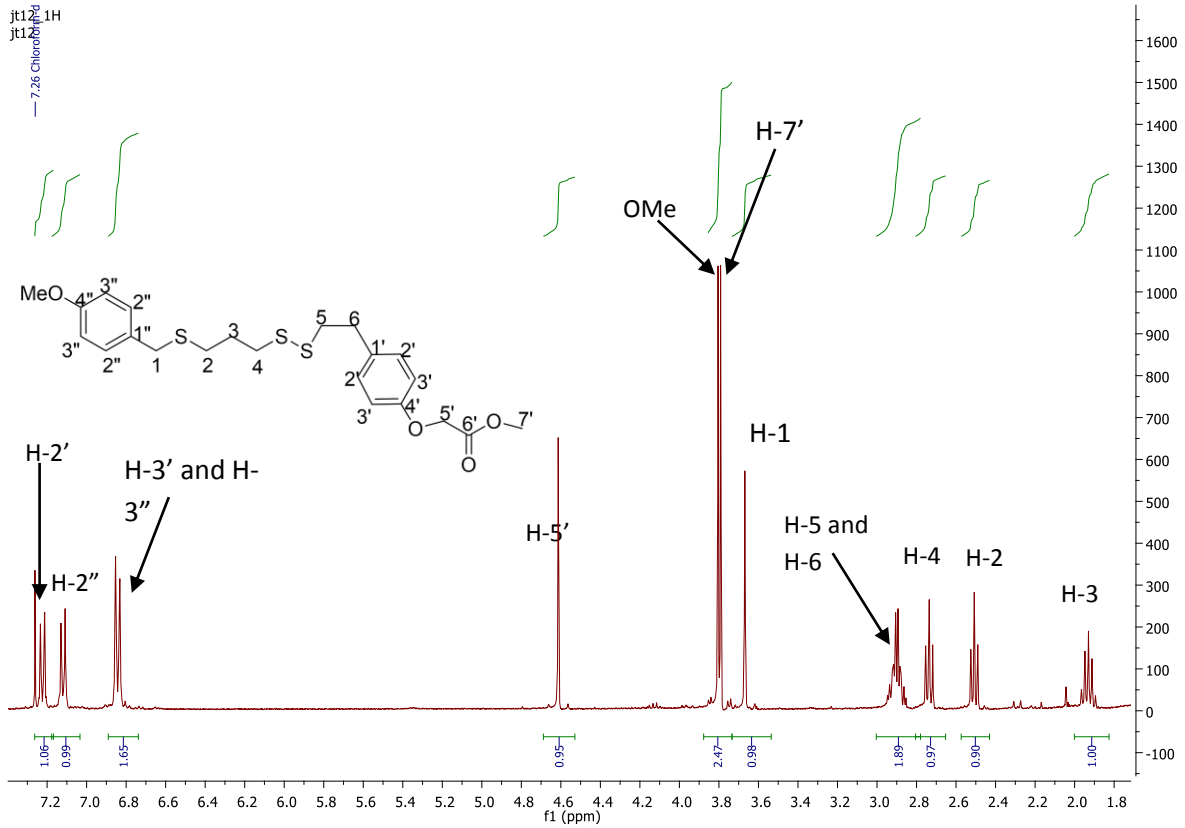

Figure 19: The ^{1}H NMR spectrum of trisulfide-ester **13c**

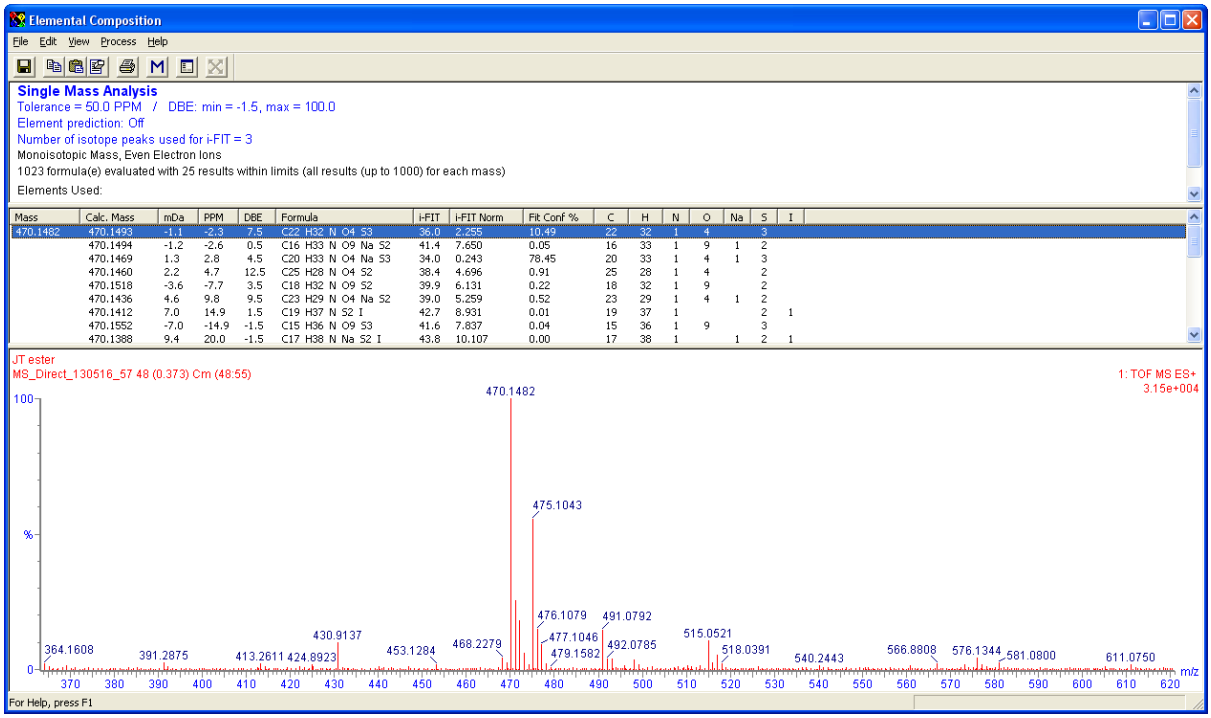

Figure 20: The High-Resolution Mass Spectrum of **13c**

3.2.3 Trisulfide-amide 13d

The final derivative, primary amide **13d**, was chosen in view of the amide's ability to hydrogen bond to water and hence significantly improve aqueous solubility. As with ester **13c**, it could be accessed via S_N2 alkylation with chloroacetamide in dry acetonitrile using the potassium phenoxide of **13a** generated using potassium carbonate as base. Stirring the heterogeneous reaction at 45 °C for 1hr resulted in complete conversion and following a conventional work-up and purification resulted in isolation of **13d** as a white powder in a good yield of 77 %. **13d** was fully characterised using IR, HRMS, HSQC, ^{1}H and ^{13}C NMR spectroscopy. Compared to **13a** the ^{1}H NMR of **13d** revealed distinctive new peaks as two broad singlets at 6.54 and 6.00 ppm corresponding to the non-equivalent amidehydrogens, as well as a sharp singlet at 4.47 ppm corresponding to the deshielded methylene protons H-5'. The H-2' and H-3' aromatic protons resonated slightly more downfield at 7.14 ppm and 6.85 ppm respectively (from 7.05 and 6.75 ppm in **13a**), presumably due to the inductive elecron-withdrawing effect by the amide. Similarly, the ^{13}C NMR spectrum revealed a new carbonyl peak at 171.2 ppm and the C-5' methylene was found relatively downfield at 67.5 ppm. Finally, the synthesis of **13d** was confirmed by High-Resolution Mass Spectrometry, with the molecular ion found at 460.1046 $[M+ Na]^+$; $C_{21}H_{27}NNaO_3S_3$ requires 460.1051.

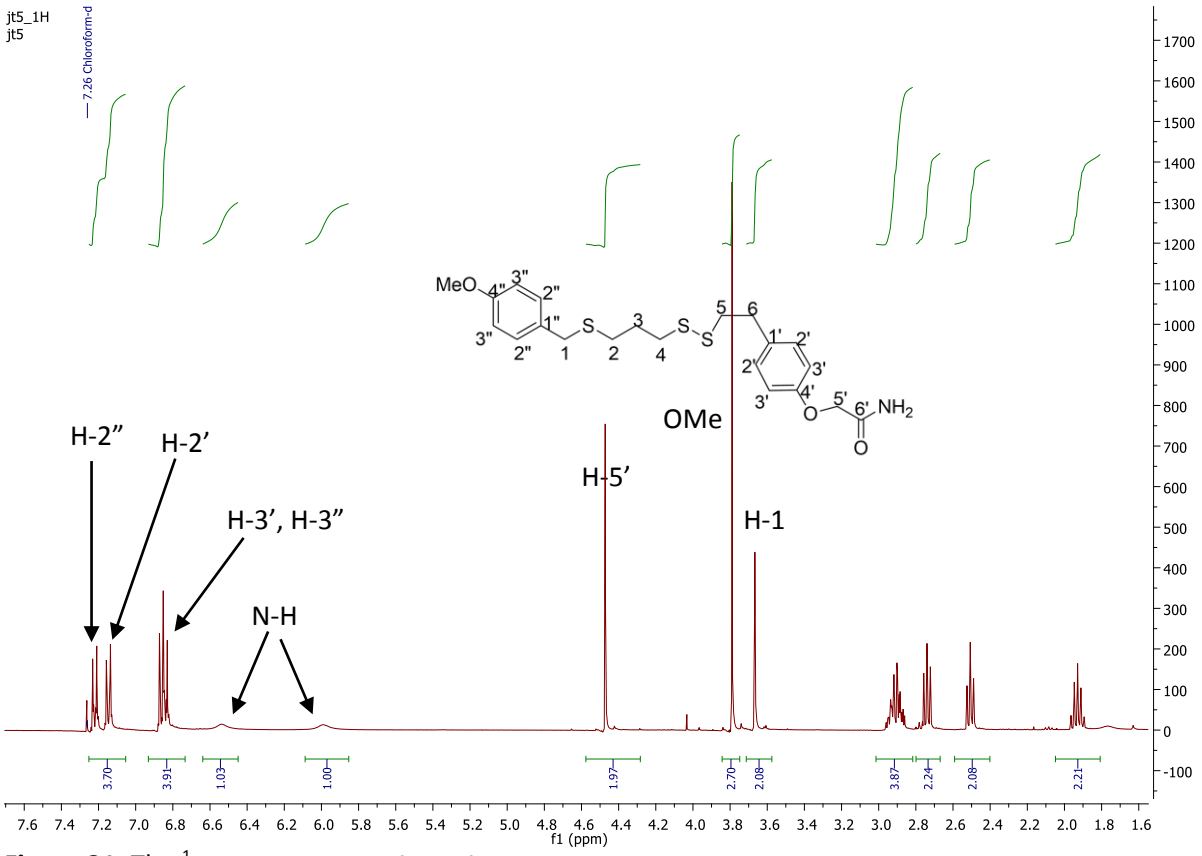

Figure 21: The ^{1}H NMR spectrum of trisulfide-amide **13d**

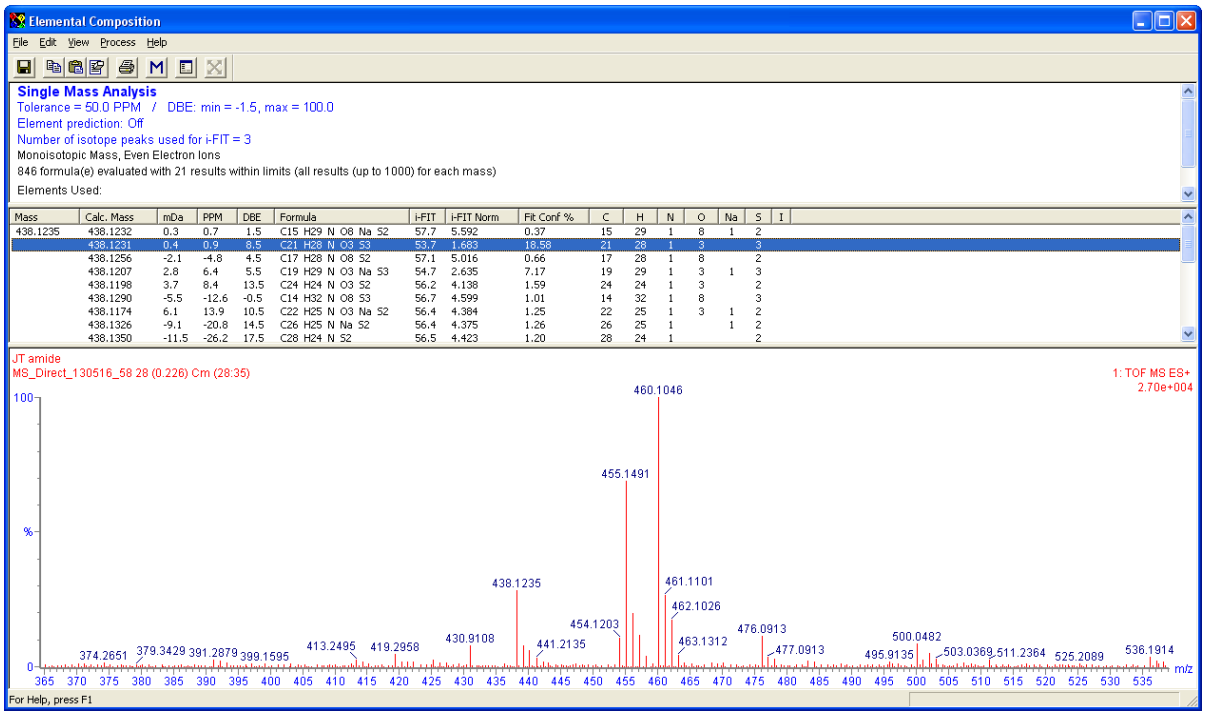

Figure 22: HRMS of trisulfide-amide **13d**

Several attempts were made to regioselectively oxidise the trisulfides **13b-13d** to their corresponding sulfoxides. However, the reaction of the trisulfides with *m*-CPBA (1.2 equiv) resulted in unstable products. In some instances there was evidence, by ^{1}H NMR spectroscopy, of the

oxidation occurring on one of the disulfide sulfurs. The instability of the products could have been due to the production of thiosulfinates. Why this only occurs for the substituted dihydroajoenes could not be rationalised, as **13a** was oxidised without any major issues.

3.2.4 Phenol-Sulfoxide, 8a

In the final step to obtain the dihydroajoene core, sulfide **13a** was regioselectively oxidised to **8a** using 1.2 equivalents of *m*-CPBA at -78 °C, allowing **8a** to be isolated as a colourless oil in 72 % yield. At -78 °C the oxidation occurs exclusively on the benzylic sulfur as it is presumably the more nucleophilic sulfur, with the disulphide sulfurs being less nucleophilic due to mutual electron withdrawal. A mechanism for the reaction is shown in Scheme 18, in which a lone pair on sulfur attacks the terminal oxygen of *m*-CPBA (which is electrophilic due to the inductive effect of the benzoic acetate) releasing the *m*-chlorobenzoate anion and giving a sulfonium cation. The reaction is completed when the benzoate anion abstracts a proton from the sulfonium cation forming the sulfoxide **8a** and *m*-chlorobenzoic acid as a by-product.

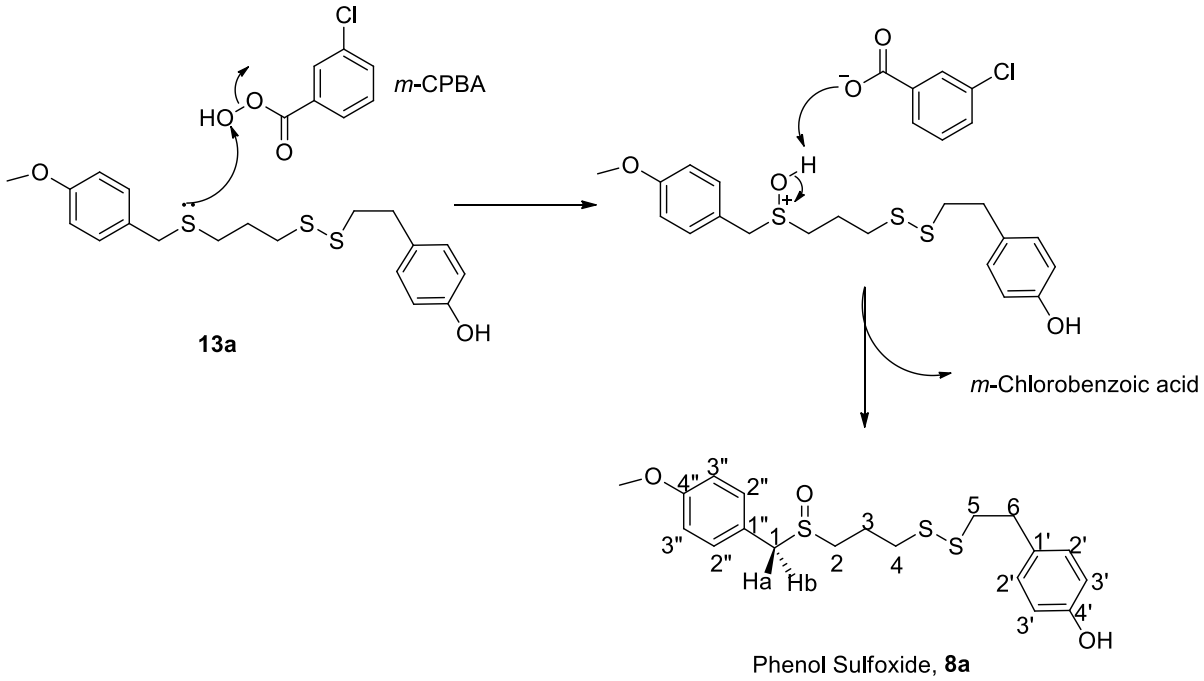

Scheme 18: Chemoselective oxidation of **13a** to the phenol-sulfoxide **8a**.

Sulfoxide **8a** is a new compound that was fully characterised using IR, HRMS, HSQC, ^{1}H and ^{13}C NMR spectroscopy. Its IR spectrum showed an absorbance at 1265 cm^{-1} confirming the presence of a sulfoxide. The ^{1}H NMR spectrum provided evidence for oxidation at the benzylic sulfur, with the H-1 protons observed as a diastereotopic pair of AB doublets at 3.95 and 4.00 ppm, which was a considerable shift downfield from 3.67 ppm in **13a**. The H-2 and H-4 methylene protons were observed as a multiplet at 2.69 ppm, also revealing a downfield shift for the H-2 protons from 2.51 ppm in **13a**. The sulfoxide is inherently chiral (Figure 23) which creates a non-equivalent

environment around C-1 resulting in the H-1a and H-1b (see Scheme 18 for numbering) protons appearing as diastereotopic doublets due to geminal coupling. The H-2 hydrogens are also diastereotopic; however, due to the overlap of shifts with H-4 protons, the expected pair of AB triplets for H-2 could not be observed. The ^{13}C NMR spectrum of **8a** revealed C-1 at 57.8 ppm and C-2 at 48.9 ppm, also significantly deshielded compared to those for **13a** (Table 6) again confirming oxidation at the benzylic sulfur. Interestingly, C-3 (22.3 ppm) and C-1" (121.4 ppm) were significantly more upfield than in **13a**, revealing that the sulfoxide has a peculiar shielding effect on the β-carbon positions. Finally, the synthesis of **8a** was confirmed by High Resolution Mass Spectrometry, the parent molecular ion was found at 397.0966 $[M+ H]^+$; $C_{19}H_{25}O_3S_3$ requires 397.0966. The purity of **8a** was determined to be greater than 95 % using Liquid-chromatography Mass Spectrometry and its biological evaluation will be discussed in Chapter 4.

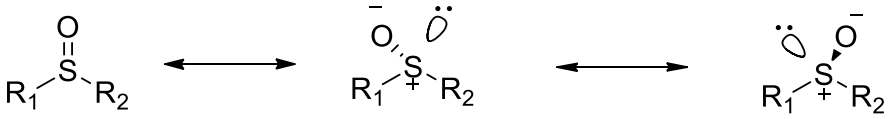

Figure 23: Chirality of the sulfoxide, **8a**.

Table 6: ^{13}C NMR spectrum shifts for compounds **8a** and **13a**

Assignment	Phenol 13a (C-13 Shifts/ppm)	Phenol-Sulfoxide 8a (C-13 Shifts/ppm)
C-1	35.9	57.8
C-2	29.9	48.9
C-3	28.6	22.3
C-4	37.7	37.3
C-5	35.0	34.9
C-6	40.7	41.1
OMe	55.5	55.5
C-1'	132.4	131.7
C-1"	130.5	121.4
C-2'	129.9	129.9
C-2"	130.0	131.4
C-3'	115.5	115.8
C-3"	114.1	114.7
C-4'	154.1	154.9
C-4"	159.0	160.0

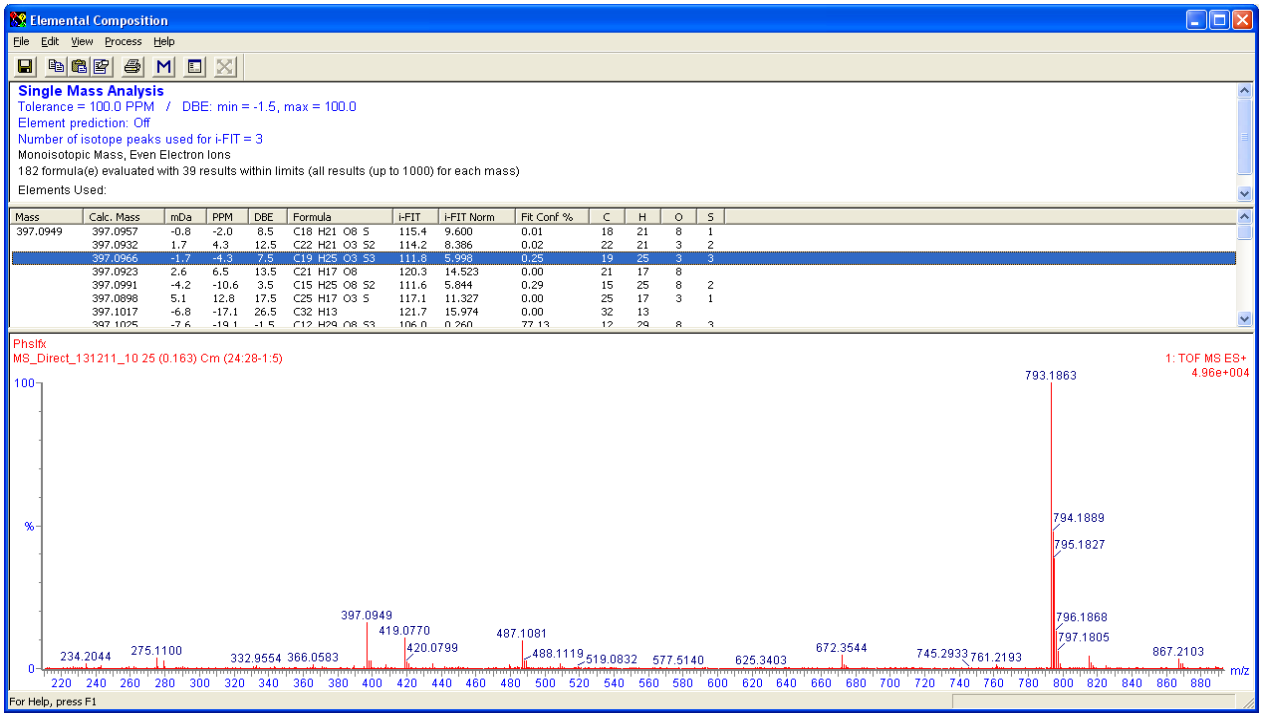

Figure 24: High-resolution Mass Spectrum for the phenol-sulfoxide, **8a**

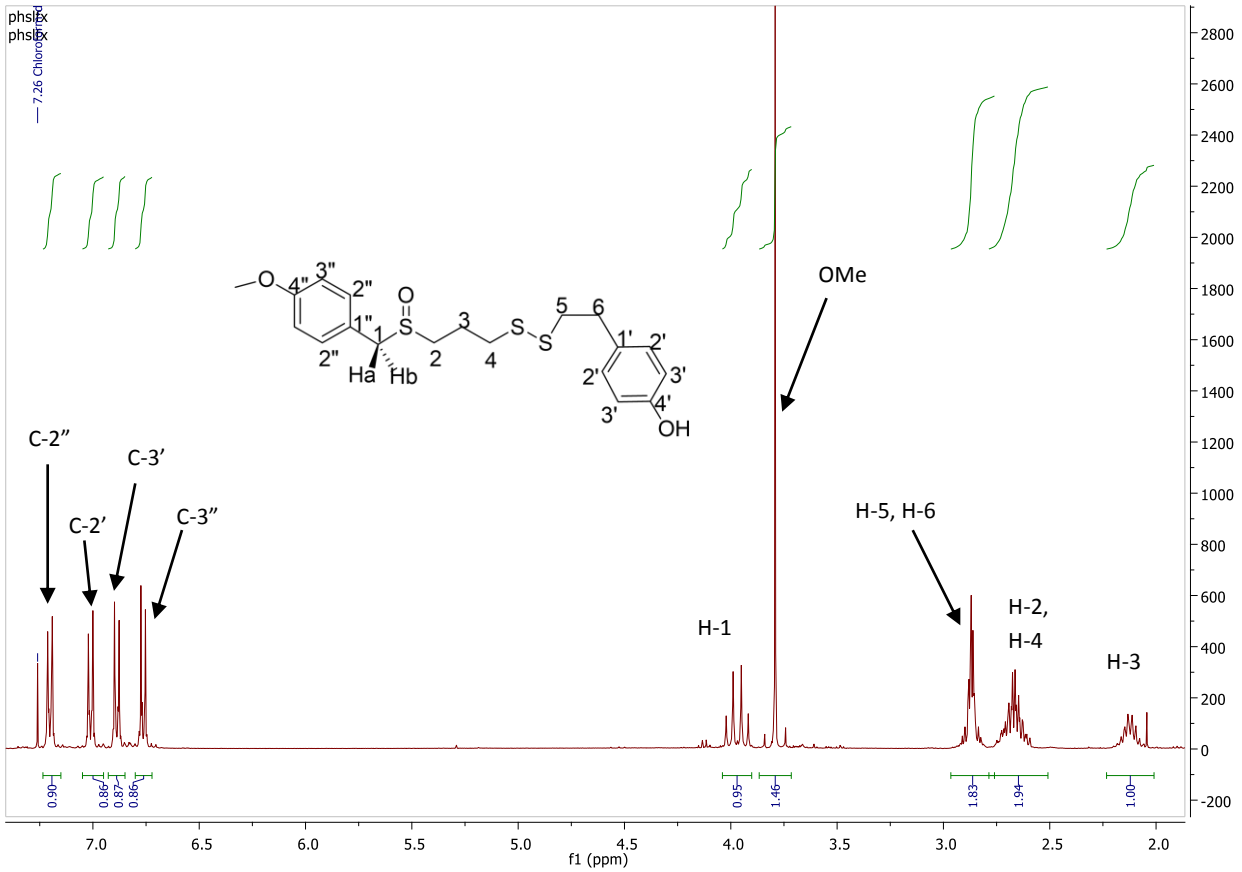

Figure 25: ^{1}H NMR spectrum for the phenol-sulfoxide, **8a**

3.2.5 Ester-Sulfoxide, 8c

As mentioned in section 3.2, the one sulfoxide (dihydroajoene) derivative that could be accessed in a divergent manner from the parent phenol-sulfoxide **8a** was ester-sulfoxide **8c**, whose synthesis was achieved via phenoxide alkylation in dry acetonitrile with methyl bromoacetate at 45 °C. The reaction was complete in 1 h and using column chromatography, the product being isolated as a yellow oil in a good yield of 77 %.

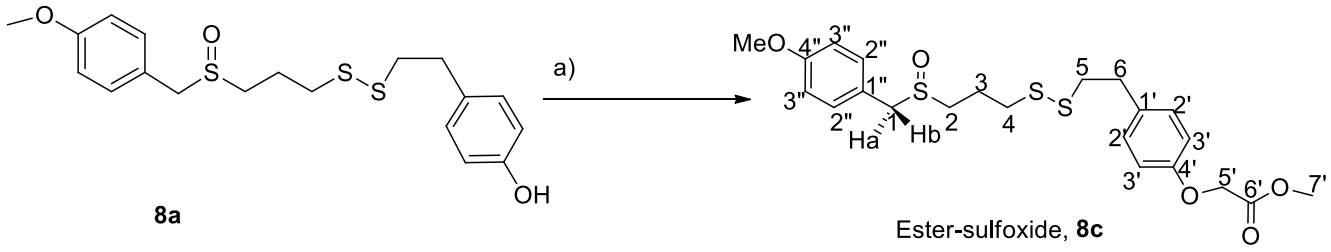

a) Methyl bromoacetate / K_2C0_3 / 45 °C / CH_3CN

Scheme 19: Alkylation of Phenol-sulfoxide **8a** to the Ester-sulfoxide **8c**

Compound **8c**, was characterised using IR, HSQC, LCMS, ^{1}H and ^{13}C NMR spectroscopy. Its IR spectrum revealed an absorption at around 1750 cm^{-1} corresponding to a carbonyl group. Compared to **8a**, the ^{1}H NMR spectrum of **8c** revealed two new singlets at 3.55 ppm and 4.55 ppm corresponding to H-7' and H-5' respectively, while the aromatic region was slightly altered from the starting material with the H-2' protons appearing further downfield at 7.10 ppm (7.01 ppm in **8a**). The ^{13}C NMR spectrum confirmed the incorporation of the ester, by virtue of a new ester carbonyl (C-6') at 169.6 ppm, also with two new singlets for C-7' and C-5' 52.4 ppm and 65.6 ppm respectively similar to resonances for the sulfide analogue **13c**. Finally, synthesis of **8c** was confirmed using Liquid Chromatography-Mass Spectrometry (LCMS), the major molecular ion being found at 491.0 $[M\text{-}Na]^{+}$; $C_{22}H_{28}NaO_5S_3$ requires 491.1. LCMS was used (in place of HRMS) as it was important to determine the purity of the sample before proceeding with the biological evaluation.

Compound **8c** was not evaluated biologically, as there was evidence of minor degradation on TLC with a faint less polar spot observed after storing the compound at - 20 ° C for 24 h. Interestingly, after 5 months of storing **8c** at -20 °C degradation was more evident on TLC but could not be observed by either ^{1}H or ^{13}C NMR spectroscopy. However, using LCMS the purity of this sample was determined to be 72 %.

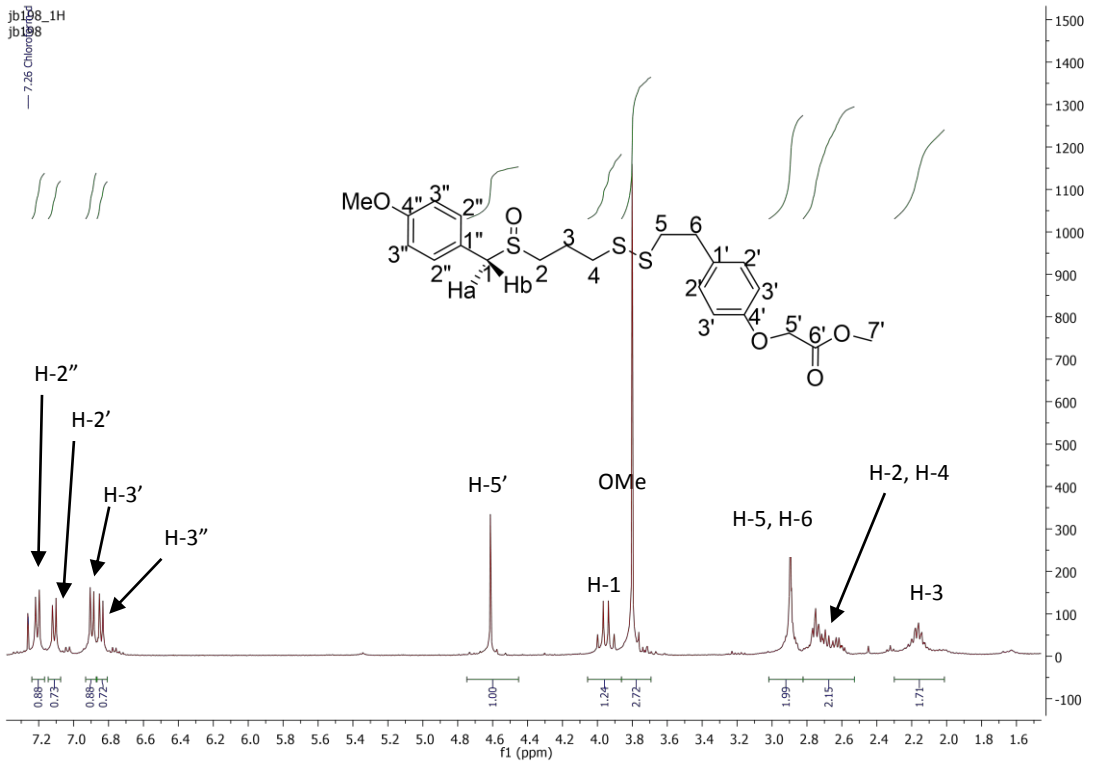

Figure 26: ^{1}H NMR spectrum of Ester-sulfoxide **8c**.

The oxidation of the trisulfides **13b**, **13c** and **13d** resulted in unstable products which were difficult to isolate. Thus the sulfoxides, **8b** and **8d** were not pursued further.

3.3 Studies towards the synthesis of an ajoene chemosensitization agent

3.3.1 Introduction

As described in section 1.6.3, ajoene has been shown to enhance the activity of the leukaemic drugs cytarabine and fludarabine, and this area of ajoene-induced chemosensitisation has not been fully explored. A study was thus initiated towards the development of an ajoene-fludarabine conjugate. The target conjugate would have ajoene and fludarabine linked by a biologically hydrolysable bond in order to release the two drugs in the hope of achieving synergism. Previous work had shown that the ajoene analogue, **7a**, with a phenol substituent retained very good cell anti-proliferation *in vitro*. It was envisaged that the phenolic hydroxyl group would provide a suitable site for attachment of an electrophilic position on a linker, which would link at the other end to the phosphate functionality of commercially available fludarabine via a phosphate ester bond using a methodology reported by H. Brachwitz.[48a] The synthons in this plan are shown in Scheme 20.

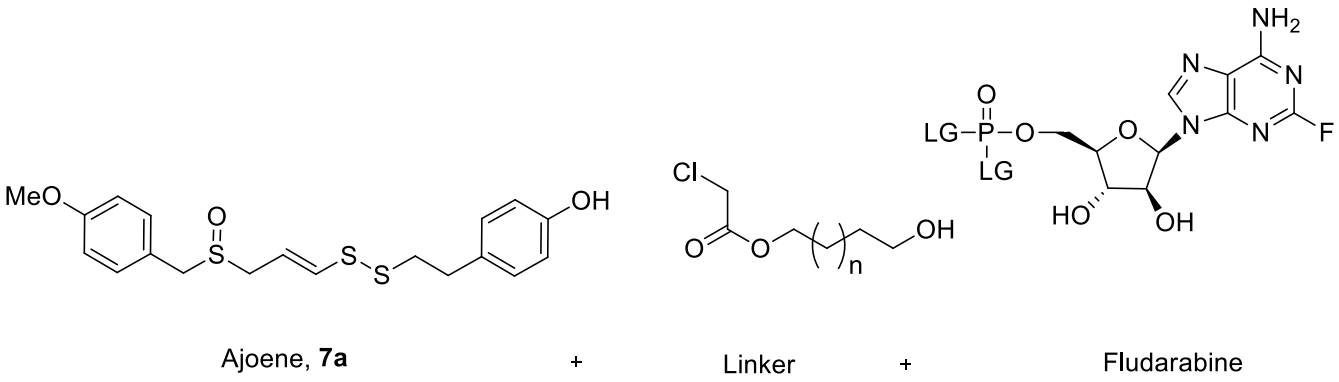

LG = leaving group

Scheme 20: Connection chemistry of the ajoene-fludarabine conjugate

3.3.2 Synthesis of ajoene 7a

The first task towards an ajoene-fludarabine conjugate was the synthesis of the ajoene analogue **7a**. A retrosynthetic analysis of **7a** is shown in Scheme 21, based on the UCT synthesis described in section 2.3, and involving thiotosylate, **11**, developed for the dihydroajoene synthesis.

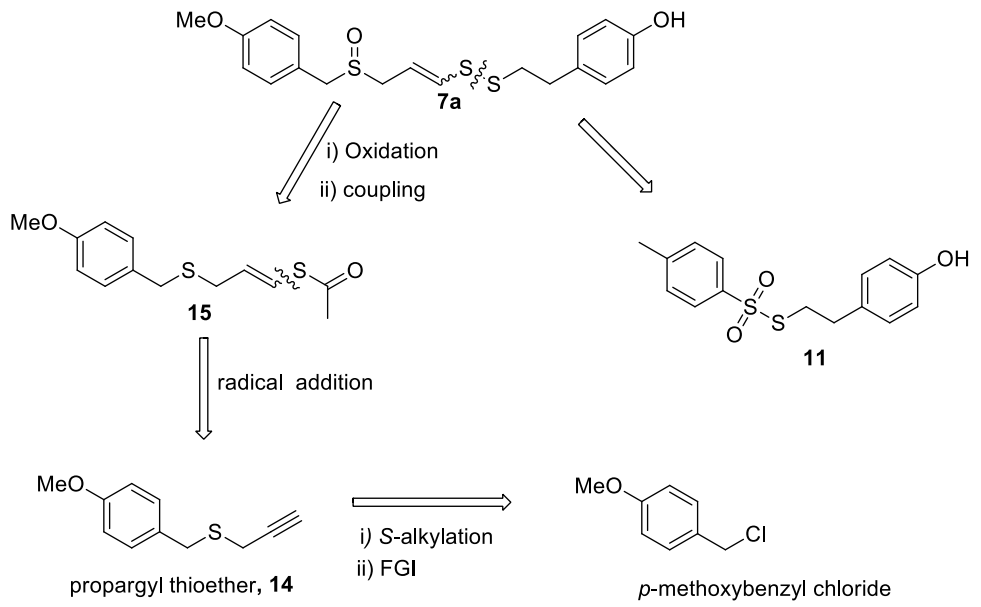

Scheme 21: Retrosynthetic analysis of ajoene analogue **7a**

3.3.2.1 Propargyl thioether, 14

The synthesis of **7a** began with the preparation of the propargyl thioether **14**, via *in situ* propargylation of *p*-methoxybenzyl thiol. The latter was accessed by refluxing commercially available *p*-methoxybenzyl chloride (1.0 equiv) and thiourea (1.2 equiv) in acetonitrile (Scheme 22 (i)) followed by base hydrolysis of the intermediate salt.

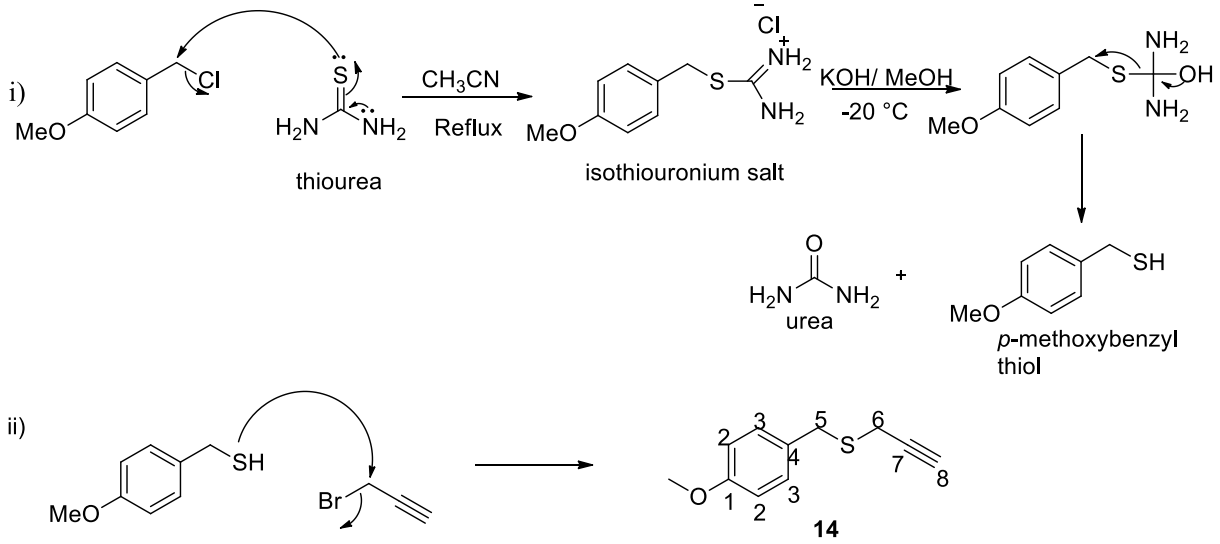

Scheme 22: Synthesis of propargyl thioether, **14**

Thiourea is more nucleophilic on the sulfur due to the donation of lone pairs by the neighbouring nitrogens into the thiocarbonyl, thus when refluxed with *p*-methoxybenzyl chloride the sulfur attacks the benzylic carbon (Scheme 22 (i)). The resulting isothiouronium salt was isolated using a cold filtration in a crude yield of 91 %, which was used without further purification. The latter (1.0 equiv) was then dissolved in degassed methanol containing KOH (2.5 equiv) at -20 ° C. After stirring the solution for 2 h the reaction temperature was allowed to rise to 0 °C at which point propargyl bromide was added. Addition of the hydroxide anion resulted in hydrolysis of the salt, releasing urea and a benzyl thiol (Scheme 22 (i)). Hydrolysis of the isothiouronium salt is entropy-favoured due to the realease of urea. It was important to use 2.5 equiv of KOH for the hydrolysis and the quenching of the HBr by-product formed in the propargylation step. Following a conventional work-up the propargyl thioether, **14**, was isolated as a gold-coloured oil in 90 % yield over the two steps. It was characterised using IR, ^{1}H and ^{13}C NMR spectroscopy. The ^{1}H NMR spectrum revealed a doublet integrating for two protons at 3.11 ppm corresponding to H-6 as well as a triplet at 2.36 ppm integrating for 1 proton, H-8, the two connected by long-range coupling through the triple bond. The ^{13}C NMR spectrum revealed the expected alkyne carbons at 71.2 and 80.0 ppm corresponding to C-8 and C-7 respectively. All ^{1}H and ^{13}C NMR spectral assignments were in agreement with the published data.[45]

3.3.2.2 Vinyl thioacetate, 15

Having obtained the propargyl thioether, **14**, attention was directed at the critical radical addition step. To this end, the alkyne (1.0 equiv), **14**, was dissolved in toluene and the temperature increased to 85 °C. At this point a catalytic amount of the radical initiator ACCN (0.1 equiv) was added followed in quick succession by the addition of thiolacetic acid (1.25 equiv). The reaction was stirred at this

temperature for 3 h and then quenched with $NaHCO_3$. **15** was isolated as a 1 : 2 mixture of *E* : *Z* isomers in a modest yield of 59 %. The proposed mechanism follows the classical radical mechanism of activation, propagation and termination as discussed in section 2.3.2. The *Z*-isomer of ajoene is reported to be the more active isomer and so it was pleasing that the reaction stereoselectivity gave the *Z*-isomer as the major product. The stereoselectivity could be explained on the basis that there is an equilibrium between the *E*- and *Z*- vinyl thioacetate radicals such that they interconvert (Scheme 7). During the termination step, in which hydrogen is abstracted from thiolacetic acid, the *Z*-vinyl thioacetate reacts faster as there is less steric interference with the approaching acid, whereas in the *E*-vinyl thioacetate there is a steric factor arising with the thioacetate substituent (Scheme 7). Thus formation of the *Z*-isomer is thus preferred kinetically (for the full mechanism see section 2.3.2).

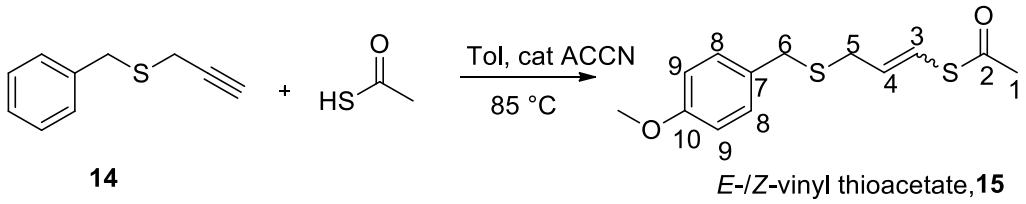

Scheme 23: Synthesis of **15**

Compound **15** was characterised using IR, HSQC, ^{1}H and ^{13}C NMR spectroscopy. Its IR spectrum showed an absorbance at 1700 cm^{-1} confirming the presence of a carbonyl group of a thioester. It was pleasing to note that the ^{1}H NMR spectrum showed a downfield shift of the alkynyl proton in **14**, into the vinyl region. H-3 was observed as two doublet of triplets at 6.52 (J_{cis} = 12.0 Hz) and 6.69 ppm (J_{trans} = 16.0 Hz), for the two geometrical isomers, with the larger vicinal coupling constant corresponding to the *E*-isomer. Similarly, the H-4 proton was observed as an overlapping doublet of triplets in the region 5.70-5.89 ppm coupling to both H-5 and H-3. Interestingly, for both isomers, H-5 was observed as a doublet of doublets coupling to both H-4 (*J* = 7.8 Hz) and to H-3 (*J* = 1.0 Hz) via allylic coupling. The other diagnostic peaks observed were the two singlets for the methyl of the acetyl at 2.39 and 2.40 ppm, corresponding to *E*- and *Z*-isomers respectively.

The ^{13}C NMR spectrum confirmed the presence of two isomers as all the expected 26 signals were observed (13 for each isomer). The most significant diagnostic peaks were the two downfield signals observed at 191.4 and 193.0 ppm corresponding to the acetyl carbonyl, C-2, *Z*- and *E*- respectively. The vinyl carbons were found at 119.7 and 119.5 ppm for C-3, 130.3 and 130.5 ppm for C-4, with C-3 more upfield due to the shielding effect sulfur has on its neighbouring carbon atoms due to resonance. The methoxy signal was observed as expected at 55.4 ppm for both isomers. All proton assignments were correlated to their carbons using HSQC as an aid.

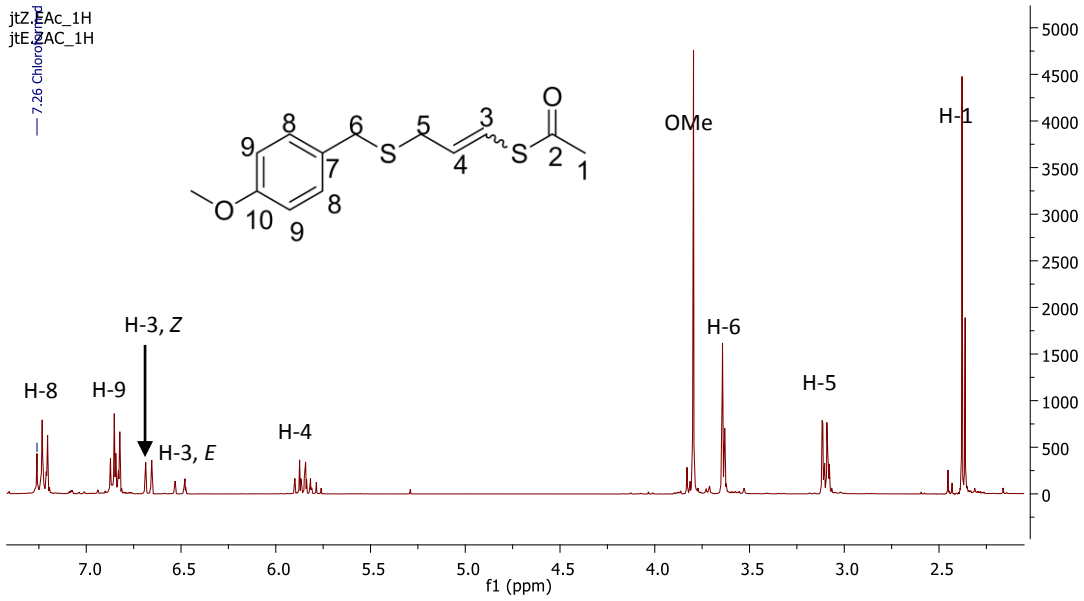

Figure 27: The ^{1}H NMR spectrum of **15**

3.3.2.3 Phenol disulfide, 16

The next step involved deacetylation and thioalkylation of the resultant enethiolate. This was achieved by hydrolyzing the thioacetate with KOH in methanol at -40 °C followed by soft-S-alkylation of the resultant enethiolate with thiotosylate **11**. The reaction was allowed to proceed overnight, at which point it was quenched, the product isolated via an extractive workup and the residue purified using column chromatography. The disulfide **16** was isolated in 79 % yield as a dark-yellow oil and as a 4: 5 mixture of *E*- : *Z*-isomers. Scheme 24 shows the reaction mechanism leading to the phenol disulfide. KOH deprotects the thiol via a base hydrolysis to give a very reactive enethiolate, thus the reaction temperature was kept at – 40 °C to avoid protonation and resulting *Z*- to *E*-isomerization. In the subsequent coupling step the temperature was lowered further to - 78 °C to retard the reactivity of the enethiolate. Past experience (3.1.5) had shown that this limited secondary reactions. It was displeasing to note that from thioacetate **15** to coupled product **16** the *Z* : *E* ratio decreased from 2 : 1 to 5 : 4.

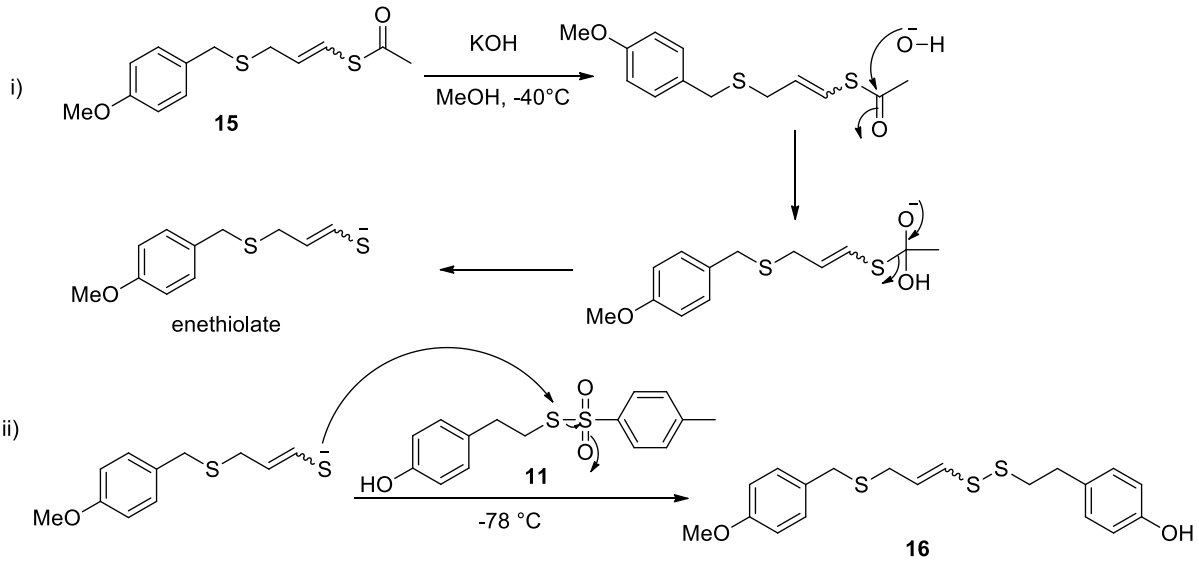

Scheme 24: Synthesis of coupled product, **16**.

Although a full mechanism on this is unknown, the loss of *Z*-selectivity might be explained by the fact that in methanol (protic solvent), the enethiolate can protonate and tautomerize to the thioaldehyde. In the case of the *Z*-enethiolate the thioaldehyde can rotate about C1-C2 to minimise steric strain and when it deprotonates back to the enethiolate the geometry around the double bond has changed to the *E*-configuration. Scheme 25 shows the proposed mechanism for the inversion in stereochemistry.

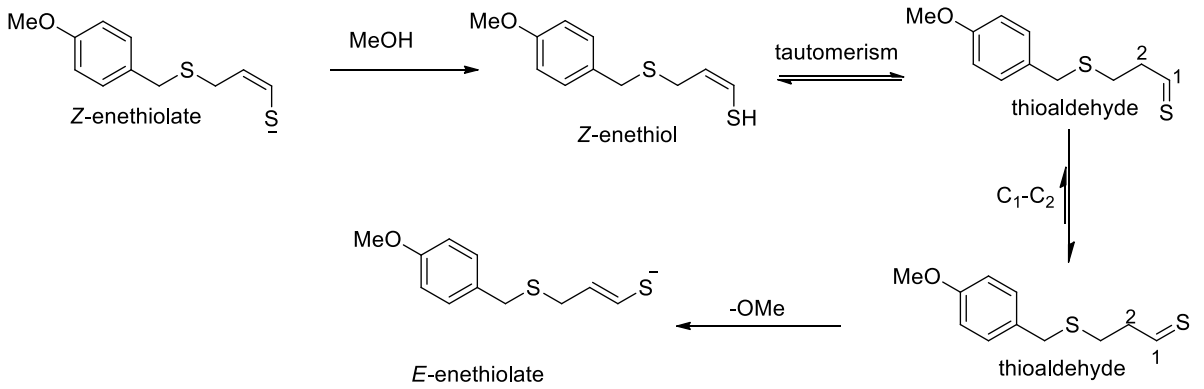

Scheme 25: Mechanistic explanation for inversion of enethiolate stereochemistry

16 was fully characterised using HRMS, IR, HSQC, ^{1}H and ^{13}C NMR spectroscopy. Its IR spectrum showed an absorbance at 3152 cm^{-1} corresponding to an aromatic OH, while the ^{1}H and ^{13}C NMR spectra revealed the replication of peaks characteristic of a mixture of isomers.

The ^{13}C NMR spectrum revealed the C-4 downfield at 128.4 ppm (*E*-isomer) and 132.4 ppm (*Z*-isomer), C-3 at 128.2 ppm (*E*-isomer) and 128.3 ppm (*Z*-isomer). All 8 aromatic carbon peaks were observed in the aromatic region and all protons were correlated to their carbons using HSQC. Finally,

the synthesis of **16** was confirmed using HRMS, in which the major molecular ion was found at 379.0849 $[M+H]^+$ $C_{19}H_{23}O_2S_3$ requires 379.0860.

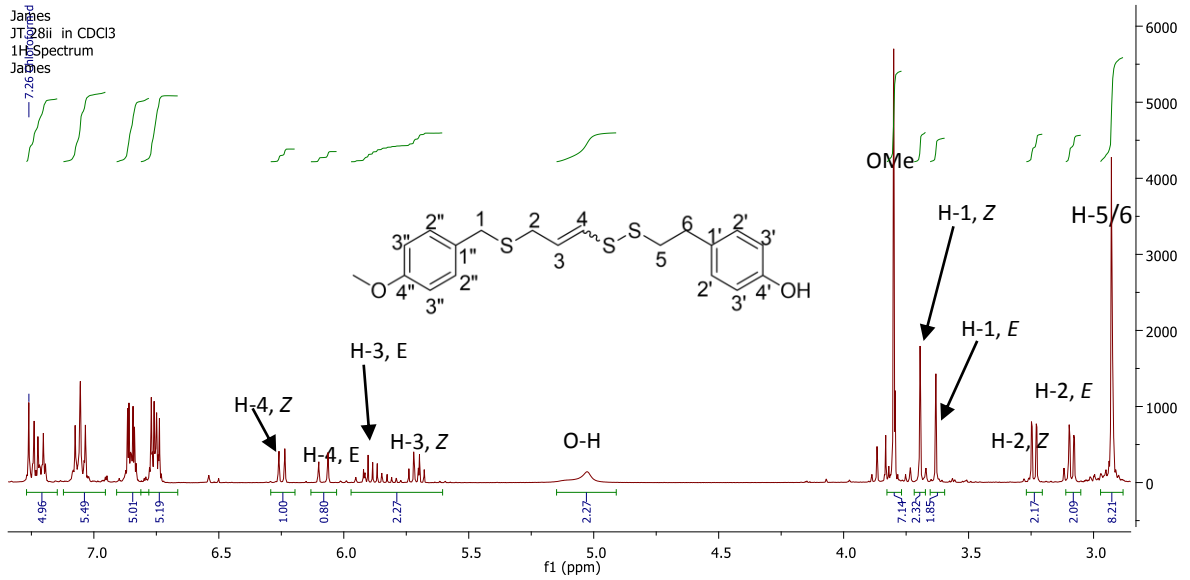

Figure 28: The ^{1}H NMR spectrum of **16**

3.3.2.4 Ajoene-analogue, 7a

The penultimate step in the synthesis of ajoene analogue **7a** was the chemoselective oxidation of the coupled product **16**, which was achieved as before using *m*-CPBA in DCM at -78 °C The reaction mixture was stirred for 5 h, at which point there was complete disappearance of the sulfide spot and appearance of a new polar spot on TLC. The reaction was quenched with 1 M $NaHCO_3$, and following an extractive work-up the residue was purified using column chromatography to give **7a** as a light-brown oil in a yield of 68 % and as a 1: 1 mixture of *E*: *Z* isomers. The oxidizing agent showed selectivity to the sulfide over the disulfide, due to the greater nucleophilicity of the sulfide as revealed by ^{1}H NMR data, which showed a significant downfield shift for the H-1 and H-2 hydrogens, and crucially that H-2 resonated as two diastereotopic hydrogens with geminal coupling (a ddd due to geminal, vicinal and allylic coupling, Figures 29 and 30).

Similarly, the ^{13}C NMR spectrum revealed all the expected 32 carbon peaks (16 for each isomer). The sulfoxide had a significant deshielding effect on C-1, which was observed at 56.4 and 57.0 ppm for the *Z*- and *E*-isomers respectively compared to 35.6 and 34.8 ppm in *Z*-**16** and *E*-**16** respectively. C-2 was also found to be significantly deshielded at 53.0 and 49.6 ppm from 29.5 and 32.9 ppm in **16** for the *Z*- and *E*-isomers respectively. Interestingly, the peculiar sulfoxide β-carbon position shielding effect noted in section 3.2.4 was also observed for compound **7a** **(**C-3 and C-1”). All proton assignments were correlated to their carbon assignments using HSQC. Finally the synthesis of **7a** was

confirmed using High-Resolution Mass Spectrometry, in which the major molecular ion was found at 393.0646 $[M-H]^+$; $C_{19}H_{21}O_3S_3$ requires 393.0653.

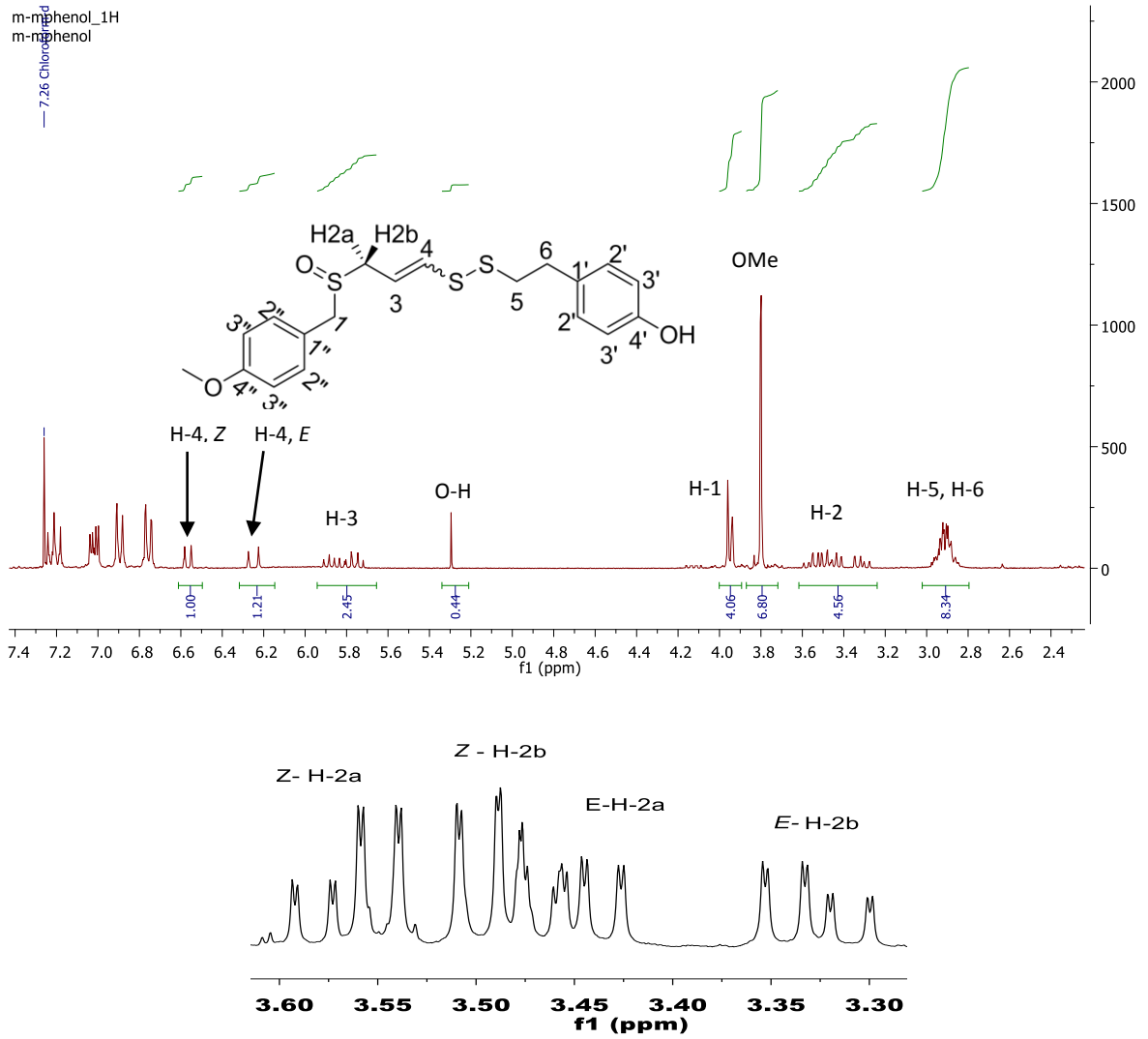

Figure 29: ^{1}H NMR spectrum of **7a** and an expansion showing the H-2 splitting pattern. Note assignment of H-2a/b was arbitrarily done.

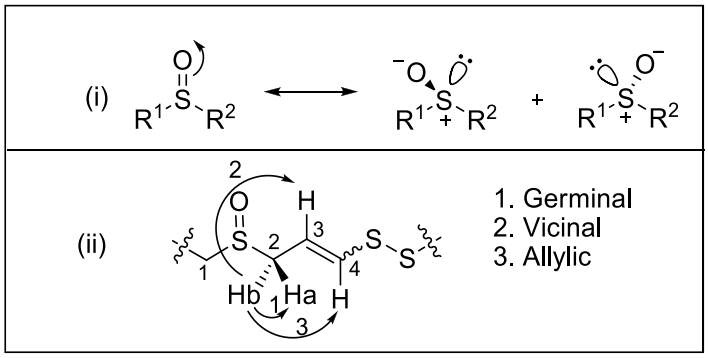

Figure 30: (i) Inherent chirality of the sulfoxide, (ii) H-2 coupling pattern

With the ajoene-analogue **7a** in hand the next part in the synthesis was focused on obtaining the linker. For this preliminary study it was decided to use a four-chain alkyl linker, **18**, containing an electrophilic chloroacetate functionality at one end and a protected nucleophilic hydroxyl group at the other (Figure 31).

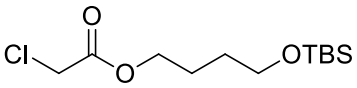

18

Figure 31: Structure of the linker, **18**

3.3.3 Synthesis of 18

3.3.3.1 Mono-protected diol, 17

The synthesis of the linker **18** commenced with mono-protection of 1,4-butanediol with a TBS silyl ether, which was achieved using the original Corey conditions of TBSCl (formerly known as TBDMSCl) in DMF using imidazole as base to form alcohol **17**. The alcohol had to be protected to avoid chemoselectivity issues in the connection chemistry, and the choice of protection group was influenced by the fact that the subsequent steps involve base-assisted alkylation, but importantly the deprotection had to be achieved using mild acidic conditions under which the ajoene-analogue had been determined to be stable. The TBS group was a suitable candidate for this purpose because of its reasonable stability under basic conditions and susceptibility to deprotection under mildly acidic conditions.[51] The product **17** was isolated as a colourless liquid in 69 % yield and was characterised using IR, HSQC, ^{1}H and ^{13}C NMR spectroscopy.

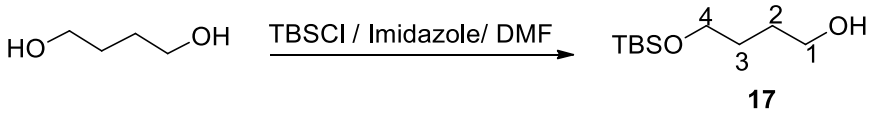

17

Scheme 26: Synthesis of mono-protected diol, **17**

Its IR spectrum revealed the expected OH stretch at 3400 cm^{-1}, while the ^{1}H NMR spectrum revealed the $Si(CH_3)$ at 0.00 ppm and the tertiary butyl methyl protons at 0.84 ppm. A diagnostic OH signal was observed at 3.06 ppm, while the H-3 and H-2 signals were observed upfield at 1.57 ppm and the H-1 and H-4 further downfield at 3.58 ppm. The ^{13}C NMR spectrum revealed a deshielded $SiCH_3$ at -5.20 ppm, the quaternary $SiCMe_3$ at 18.3 ppm, while the *t*-butyl methyl carbons were observed at 26.0 ppm. The methylene C-3 and C-2 carbons were observed at 29.8 and 30.0 ppm respectively, while C-4 and C-1 were further downfield at 62.6 and 63.3 ppm.

3.3.3.2 4-((*tert*-Butyldimethylsilyl)oxy)butyl 2-chloroethanoate, 18

For the alkylation step to incorporate the electrophilic functionality of the linker, **17** was subjected to a standard S_NAc reaction with chloroacetyl chloride with triethylamine as base to neutralise the HCl produced. In such a way **18** was isolated as a colourless oil in a good yield of 72 %, Scheme 27

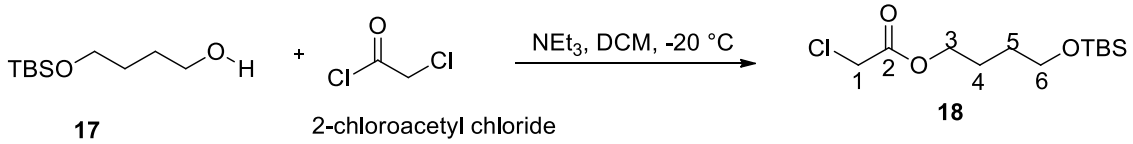

17 2-chloroacetyl chloride **18**

Scheme 27: Synthesis of the linker compound, **18**

18 was characterised using IR, HSQC, ^{1}H and ^{13}C NMR spectroscopy, with the key diagnostic signals being a carbonyl absorbance at 1755 cm^{-1}, the disappearance of the hydroxyl peak in the ^{1}H NMR spectrum, and a new singlet for the methylene H-1 hydrogens reasonably downfield at 4.04 ppm. Similarly, the ^{13}C NMR spectrum revealed the carbonyl resonance at 167.5 ppm and a new relatively deshielded methylene peak at 41.0 ppm corresponding to C-1.

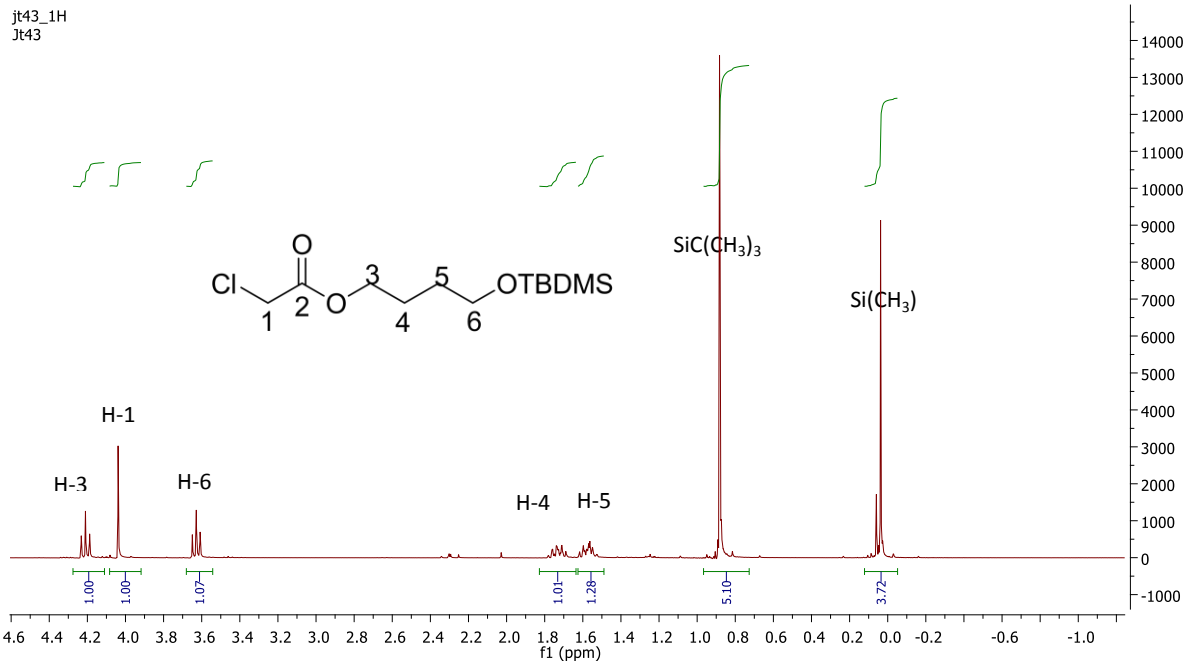

Figure 32: The ^{1}H NMR spectrum of **18**

3.3.3.2 Alkylation of ajoene-analogue 7a

With the ajoene **7a** and the electrophilic linker **18** in hand attention was turned to the alkylation step to join them together (Scheme 28). Several efforts to achieve this transformation did not give the desired product. Alkylation using K_2CO_3 in acetonitrile only proceeded at temperatures above 40 °C, but the subsequent work-up and purification did not deliver the desired alkylated-ajoene **19**. The ^{1}H NMR spectrum of the isolated product showed evidence of alkylation of sulfide **7a**, but it was not clear where the alkylation had occurred, as the aromatic ring containing the hydroxyl group was missing. It was postulated that the unexpected result may be due to the participation of the sulfoxide, as there had been a similar issue in alkylation of phenol-sulfoxide **8a**. With this in mind it was decided to alkylate the ajoene precursor **16** instead Scheme 29**.**

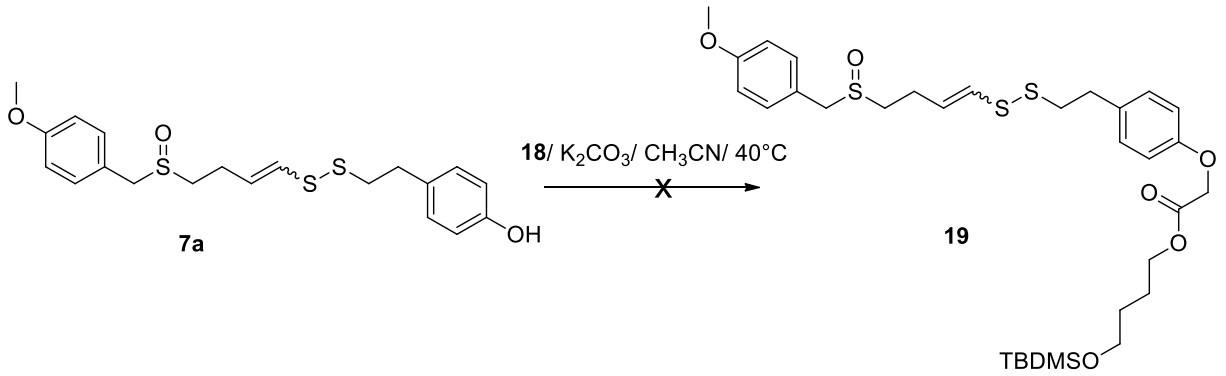

Scheme 28: Alkylation of Ajoene-analogue **7a**

3.3.3.2 Trisulfide-linker conjugate, 20

Alkylation of sulfide **16** was achieved using the same conditions used in the attempted alkylation of **7a** using chloroacetate, **18** (2.0 equiv), with K_2CO_3 (2.0 equiv) in dry acetonitrile at 40 °C for 72 h, which gave the desired alkylated product **20** as a yellow oil and as a 7: 5 mixture of *E*-: *Z*-isomers in 45 % yield. The poor yield was attributed to the formation of multiple by-products that were observed on TLC.

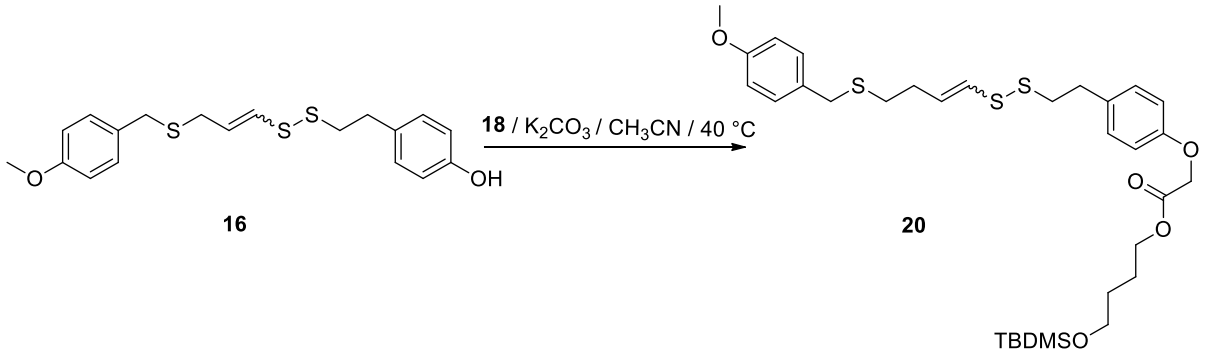

Scheme 30: Synthesis of advanced intermediate **20**

20 was characterised using IR, HSQC, ^{1}H and ^{13}C NMR spectroscopy. Signals for each reactant could be observed with correct integration in the product. Notably, the silyl grouping compared favourably against the aromatic and vinyl integrations. Otherwise, the expected signals were observed as in the precursors. The ^{13}C NMR spectrum revealed all of the expected 46 peaks (23 for each isomer), while a carbonyl resonance was observed at 170.0 ppm for the ester (C-6'), The ^{1}H NMR spectrum with assignments is shown in Figure 33.

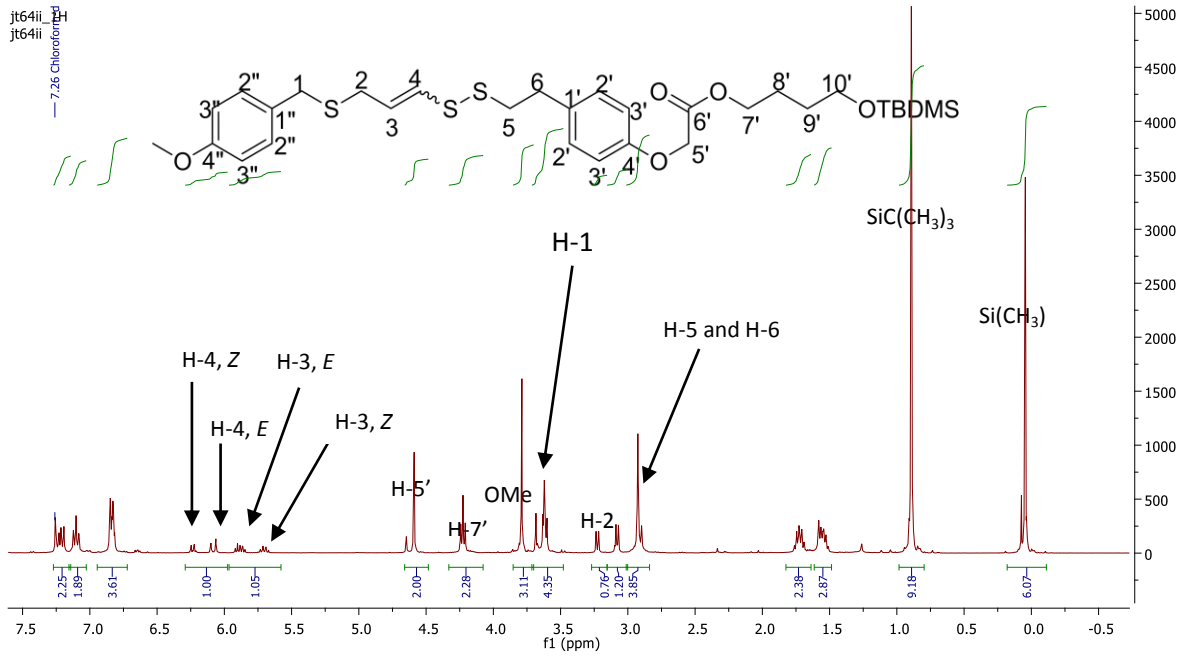

Figure 33: ^{1}H NMR spectrum of trisulfide-linker conjugate **20**

The full synthesis to the ajoene-fludarabine conjugate was not achieved due to time constraints. Small-scale preliminary studies seemed to show that the sulfide **20** could be chemoselectively oxidised to the sulfoxide **19** using *m*-CPBA (this was based on monitoring TLC reaction progress, where a similar reaction profile was observed to that for the oxidation to **7a**, (page 67), while silyl deprotection studies on **19** and **20** with catalytic amounts of acetyl chloride in methanol showed that it was much more convenient to work with the sulfide **20**, as the sulfoxide **19** (used without purification from reaction above) gave unstable by-products upon deprotection.

Regarding preparation of the commercially available (and very polar) fludarabine phosphate group for coupling, literature reports had suggested that a sequence of hydroxyl protection on fludarabine followed by activation of the hydroxyl groups of the phosphoric acid moiety using 2,4,6-TIPSCl (triisopropylphenylsulfonyl chloride), both steps carried out *in situ*, would furnish a derivative appropriate for coupling with the ajoene-alcohol (from deprotection).[48a]

As part of a preliminary model study on this, protection of the fludarabine hydroxyl groups of fludarabine phosphate with TBSCl (2.5 equiv) and imidazole was attempted, Scheme 31.

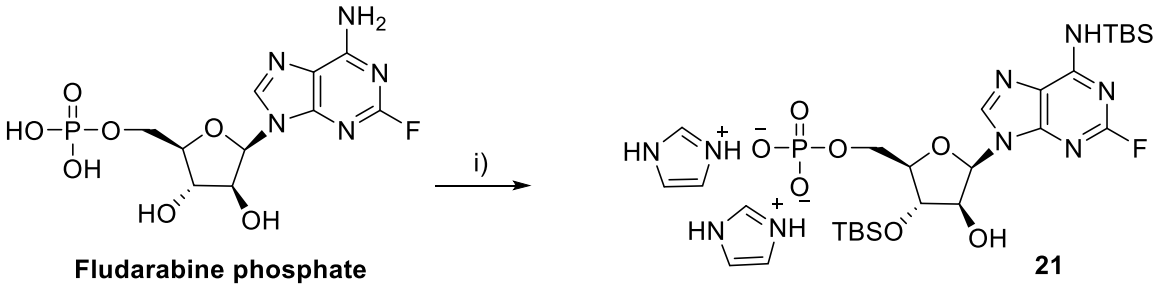

Fludarabine phosphate

i) TBSCl (2.5 eq), imidazole (2.5 eq), DMF

Scheme 31: TBS protection of fludarabine

Following a difficult chromatographic isolation using a very polar mobile phase of 4:20:76 (NEt_3: MeOH: DCM) product **21** was obtained. Its ^{1}H NMR spectrum is shown in Figure 34 together with assignments. Although there are impurities in the spectrum, the structure as shown in Figure 34 for **21** was assigned. When excess TBSCl was used the protection of both 2' and 3' hydroxyl groups was not observed, and this is most likely due to the steric strain that would result in such a case. Chhikara *et al* reported that silylation of cytarabine with TBSCl occurs more readily on the 3' hydroxyl group in.[48b] Thus it is suspected that this might be the case in fludarabine with silylation occurring on the less hindered face of the arabinose sugar as depicted in Scheme 31. Owing to time constraints this is where the project stopped.

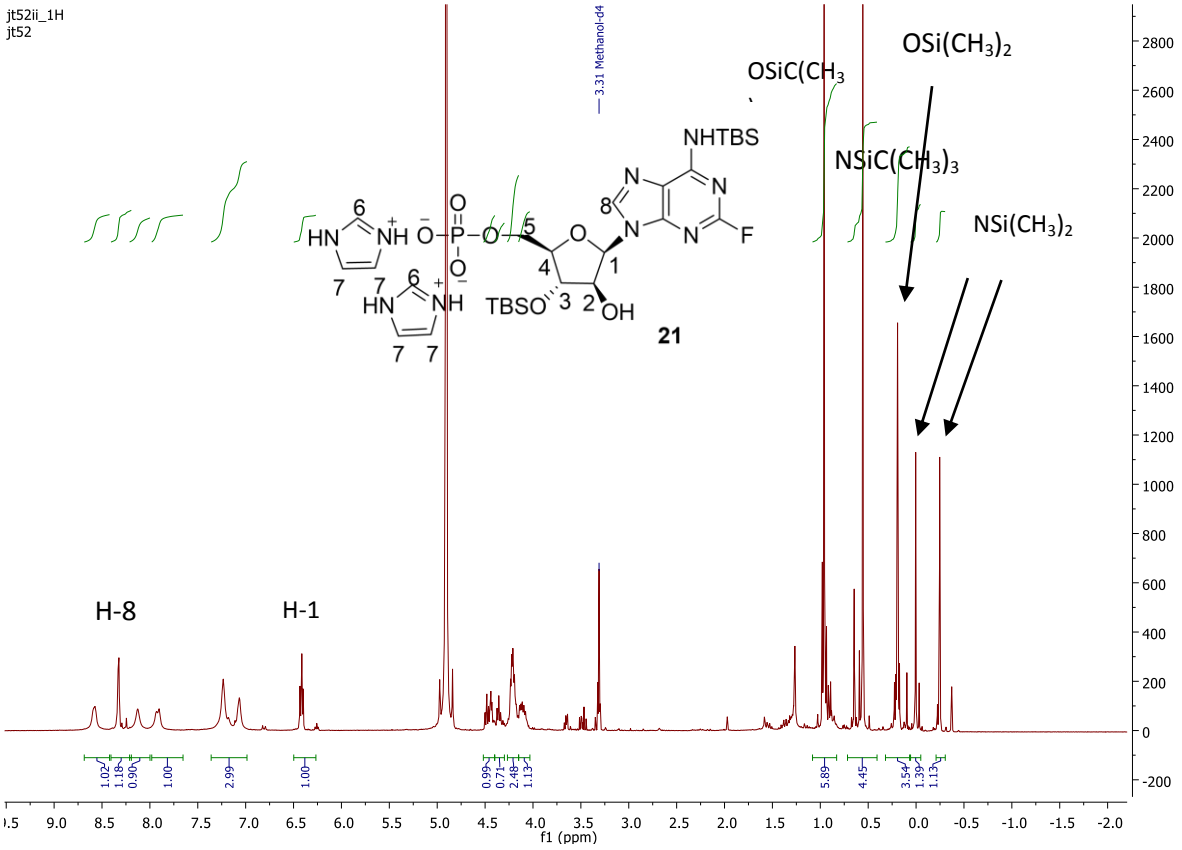

Figure 34: ^{1}H NMR of **21**

3.4 Conclusions on the Synthesis Studies

Analogues of ajoene lacking the double bond (dihydroajoene series) were successfully synthesized for the purposes of a Structure-Activity Relationship (SAR) study, in which analogues **8a**, and **13a-d** were evaluated for their biological activity against the oesophageal cancer cell line WHCO1. The Ester-Sulfoxide, **8c**, was not evaluated as it was deemed not to be of the required purity (>95 %) by LCMS. It was also displeasing that the two analogues **8b** and **8d** could not be obtained in good enough purity for the SAR study.

A preliminary study towards an ajoene-fludarabine conjugate was explored. An advanced intermediate **20** was successfully synthesized, as well as preliminary studies carried out on preparation of the fludarabine partner for coupling, but owing to time constraints the full synthesis of an ajoene-fludarabine conjugate was not achieved

The next Chapter discusses the biological evaluation of the synthesized dihydroajoene analogues.

Chapter 4: Biological Evaluation of Ajoene Analogues

4.1 Introduction

In previous work, several ajoene analogues were evaluated in an SAR study and a lead compound **6a**, was identified.[45] **6a** was found to exhibit the strongest activity against WHCO1 cell proliferation with an IC_{50} of 2.1 μM.[45] In a subsequent study several analogues (**7a-d**) were synthesized to improve the aqueous solubility of **6a** and these analogues were found to retain good activity against the same cancer cell-line, see Figure 34 below for structures.[47] Here, several aqueous enhancing groups were incorporated on the phenol end of the molecule to be amide, acetate and ester functional groups (Fig 34) that increased water solubility via hydrogen-bonding. Indeed the aqueous solubilities of **7a-d** were all improved compared to that of the lead **6a** as shown in a turbidmetric study.[47]

In two *in vivo* experiments the compounds **6a** and **7d** were found to be ineffective at reducing tumour cell growth.[45, 47] The failure of the lead **6a** was possibly attributed to its insolubility in the delivery intralipid vehicle. In the case of **7d** however, the analogue was much more soluble in the intralipid vehicle, hence it was felt that its failure could not be attributed to solubility issues alone. Thus a second consideration was that the compounds were likely to be metabolically unstable which may prevent their delivery to the tumour site.[47]

The metabolic stability of **6a** was therefore evaluated *in vitro* in mouse blood where a degree of stability was noted in plasma but **6a** was found to be unstable in both the whole blood and red blood cell fractions as demonstrated by an HPLC blood aliquot monitoring experiment (see Figure 11).[47] This result suggested that the compound was interacting with red blood cells causing rapid degradation of the compound. We went on to speculate that this instability may be structurally related to the presence of the vinyl disulfide functionality.

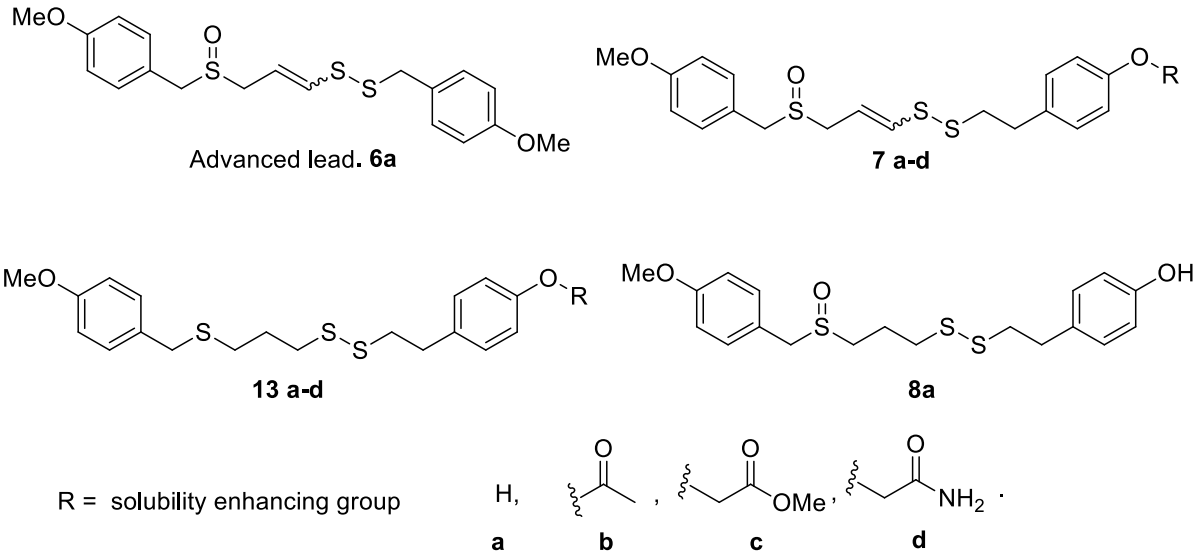

Fig 34: Structures of the lead compound **6a**, ajoenes **7a-d** and the dihydroajoenes **13a-d** and **8a**.

To test this hypothesis, a new set of compounds (dihydroajoenes) mirroring the analogues **7a-d** but lacking the vinyl disulfide were designed to possibly circumvent the metabolic stability issues of **6a**. Owing to synthetic challenges the whole library of analogues mirroring **7a-d** were not obtained. The dihydroajoene analogues synthesized have been discussed previously in Chapter 3 and shown here in Figure 34.

Thus, the biological evaluation set about to establish if *in vitro* WHCO1 anti-proliferation activity could be retained in analogues **8a**, **13a-d** lacking the vinylic-disulfide bond, and finally whether these analogues were stable in blood.

4.2 Determination of the IC_{50} of Ajoene Analogues

4.2.1 Measurement of Anti-Cancer Activity

The ajoene analogues synthesized were tested for their ability to inhibit cell proliferation of WHCO1 cancer cells using an MTT assay. The oesophageal cancer cell-line WHCO1 was derived from a biopsy of a primary oesophageal squamous cell carcinoma of South-African origin.[45] The MTT assay is based on the ability of metabolically active cells to cleave [3-(4,5-dimethylthiazol-2-yl)-2,5-diphenyltetazolium bromide] salt (MTT) to formazan crystals (Figure 35).

Living cells have active mitochondrial reductase which can metabolise MTT to formazan (Figure 35) which does not occur in metabolically inactive cells. The assay relies on colorimetric evaluation to assess cell viability. The tetrazolium salt (MTT) is yellow coloured and water soluble whilst formazan crystals are purple coloured and insoluble in aqueous media. The resulting crystals are solubilised in

solubilizing reagent and quantitated colorimetrically using a scanning multiwall spectrophotometer, with the absorbance measured at 595 nm. The amount of formazan formed is proportional to the number of viable cells.

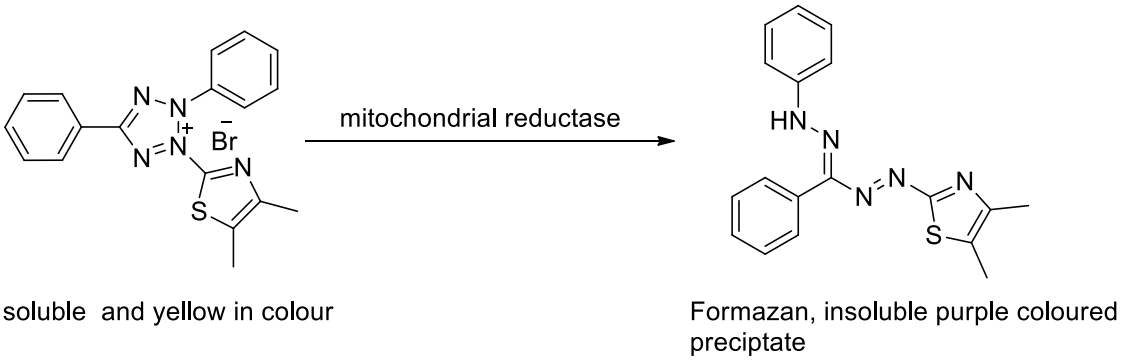

Figure 35: Conversion of MTT by the mitochondrial reductase

The absorbance results from the assay were analysed using Graphpad prism 6 software, using the sigmoidal dose-response (variable slope) to fit the curve and determine the IC_{50} value. The IC_{50} is defined as the concentration of compound required to inhibit 50 % of cell proliferation.

4.2.2 MTT Assay

WHCO1 cells were plated in 96-well plates and allowed to recover and settle overnight. The following day they were treated with drug dissolved in DMSO and diluted in media such that the final concentrations were 0-150 µM drug and 0.1 % DMSO. The duration of drug treatment was 48 h and at that point MTT solution was added. After 4 h incubation with the MTT reagent, solubilisation reagent was added to each well and the cells were incubated overnight. The following day, the absorbance was measured at 595 nm. The spectrophotometric data was analysed using Graphpad prism 6, fitted to a sigmoidal dose-response curve with a non-variable slope from which the IC_{50} was determined. Figure 36 shows representative sigmoidal dose-response graphs for each of the compounds. Each compound IC_{50} is calculated as the mean of at least three independent determinations (± standard deviation), the results are summarised, together with some previous results, in Table 7 below.

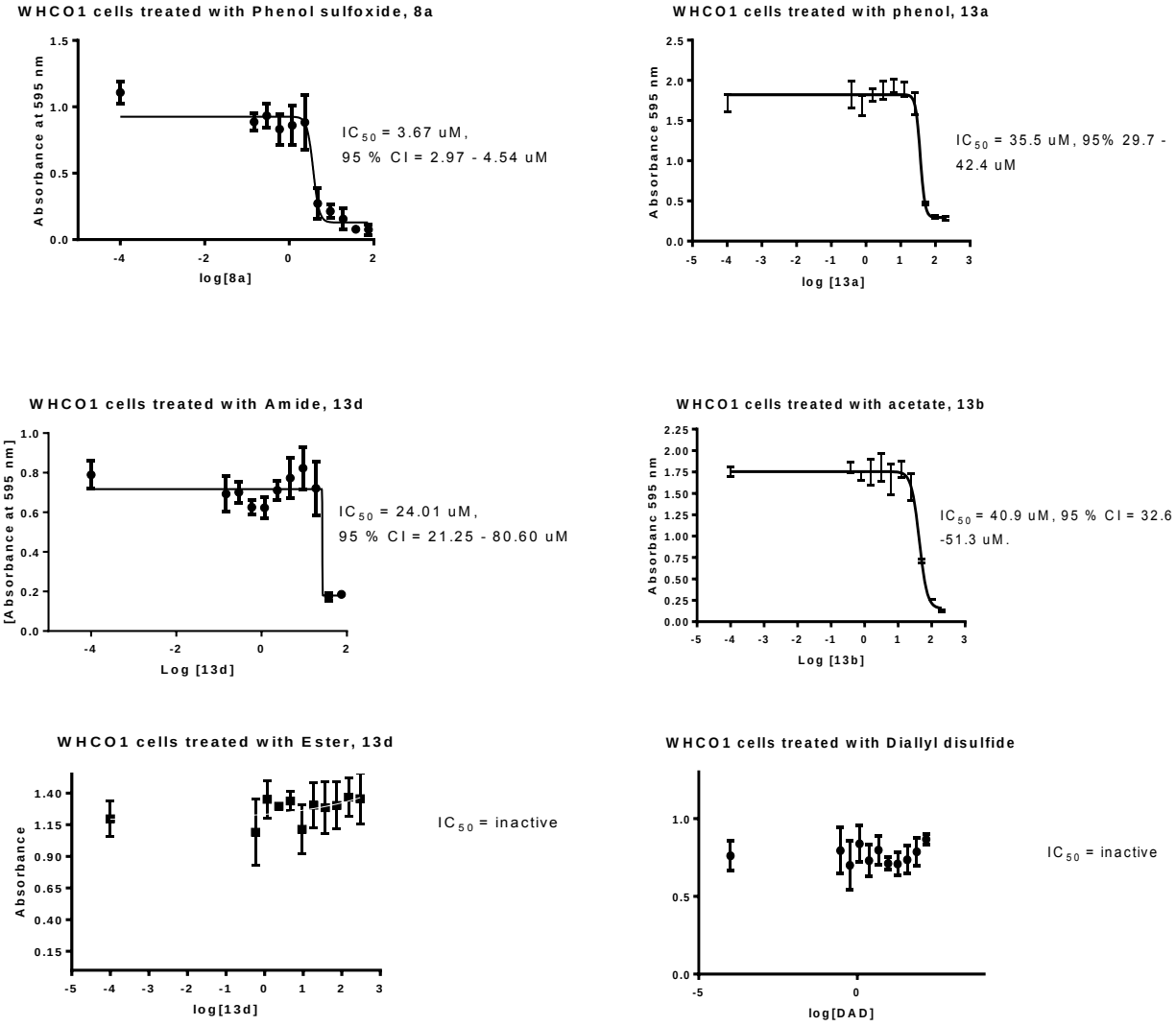

Figure 36: Representative sigmoidal dose-dependent curves of absorbance at 595 nm vs concentration for the determination of IC_{50}s.

4.2.3 MTT Assay Results and SAR Analysis

All dihydroajoene analogues synthesized with the exception of the ester analogue **13c**, were found to be active *in vitro* with an anti-proliferative IC_{50} in the range 1-40 µM as shown in Table 7. The phenol-sulfoxide **8a** was found to be the most active with an IC_{50} of 4.1 µM, which is comparable to that of the advanced lead compound **6a** of 2.1 µM against the same cell-line. The dihydroajoenes in which both the vinyl disulfide and sulfoxide were removed, namely phenol, **13a** (39 µM), acetate **13b** (39 µM) and amide **13d** (29 µM), all displayed roughly 10-fold reduced activity compared to the analogous derivatives containing a sulfoxide and double bond **7a** (1.9 µM), **7b** (3.6 µM), **7c** (1.7 µM) and **7d** (7.7 µM**)** which were synthesized and evaluated in a prior study. It is not clear why the

dihydroajoene ester **13c** is inactive but there is likely to be another, as yet to be identified, factor involved for this compound.

Table 7: A comprehensive table of anti-proliferative IC50's (WHCO1 cells) for previously synthesized ajoene analogues together with the analogues synthesized in the current study.

Dihydroajoene-analogues	IC_{50} ± SD	Ajoene analogues	IC_{50} ± SD
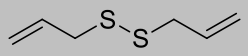 **diallyl disulfide**	> 200	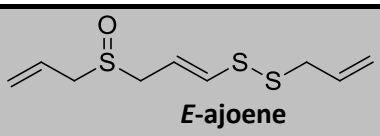 ***E*-ajoene** 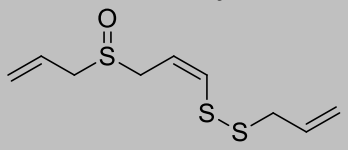 ***Z*-ajoene**	39 ± 7.8[45] 25 ± 2.8[45]
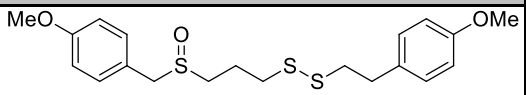 **6e**	16 ± 3.7 [47]	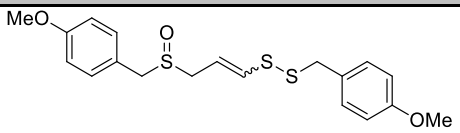 **6a**	2.1 ± 0.4[45]
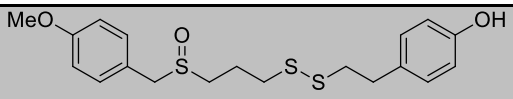 **8a** 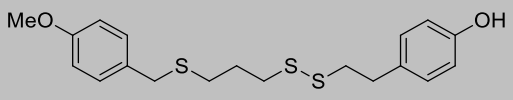 **13a**	4.1 ± 0.6 39 ± 13	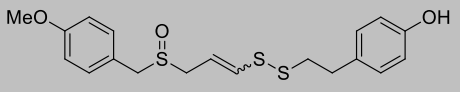 **7a**	1.9 ± 0.8[47]
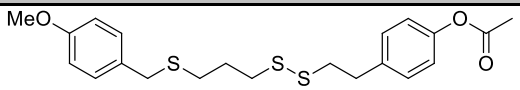 **13b**	39 ± 12	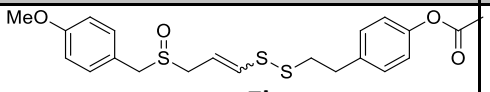 **7b**	3.6 ± 0.04[47]
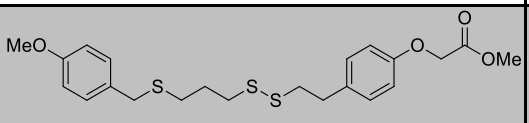 **13c**	> 200	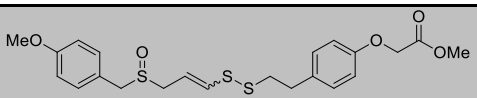 **7c**	1.7 ± 0.9 [47]
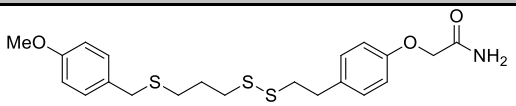 **13d**	29 ± 16	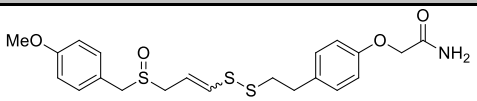 **7d**	7.7 ± 1.7[47]

Interestingly, diallyl disulfide was found to be inactive against WHCO1 cancer cell proliferation when tested up to 200 µM implying that the presence of the disulfide functional group alone is not sufficient for strong activity.

Previously an 8-fold reduction in activity was found when the vinyl group of compound **6a** was removed in **6e**. For the phenol series (**7a**, **8a** and **13a)** removal of the vinyl group in **7a** still resulted in decreased activity however to a lesser extent (only 2-fold) compared to **6a**, with the resulting derivative **8a** still exhibiting good activity of 4 μM.

Certain conclusions on the SAR can be drawn:

- Most importantly, activity can be retained in the absence of the vinyl group as all dihydroajoene compounds, except for the ester **13c**, were found to exhibit good anti-proliferation activity.
- Removal of the vinyl group results in a reduced activity: a 2-fold reduction of activity in the phenol series **7a** to **8a**; and an 8-fold in the bis-paramethoxy series **6a** to **6e**.
- When the vinyl group is removed, the sulfoxide is necessary for retention of good activity. When the both the double bond and sulfoxide were removed from **7a** to analogue **13a** the activity dropped about 20-fold, while removal of only the vinyl group as in **8a** retains good activity.

The previous SAR study already established that the disulfide bond is the pharmacophore and that the vinylic bond serves to activate the pharmacophore.[45] The results presented show that the relative activity of the ajoene analogues is dependent on the electrophilicity of the disulfide bond. With the vinyl bond and sulfoxide amplifying this electrophilicity via a resonance and an inductive electron withdrawing effect respectively (Scheme 32). This observation suggests that the mode of action of these compounds is via a disulfide exchange mechanism, in which a mixed disulfide is formed between ajoene analogues and an accessible thiol on a cysteine residue. This is in support of work reported by Krauth-Siegel *et al* who showed that ajoene forms a mixed disulfide with Cys-58 of glutathione reductase.[40]

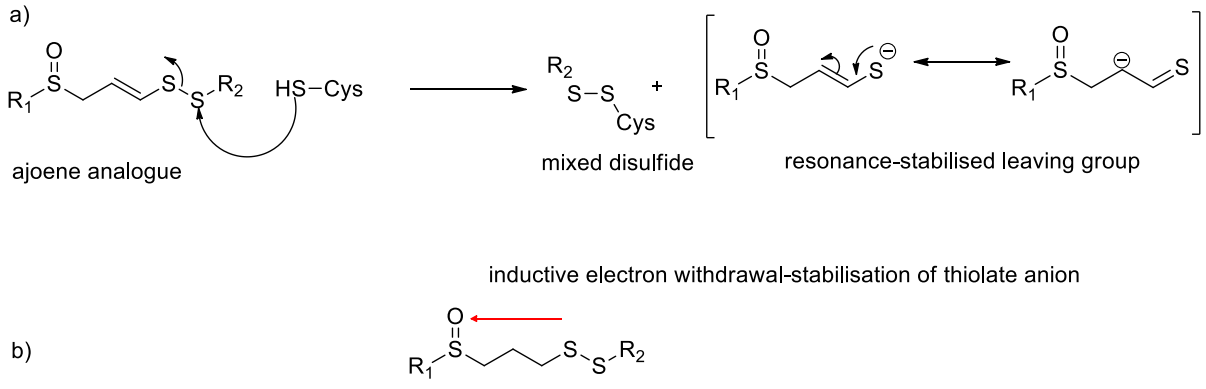

Scheme 32: Induced electrophilicity on the disulfide bond through a) resonance stabilisation of the leaving group and b) the inductive electron-withdrawing effect of the sulfoxide.

Having ascertained that analogues lacking the vinyl group and with increased water solubility retained anti-proliferative activity, the focus was turned to the metabolic stability of these analogues in mouse blood.

4.5 Blood Stability Study

A preclinical matrix stability study on ajoene analogues was performed on our behalf, at the Division of Pharmacology at the University of Cape Town. Analogues were evaluated for their *in vitro* stability in both mouse plasma and in the red blood cell fraction of mouse blood. Only the following compounds were evaluated in this study: **6a**, **7a-7d** and **13b-13d**.

Stock solutions of the compounds were prepared in DMSO at a concentration of 20 mg/mL. The stock solutions were diluted 10-fold to 2 mg/mL and then a further 10-fold to yield 200 µg/mL solutions. Blood was collected from 10 mice and stored at room temperature in K_2EDTA coated tubes. Two matrixes were prepared namely plasma and red blood cell matrixes. The experiment commenced with each matrix being spiked with analogue compound to give a final concentration of 20 µg/mL and then incubated at 37 ° C. Aliquots of 10 µL were removed at the following times: 0 (baseline), 20, 60 and 120 minutes and analysed by High Performance Liquid Chromatography coupled to Mass Spectroscopy to detect and quantify the parent molecular ion. The results are shown in the charts below, where analyte peaks were calculated as a percentage of the baseline value measured at 0 minutes.

The compounds (**6a, 7a-d and 13b-d**) were found to have vastly different stabilities in the plasma matrix, with the dihydro derivatives considerably more stable compared to their ajoene counterparts, apart from bis-pmb **6a.** In the dihydroajoene series the ester **13c** was the least stable of the three derivatives tested (Figure 35), although as this derivative was inactive *in vitro* it was of no consequence that it was found to be relatively unstable in the plasma fraction. However, it was extremely pleasing that the two dihydro analogues **13b** and **13d** (active *in vitro*) were relatively stable in plasma.

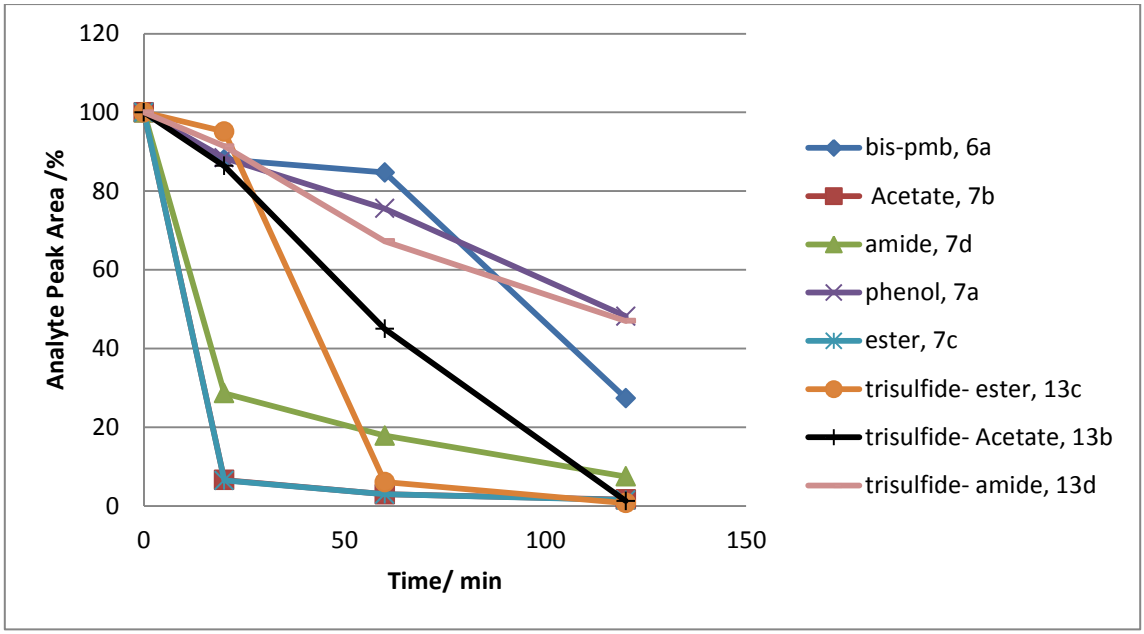

Figure 35 Stability of ajoene analogues in blood plasma.

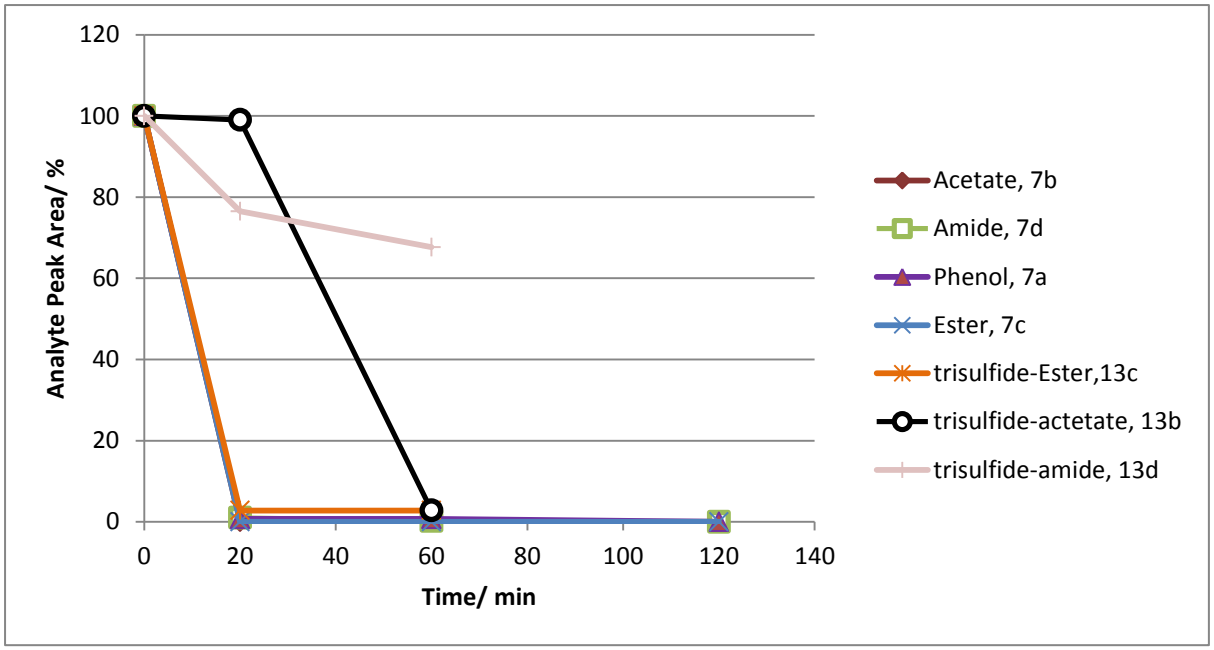

Figure 36: Stability of ajoene analogues in red blood cells

With the stability of the compounds in plasma setting the scene, it was informative to note that their stability in red blood followed a similar trend, with the dihydro compounds much more stable than the ajoene derivatives. As with the plasma results ester **13c** proved to be the least stable. Overall, amide **13d** emerged as having the best characteristics in both systems. The results support the hypothesis that the double bond of the vinyl disulfide gives rise to instability of ajoene analogues in

blood. The relative stability, in RBCs, of the dihydroajoene series compounds **13b** and **13d** was pleasing as this was an improvement on the stability of the lead compound **6a**. In light of this improved metabolic stability of **13b** and **13d,** it may be interesting to test whether these compounds are stable enough to reach the tumour site and deliver their apoptosis-inducing potential in an *in vivo* experiment.

4.6 Conclusion

Most of the analogues synthesized in this project (dihydroajoene series) had comparable or superior activity to that of the parent compound ajoene at inhibiting proliferation of WHCO1 cancer cells. The phenol-sulfoxide **8a** was the most promising analogue with an IC_{50} of 4.1 μM, which was only 2-fold less active than the lead bis-pmb, **6a**.

Dihydroajoene analogues **13b** and **13d** were significantly much more stable in the red blood cell fraction of blood than the vinyl disulfide analogues **7a-7d**. This result agrees with our initial hypothesis that the double bond of the vinyl disulfide may be the source of instability of ajoene analogues in blood. Though compound **8a** was not evaluated for metabolic stability, it is predicted that this compound would be much more stable than lead **6a** in RBCs owing to the absence of the vinyl disulfide. The sulfoxide and phenolic OH group should also enhance **8a**'s water solubility. Coupled with its good activity the results make **8a** a suitable candidate for an *in vivo* animal evaluation.

This study aimed to address two questions:

Is the double bond essential for activity? and
Does its removal aid in increasing metabolic stability
In conclusion, this study has found that: 1) the double bond is not essential for retention of activity and 2) that its removal is associated with a significant increase in metabolic stability.

Chapter 5: Conclusion

In conclusion, new analogues of ajoene were synthesized. The developed synthetic route is divergent and spans over 7 steps with the focus on obtaining a phenol derivative, on which various water enhancing groups can be installed. The analogues retained good anti-proliferation activity against WHCO1 cancer cell line, with the phenol-sulfoxide **8a** derivative being the most active. From an SAR study it was established that the vinyl double bond is not essential for retention of activity but the sulfoxide was important for enhancing the activity in the absence of the vinyl bond. It was exciting to note that the dihydroajoene analogues acetate, **13b**, and amide, **13d**, were much more stable in blood than ajoene analogues containing a double bond. Overall, the results give hope that a successful *in vivo* ajoene analogue candidate will be found.

A preliminary study towards the synthesis of an ajoene-fludarabine conjugate was initiated and an advanced intermediate of ajoene coupled to a linker, **20**, was obtained. Preliminary preparation of a fludarabine coupling counterpart was also explored (not reported). With further work it is possible that the ajoene-fludarabine conjugate can be achieved using this preliminary study.

Chapter 6: Experimental

6.1 General:

All reaction solvents were freshly distilled under a nitrogen atmosphere. DCM was distilled over phosphorus pentoxide, acetonitrile was distilled over calcium hydride and THF was distilled over sodium wire and benzophenone. Anhydrous methanol was degassed using nitrogen gas. Reagents were obtained from commercial sources (Sigma–Aldrich, Fluka, Merck).

All reaction flasks were dried in the oven (50 °C) and all reactions were carried out using magnetic stirrers. Unless otherwise stated all reactions were carried under a nitrogen atmosphere. Low-temperature reactions were carried out using acetone in liquid nitrogen (-94 °C), ice and NaCl (-20 °C), ice and calcium chloride (- 10 °C) or an ice bath (0 °C).

Thin layer chromatography (TLC) was used to monitor reactions using aluminium-backed Merck silica-gel 60 F_{254} plates. Compounds on TLC plates were observed using ultraviolet light and stained with either: 2.5 % solution of anisaldehyde in a mixture of sulphuric acid and ethanol (1:10 v/v) or iodine vapour and then heated. Column chromatography was carried out using silica-gel 60 mesh (Merck).

Nuclear Magnetic Resonance (NMR) spectra were recorded on either a Bruker XR400 MHz spectrometer (at 399.95 MHz for H^1, 100.58 MHz for ^{13}C), or a Varian Mercury XR400 MHz spectrometer (at 399.95 MHz for H^1 and at 100.58 MHz for ^{13}C), or a Varian Mercury XR300 MHz spectrometer (at 300.08 MHz for H^1 and at 75.46 MHz for ^{13}C). Chemical shifts are reported in ppm and *J* values are reported in Hz, with internal references for $CHCl_3$ in the $CDCl_3$ taken as 7.26 ppm for ^1H and 77.16 ppm for ^{13}C NMR spectra. High Resolution Mass spectrometry was performed on a Water API Q-TOF Ultima machine at The University of Stellenbosch Central Analytical Facilities. Infrared spectra were obtained on a Perkin-Elmer Paragon 1000 FT-IR spectrometer. Melting point measurements were taken on a Reichert-Jung Thermovar hot-stage microscope and are uncorrected.

6.2 Synthesis Experimental

4-(2-Hydroxyethyl)phenol (1)[49]

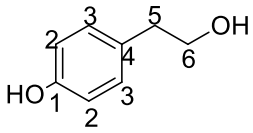

Methyl 4-hydroxyyphenylacetate (3.00 g, 18.05 mmol) was added slowly to a stirring suspension of $LiAlH_4$ (1.39 g, 36.0 mmol) in THF (60 mL) at -78 °C. The reaction proceeded under N_2 for 2 h at which point the reaction mixture was quenched with 1 M HCl (to pH 4). The resulting suspension was filtered through Celite washing with warm EtOAc (40 mL). The aqueous layer was extracted using EtOAc (3 x 40 mL). The combined organic extracts were washed with water (3 x 20 mL), then brine (20 mL) and dried over $MgSO_4$. Solvent was removed under reduced pressure and the crude product purified by flash chromatography using petroleum ether/ EtOAc mixtures. The product (**1**) was recrystallised from ethyl acetate and hexane and isolated as a white powder (2.00 g, 82 %).

R_f = 0.2 (Hexane / EtOAc = 80 / 20); Mp: 86-88 °C, lit[39] Mp: 87-89 °C; IR ν_{max}/ cm-[1] (KBr): 3391 (ROH), 3152 (ArOH); ^{1}H NMR (400 MHz,d_6-acetone) δ 2.71 (2H, t, *J* = 7.1 Hz, H-5), 3.53 (1H, brs, OH), 3.69 (2H, t, *J* = 7.1 Hz, H-6), 6.74 (2H, d, *J* = 8.4 Hz, H-2), 7.05 (2H, d, *J* = 8.4 Hz, H-3), 8.00 (1H, brs, PhOH); ^{13}C NMR (100 MHz, d_6-acetone): δ 39.6 (C-5), 64.3 (C-6), 116.0 (C-2), 130.8 (C-3), 131.1 (C-4), 156.6 (C-1).

4-(2-Iodoethyl)phenol (2)[50]

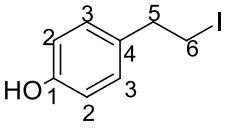

Iodine (0.548 g, 2.16 mmol), triphenylphosphine (0.566 g, 2.16 mmol) and imidazole (0.147 g, 2.16 mmol) were dissolved in THF (7 mL) at room temperature. Alcohol **1** (0.251 g, 1.82 mmol) in THF (2 mL) was added to the reaction vessel and the reaction was allowed to proceed for 3 h under N_2 at room temperature. Thereafter the reaction was quenched using a concentrated solution of Na_2SO_3 (10 mL) and the mixture stirred for 10 minutes. The aqueous layer was extracted using EtOAc (3 x 15 mL), the combined organic extracts were washed with a concentrated solution of Na_2SO_3 (15 mL), 1 M HCl (10 mL) and $NaHCO_3$ (10 mL) and dried over $MgSO_4$. The solvent was removed under reduced pressure and the residue purified by column chromatography using a mixture of EtOAc and hexane to give the product (**2**) as a white powder (0.433 g, 91 %).

R_f = 0.6 (Hexane / EtOAc = 80 / 20); Mp: 112-113 °C, lit [40] Mp: 111-112°C; IR *v*max/ cm^{-1} ($CHCl_3$): 3152 (ArOH), 500 (C-I); ^{1}H NMR (400 MHz, $CDCl_3$): δ 3.10 (2H, t, *J* = 8.0 Hz, H-5), 3.31 (2H, t, *J* = 8.0 Hz, H-6), 4.87 (1H, s, PhOH), 6.78 (2H, m, H-2), 7.06 (2H, m, H-3); ^{13}C NMR (100 MHz, $CDCl_3$) δ 6.2 (C-6), 39.5 (C-5), 115.5 (C-2), 129.5 (C-3), 133.1 (C-4), 154.4 (C-1).

_S_-4-Hydroxyphenethyl 4-methylbenzenesulfonothioate (3)

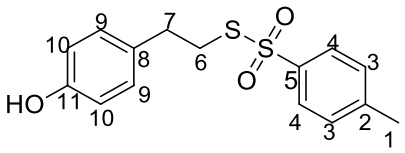

4-(2-Iodoethyl)phenol (**2**) (0.862 g, 3.48 mmol) was dissolved in anhydrous DMF (10 mL) and then potassium thiotosylate (2.36 g, 10.44 mmol) was added to the solution. The reaction mixture was stirred at room temperature under N_2 for two hours, at which point there was complete conversion of the substrate based on the appearance of a new polar spot on TLC. The reaction mixture was suspended in H_2O (10 mL) and then diluted with EtOAc (15 mL). The aqueous layer was extracted using EtOAc (3 x 15 mL), the combined organic fractions were then washed with H_2O (5 x 10 mL) and dried over $MgSO_4$. The solvent was removed under reduced pressure and the residue was purified by column chromatography using mixtures of hexane and EtOAc to yield (**3**) as a brown oil (0.976 g, 91 %).

R_f = 0.5 (Hexane / EtOAc = 80 / 20); IR v_{max}/cm^{-1} ($CHCl_3$): 3152 (ArOH), 1228 (O=S=O); HRMS (ES) *m/z*: 309.0615 [M+ H] $^+$, $C_{15}H_{17}O_3S_2$ requires 309.0619; ^{1}H NMR (400 MHz, $CDCl_3$) 2.45 (3H, s, H-1), 2.83 (2H, t, *J* = 7.6 Hz, H-6), 3.18 (2H, t, *J* = 7.6 Hz, H-7), 3.38 (1H, s, OH), 6.74 (2H, d, *J* = 8.5 Hz, H-10), 6.95 (2H, d, *J* = 8.5 Hz, H-9), 7.34 (2H, d, *J* = 8.5 Hz, H-3), 7.81 (2H, d, *J* = 8.5 Hz, H-4); ^{13}C NMR (101 MHz, $CDCl_3$) 21.8 (C-1), 34.4 (C-6), 37.6 (C-7), 115.7 (C-10), 127.2 (C-9), 129.9 (C-4), 130.0 (C-3), 131.0 (C-8), 142.3 (C-5), 144.9 (C-2), 154.7 (C-11).

3-((4-Methoxybenzyl)thio)propane-1-thiol (4)

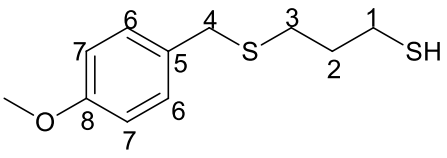

Propane-1,3-dithiol (486 mg, 4.50 mmol) was dissolved in degassed anhydrous methanol (15 mL) in a three-necked flask. Potassium hydroxide pellets (328 mg, 5.80 mmol) were added to the reaction vessel and the solution was stirred for 5 minutes under N_2 at 0 °C. PMBCl (642 mg, 4.10 mmol) was

added to the reaction vessel dropwise and the reaction was left to proceed for 2 hours at 0 °C. Thereafter, the reaction mixture was quenched with 1 M HCl (10 mL). The aqueous layer was extracted using EtOAc (3 x 30 mL) and the combined organic extracts were washed with water (3 x 30 mL) and brine (10 mL) and then dried over $MgSO_4$. The solvent was removed under reduced pressure, and the crude mixture purified by column chromatography using EtOAc and Hexane (3 : 97) to yield (**4**) as an odoriferous lime-green-coloured oil (661 mg, 71 %).

R_f = 0.85 (Hexane / EtOAc = 90 / 10) ^{1}H NMR (400 MHz, $CDCl_3$): δ 1.31 (1H, t, *J* = 8.0 Hz, S-H), 1.84 (2H, quin, *J* = 7.2 Hz, H-2) , 2.52 (2H, t, *J* = 7.2 Hz, H-3), 2.58 (2H, q, *J* = 7.6 Hz, H-1), 3.66 (2H, s, H-4), 3.80 (3H, s, OMe), 6.84 (2H, d, *J* = 8.8 Hz, H-7), 7.22 (2H, d, *J* = 8.8 Hz, H-6); ^{13}C NMR (100 MHz, $CDCl_3$): δ 23.6 (C-1), 29.7 (C-3), 33.2 (C-2), 35.8 (C-4), 55.4 (OMe), 114.0 (C-7), 130.0 (C-6), 130.4 (C-5), 158.8 (C-8).

1-(*p*-Methoxyphenyl)-9-(4-hydroxyphenyl)-2,6,7-trithianonane (5)

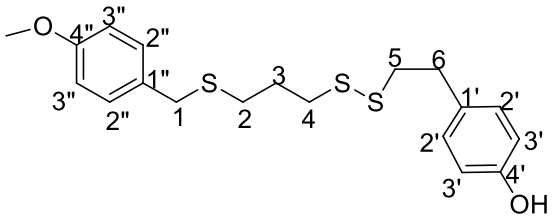

Thiol (**4**) (250 mg, 1.1 mmol) dissolved in triethylamine (0.31 mL, 2.25 mmol) was added dropwise to a solution of sulfonylthioate (**3**) (0.704 g, 2.2 mmol) in anhydrous methanol (10 mL) at -78°C. The reaction was allowed to proceed for 30 mins, after which there was full conversion of the thiol substrate according to TLC, at which point the methanol and excess triethylamine were removed under reduced pressure. The crude product was purified directly by column chromatography using EtOAc and Hexane (5-20% EtOAc) to afford (**5**) as a yellow oil (368 mg, 88%).

R_f = 0.4 (Hexane / EtOAc = 70 / 30); IR ν_{max}/cm^{-1} (CH_2Cl_2): 3054 (ArOH), 705 (C-S); *m/z* (ES) : 379.0860 $[M-H]^+$ $C_{19}H_{23}O_2S_3$ requires 379.0866; ^{1}H NMR (400 MHz, $CDCl_3$) δ 1.93 (2H, quin, *J* = 7.2 Hz, H-3), 2.51 (2H, t, *J* = 7.2 Hz, H-2), 2.73 (2H, t, *J* = 7.2 Hz, H-4), 2.89 (4H, brs, H-5, H-6), 3.67 (2H, s, H-1), 3.79 (3H, s, OMe), 4.77 (1H, s, O-H), 6.75 (2H, d, *J* = 8.8 Hz, H-3'), 6.84 (2H, d, *J* = 8.8 Hz, H-3"), 7.05 (2H, d, *J* = 8.8 Hz, H-2'), 7.22 (2H, d, *J* = 8.8 Hz, H-2"); ^{13}C NMR (100 MHz, $CDCl_3$): δ 28.6 (C-3), 29.9 (C-2) 35.0 (C-5), 35.9 (C-1), 37.7 (C-4), 40.7 (C-6), 55.5 (OMe), 114.1 (C-3"), 115.5 (C-3'), 129.9 (C-2'), 130.0 (C-2''), 130.5 (C-1"), 132.4 (C-1'), 154.1 (C-4'), 159.0 (C-4").

9-(*p*-Acetyloxyphenyl)-1-(*p*-methoxyphenyl)-2,6,7-trithianonane (6)

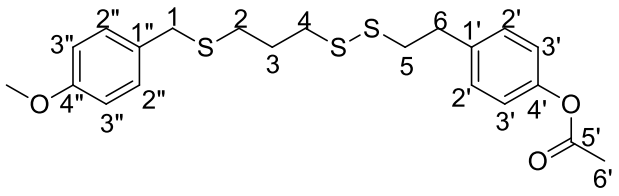

To a solution of phenol (**5)** (0.150 g, 0.395 mmol) and triethylamine (0.08 mL, 0.56 mmol) in DCM (5 mL) at – 78 °C, was added acetyl chloride (0.043 ml, 0.56 mmol) drop-wise. The reaction was stirred under N_2 for 1 h at which point 1 M HCl (5 mL) was used to quench the reaction. The aqueous layer was extracted with DCM (3 x 10 mL), the combined extracts were washed with H_2O (3 x 10 mL) and dried over $MgSO_4$. The solvent was removed under reduced pressure and the residue purified by column chromatography using mixtures of EtOAc and hexane to give the desired product (**6**) as a yellow oil (0.110 g, 64 %).

R_f = 0.5 (Hexane / EtOAc = 70 / 30); IR ν_{max}/cm^{-1} (CH_2Cl_2): 1750 (C=O), 705 (C-S); *m/z* (ES): 445.0933 $[M + Na]^+$, $C_{21}H_{26}NaO_3S_3$ requires 445.0942; ^{1}H NMR (400 MHz, $CDCl_3$): δ 1.96 (2H, quin, *J* = 7.2 Hz H-3), 2.30 (3H, s, H-6'), 2.53 (2H, t, *J* = 7.2 Hz, H-2), 2.76 (2H, t, *J* = 7.2 Hz, H-4), 2.91 (2H, m, H-5), 3.00 (2H, m, H-6), 3.71 (2H, s, H-1), 3.82 (3H, s, OMe), 6.87 (2H, d, *J* = 8.8 Hz, H-3"), 7.04 (2H, d, *J* = 8.8 Hz, H-2'), 7.25 (4H, m, H-2"and H-3'); ^{13}C NMR (100 MHz, $CDCl_3$): δ 21.1 (C-6'), 28.5 (C-3), 29.8 (C-2), 35.1 (C-5), 35.7 (C-1), 37.5 (C-4), 40.0 (C-6), 55.3 (OMe), 114.0 (C-3"), 121.6 (C-2'), 129.6 (C-2"), 130.0 (C-3'), 130.3 (C-1"), 137.5 (C-1'), 149.4 (C-4'), 158.9 (C-4"), 169.5 (C-5').

1-(*p*-Methoxycarbonylmethyloxyphenyl)-9-(*p*-methoxyphenyl)-2,6,7-trithianonane (7)

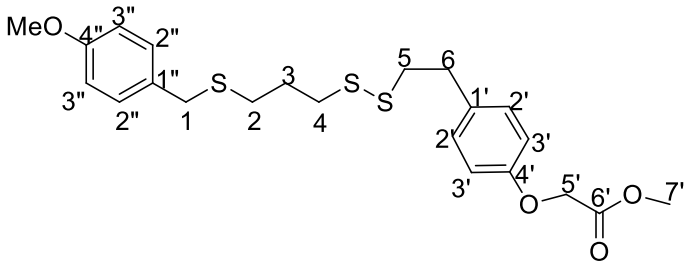

Potassium carbonate (35 mg, 0.26 mmol) was added to a stirring solution of phenol (**5**) (65 mg, 0.17 mmol) in dry acetonitrile (2 mL). After stirring the reaction for 5 min at room temperature, methyl 2-bromoacetate (40 mg, 0.26 mmol) was added, the reaction temperature was raised to 45 °C and the contents stirred overnight under N_2. The reaction was diluted with H_2O (15 mL), and the aqueous layer extracted using EtOAc (3 x 10 mL). The combined organic extracts were washed with H_2O (3 x 10 mL) followed by brine (10 mL). The extracts were dried over $MgSO_4$, the solvent

removed under reduced pressure and the residue purified by column chromatography using mixtures of EtOAc and hexane. The product (**7**) was isolated as a dark-yellow oil (60 mg, 78%).

R_f = 0.15 (Hexane / EtOAc = 90 / 10); IR ν_{max}/cm^{-1} (CH_2Cl_2): 1750 (C=O); HRMS *m/z* (ES): 475.1047 [M+ Na]$^+$, $C_{22}H_{28}NaO_4S_3$ requires 475.1047; ^{1}H NMR (400 MHz, $CDCl_3$): δ 1.94 (2H, quin, *J* = 7.1 Hz, H-3), 2.50 (2H, t, *J* = 7.0 Hz, H-2), 2.73 (2H, t, *J* = 7.0 Hz, H-4), 2.89 (2H, m, H-5), 2.90 (2H, m, H-6), 3.67 (2H, s, H-1), 3.79 (3H, s, H-7'), 3.80 (3H, s, OMe), 4.61 (2H, s, H-5'), 6.83 (4H, d, *J* = 7.2 Hz, H-3' and H-3"), 7.11 (2H, d, *J* = 8.4 Hz, H-2'), 7.20 (2H, d, *J* = 8.4 Hz, H-2"); ^{13}C NMR (100 MHz, $CDCl_3$): δ 28.6 (C-3), 29.8 (C-2), 35.0 (C-5), 35.8 (C-1), 37.7 (C-4), 40.4 (C-6), 52.5 (C-7'), 55.4 (O-Me), 65.7 (C-5'), 114.1 (C-3"), 114.9 (C-3'), 129.9 (C-2"), 130.0 (C-2'), 130.4 (C-1"), 133.5 (C-1'), 156.7 (C-4" and C-4'), 169.7 (C-6').

9-(*p*-Acetamidophenyl)-1-(*p*-methoxyphenyl)-2,6,7-trithianonane (8)

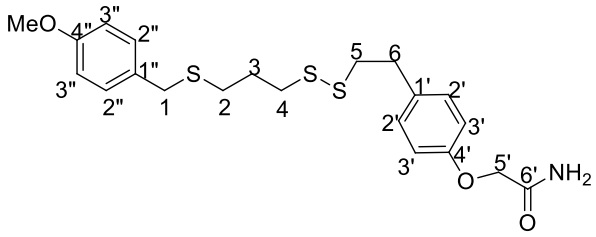

Phenol (**5**) (0.150 g, 0.39 mmol) dissolved in dry acetonitrile (1 mL) was added to a mixture of potassium carbonate (0.082 g, 0.59 mmol) in dry acetonitrile (2 mL), the mixture was stirred for 5 mins before addition of chloroacetamide (55 mg, 0.59 mmol). The temperature was then raised to 45 °C and the reaction mixture stirred under N_2 for 12 h. The reaction was diluted with H_2O (10 mL) and the aqueous layer extracted using EtOAc (3 x 30 mL). The combined organic extracts were washed with H_2O (3 x 30 mL) and dried over $MgSO_4$.The solvent was removed under reduced pressure and the residue purified by column chromatography using mixtures of methanol and DCM to yield the title compound (**8**) as a white powder (0.133 g, 77 %).

R_f = 0.2 (Hexane / EtOAc = 50 / 50); Mp: 83-85 °C; HRMS (ES) *m/z*: 460.1046 [M+ Na]$^+$ $C_{21}H_{27}NNaO_3S_3$ requires 460.1051; ^{1}H NMR (400 MHz, $CDCl_3$): δ 1.93 (2H, quin, *J* = 7.0 Hz, H-3), 2.51 (2H, t, *J* = 7.2 Hz, H-2), 2.74 (2H, t, *J* = 7.2 Hz, H-4), 2.81 (4H, m, H-5 and H-6) 3.67 (2H, s, H-1), 3.79 (3H, s, O-Me), 4,47 (2H, s, H-5'), 6.00 (1H, s, N-H), 6.54 (1H, s, N-H), 6.85 (4H, m, H-3' and H-3"), 7.14 (2H, d, *J* = 8.8 Hz, H-2'), 7.21 (2H, d, *J* = 8.8 Hz, H-2"); ^{13}C NMR (100 MHz, $CDCl_3$): δ 28.6 (C-3), 29.9 (C-2), 34.8 (C-5), 35.8 (C-1), 37.6 (C-4), 40.4 (C-6), 55.4 (OMe), 67.5 (C-5'), 114.1 (C-3"), 114.9 (C-3'), 130.0 (C-2' and C-2"), 130.1 (C-1") 133.9 (C-1'), 156.1 (C-4'), 159.0 (C-4"), 171.2 (C-6').

9-(*p*-Hydroxyphenyl)-1-(*p*-methoxyphenyl) -2, 6, 7-trithianonane-2-oxide (9)

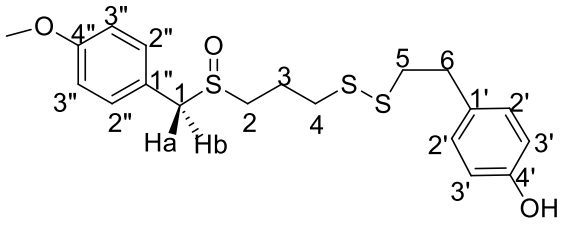

Phenol (**5**) (129 mg, 0.34 mmol) was dissolved in DCM (2 mL), the reaction temperature was lowered to –78 °C and then *m*-CPBA (91.3 mg, 77 % in H_2O, 0.53 mmol) was added slowly. After 1 hour the reaction was quenched with saturated Na_2C0_3 (6 mL). The aqueous layer was extracted with DCM (3 x 10 mL), the combined organic fractions were washed with H_2O (3 x 10 mL). The combined organic fractions were dried over $MgSO_4$, the solvent removed under reduced pressure and the residue purified by column chromatography using mixtures of DCM / methanol to yield (**9**) (100 mg, 72%) as a colourless oil.

R_f = 0.2 (DCM / Methanol = 95 / 5); HRMS (ES) *m/z*: 397.066 $[M+ H]^+$ $C_{19}H_{24}NO_3S_3$ requires 397.066; IR ν_{max}/cm^{-1} (CH_2Cl_2): 3054 (ArOH), 1265 (S=O), 705 (C-S); ^{1}H NMR (400 MHz, $CDCl_3$): δ 2.13 (2H, m, H-3), 2.69 (4H, m, H-2 and H-4), 2.88 (4H, brs, H-5 and H-6), 3.80 (3H, s, OMe), 3.95 (1H, d, *J* = 12.0 Hz, H-1a), 4.00 (1H, d, *J* = 12.0 Hz, H-1b), 6.76 (2H, d, *J* = 8.0 Hz, H-3'), 6.89 (2H, d, *J* = 8.0 Hz, H-3"), 7.01 (2H, d, *J* = 8.0 Hz, H-2'), 7.20 (2H, d, *J* = 8.0 Hz, H-2"); ^{13}C NMR (100 MHz, $CDCl_3$): δ 22.3 (C-3), 34.9 (C-5), 37.3 (C-4), 41.1 (C-6), 48.9 (C-2), 55.5 (OMe), 57.8 (C-1), 114.7 (C-3"), 115.8 (C-3'), 121.4 (C-1"), 129.9 (C-2'), 131.4 (C-2"), 131.7 (C-1'), 154.9 (C-4'), 160.0 (C-4").

9-(*p*-Methoxycarbonylmethyloxyphenyl)-1-(*p*-methoxyphenyl)-2, 6, 7-trithianonane-2-oxide (10)

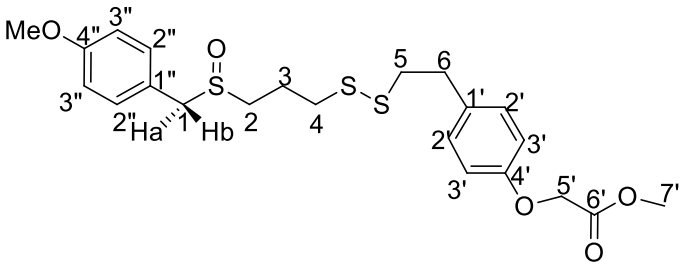

Sulfoxide (**9**) (66 mg, 0.17 mmol) and potassium carbonate were stirred in acetonitrile (5 mL) and after stirring for 5 minutes methyl bromoacetate (39.1 mg, 0.26 mmol) was added, the reaction temperature was raised to 45 °C and the reaction was stirred under N_2 for 1 h. The reaction mixture was quenched with 1 M HCl (10 mL) and the aqueous layer extracted using EtOAc (3 x 10 mL) the combined organic extracts were washed with H_2O (3 x 10 mL) and finally brine (10 mL). The extracts

were dried over $MgSO_4$, the solvent removed under reduced pressure and the residue purified by column chromatography using mixtures of DCM and methanol. The product (**10**) was isolated as a yellow oil (60 mg, 77 %).

R_f = 0.2 (DCM / Methanol = 95 / 5), LC-MS *m/z*: 491.0. $[M+ Na]^+$, $C_{22}H_{28}NaO_5S_3$ requires 491.0997; IR ν_{max}/cm^{-1} (CH_2Cl_2): 1750 (C=O), 1265 (S=O), 705 (C-S); ^1H NMR (400 MHz, $CDCl_3$): δ 2.10 (2H, m, H-3), 2.58-2.78 (4H, m, H-2 and H-4), 2.83 (4H, m, H-5 and H-6), 3.55 (6H, s, OMe and H-7') 3.84 (1H, d, J = 12.0 Hz, H-1a), 3.90 (1H, J = 12.0 Hz, H-1b), 4.55 (2H, s, H-5'), 6.76 (2H, d, *J* = 8.0 Hz, H-3'), 6.82 (2H, d, *J* = 8.0 Hz, H-3"), 7.10 (2H, d, *J* = 8.0 Hz, H-2'), 7.20 (2H, d, *J* = 8.0 Hz, H-2"),; ^{13}C NMR (100 MHz, $CDCl_3$): δ 22.3 (C-3), 34.9 (C-5), 37.4 (C-4), 40.4 (C-6), 49.0 (C-2), 52.4 (C-7'), 55.5 (OMe), 57.9 (C-1), 65.6 (C-5'), 114.7 (C-3"), 114.9 (C-3'), 121.6 (C-1"), 129.9 (C-2'), 131.4 (C-2"), 134.0 (C-1'), 156.7 (C-4'), 160.0 (C-4"), 169.6 (C-6').

***S*-(3-(*p*-Methoxyphenylmethylthio)propyl) ethanethioate (11)**

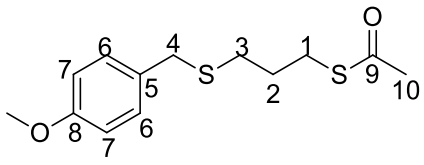

Potassium carbonate (0.726 g, 5.26 mmol) was added to thiol (**4**) (0.600 g, 3.02 mmol) dissolved in degassed acetonitrile (10 mL). After stirring the reaction for 5 mins acetic anhydride (0.30 mL, 3.16 mmol), was added slowly. Thereafter, the reaction was stirred at room temperature under N_2 for a further 90 minutes. The reaction mixture was diluted with H_2O (10 mL), the pH lowered to pH 3 using 1 M HCl and the aqueous layer extracted using EtOAc (3 x 30 mL). The combined organic extracts were washed with H_20 (3 x 30 mL) and saturated $NaHCO_3$ (20 mL), the solvent was removed under reduced pressure and the residue purified by column chromatography using mixtures of EtOAc and hexane to yield the product (**11**) as a yellow oil (0.561 g, 79%).

R_f = 0.6 (Hexane / EtOAc = 95 / 5), ^1H NMR (400 MHz, $CDCl_3$): δ 1.85 (2H, m, H-2), 2.34 (3H, s, H-10), 2.48 (2H, t, *J* = 8.0 Hz, H-3), 2.95 (2H, t, *J* = 8.0 Hz, H-1), 3.69 (2H, s, H-4), 3.82 (3H, s, OMe), 6.86 (2H, d, *J* = 8.0 Hz, H-7), 7.24 (2H, d, *J* = 8.0 Hz, H-6); ^{13}C NMR (100 MHz, $CDCl_3$): δ 28.2 (C-2), 29.2 (C-3), 29.7 (C-1), 30.2 (C-10), 35.6 (C-4), 55.4 (OMe), 114.1 (C-7), 130.0 (C-6), 130.5 (C-5), 158.8 (C-8), 159.0 (C-9).

***S*-(3-((4-Methoxyphenylmethyl)sulfinyl)propyl) ethanethioate (12)**

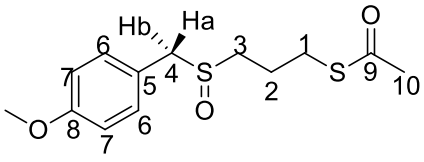

To a solution of sulfide (**11**) (0.420 g, 1.55 mmol) in DCM (10 mL) at -78 °C, was added *m*-CPBA (0.421 g, 77 % in H_2O, 2.44 mmol) slowly. The reaction was stirred at this temperature for 45 minutes under N_2 and full conversion of the sulfide substrate was confirmed by appearance of a new more polar spot on TLC, at which point the reaction was quenched with 1 M $NaHCO_3$ (10 mL). The aqueous layer was extracted using DCM (3 x 30 mL). The combined organic layers were washed with H_2O (3 x 30 mL), then $NaHC0_3$ (30 mL) and dried over $MgSO_4$. Following solvent evaporation, the residue was purified by column chromatography using mixtures of DCM and methanol, to afford (**12**) as a white powder (0.440 g, 99 %).

R_f = 0.5 (Hexane / EtOAc = 20 / 80), ^{1}H NMR (400 MHz, $CDCl_3$): δ 2.04 (2H, quin, *J* = 8.0 Hz, H-2), 2.32 (3H, s, H-10), 2.58 (2H, m, H-3), 2.96 (2H, t, *J* = 8.0 Hz, H-1), 3.80 (3H, s, OMe), 3.91 (1H, d, *J* = 12.0 Hz, H-4a), 3.95 (1H, d, *J* = 12.0 Hz, H-4b), 6.89 (2H, d, *J* = 8.0 Hz, H-7), 7.19 (2H, d, *J* = 8.0 Hz, H-6); ^{13}C NMR (100 MHz, $CDCl_3$): δ 23.2 (C-2), 28.2 (C-1), 30.7 (C-10), 49.5 (C-3), 55.5 (OMe), 57.9 (C-4), 114.6 (C-7), 121.6 (C-5) , 131.4 (C-6), 160.0 (C-9), 161.1 (C-8).

3-(4-Methoxybenzyl thio)-1-propyne (13)[45]

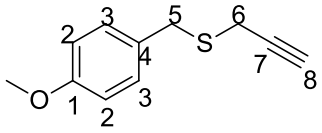

PMBCl (0.460 g, 2.95 mmol) was added to a stirring mixture of thiourea (0.270 g, 3.55 mmol) in dry acetonitrile (10 mL). The mixture was refluxed for 14 hours under N_2, at which point the reaction was cooled in an ice bath and isothiouronium salt retrieved using cold filtration washing with ice-cold acetonitrile (50 mL). The residue was dried on the high vacuum pump to afford the crude isothiouronium salt (0.700 g, 91 %).

The isothiouronium salt (0.700 g, 3.02 mmol) was added to a stirring solution of potassium hydroxide (0.423 g, 7.54 mmol) in degassed anhydrous methanol (10 mL) at – 20 °C. After stirring the reaction at this temperature for 2hrs the reaction temperature was allowed to rise to 0 °C, then propargyl bromide (0.629 g, 5.29 mmol) was added and the reaction left for 10 mins at which point it

was quenched with H_2O (10 mL). The aqueous layer was extracted with EtOAc (3 x 20 mL) and then the combined organic extracts were washed with H_2O (3 x 20 mL) and dried over $MgSO_4$. After subsequent removal of solvent under reduced pressure, the residue was purified by column chromatography using mixtures of EtOAc and hexane to afford (**13**) (520 mg, 90 %) as a gold-coloured oil.

R_f = 0.8 (Hexane / EtOAc = 40 / 60); IR ν_{max}/cm^{-1} (CH_2Cl_2): 3300 (C≡C); ^{1}H NMR (400 MHz, $CDCl_3$): 2.36 (1H, t, *J* = 6.4 Hz, 2.8 Hz, H-8), 3.11 (2H, d, *J* = 2.8 Hz, H-6), 3.82 (3H, s, OMe), 3.87 (2H, s, H-5), 6.89 (2H, d, *J* = 8.8 Hz, H-3), 7.29 (2H, d, *J* = 8.8 Hz, H-2); ^{13}C NMR (100 MHz, $CDCl_3$): δ 18.2 (C-6), 34.6 (C-5), 55.1 (OMe), 71.2 (C-8), 80.0 (C-7), 113.9 (C-2), 129.3 (C-4), 130.0 (C-3), 158.7 (C-1).

(*E*/*Z*)-*S*-3-(4-Methoxybenzylthio)prop-1-en-yl) ethanethioate (**14**)

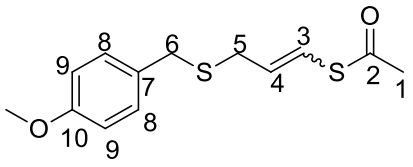

Alkyne (**13**) (0.200 g, 1.04 mmol) was dissolved in dry toluene (5 mL) and the solution heated to 85 °C under N_2, at which point ACCN (25.4 mg, 0.10 mmol) was added followed by the addition of thiolacetic acid (95.2 mg, 1.25 mmol). The reaction was stirred at 85 °C for 3 h, thereafter cooled to room temperature and quenched with saturated $NaHCO_3$ (5 mL). Toluene was removed under reduced pressure and the residue diluted with EtOAc (10 mL). The aqueous layer was extracted using EtOAc (3 x 15 mL), then the combined organic fractions washed with H_2O (3 x 15 mL), then brine (10 mL) and dried over $MgSO_4$. The solvent was removed under reduced pressure and the residue purified by column chromatography using mixtures of EtOAc and hexane (1-5% EtOAc) to afford (**14**) (164 mg, 59 %) as ≈ 1 : 2 mixture of *E* : *Z* isomers.

***E*/*Z* mixture:** R_f = 0.5 (Hexane / EtOAc = 90 / 10), IR ν_{max}/cm^{-1} (CH_2Cl_2): 1700 (C=O), 705 (C-S)

***Z*-isomer**: ^{1}H NMR (400 MHz, $CDCl_3$): δ 2.40 (3H, s, H-1), 3.14 (2H, dd, *J* = 7.8 Hz, 1.0 Hz, H-5), 3.68 (2H, s, H-6), 3.83 (3H, s, OMe), 5.89 (1H, m, H-4), 6.69 (1H, dt, *J* = 12.0 Hz, 1.0 Hz, H-3), 6.86 (2H, d, *J* = 9.0 Hz, H-9), 7.24 (2H, *J* = 9.0 Hz, H-8); ^{13}C NMR (100 MHz, $CDCl_3$): δ 30.8 (C-1), 33.3 (C-5), 35.3 (C-6), 55.4 (OMe), 114.1 (C-9), 119.7 (C-3), 130.0 (C-7), 130.2 (C-4), 130.3 (C-8), 158.9 (C-10), 191.4 (C-2).

***E*-isomer**: ^{1}H NMR (400 MHz, $CDCl_3$): δ 2.39 (3H, s, H-1), 3.12 (2H, dd, *J* = 7.2 Hz, 1.2 Hz, H-5), 3.67 (2H, s, H-6), (3H, s, OMe), 5.72 (1H, m, H-4), 6.52 (1H, dt, *J* = 16.0 Hz, 1.2 Hz H-3), 6.88 (2H, d, *J* = 8.0

Hz, H-9), 7.27 (2H, d, *J* = 8.0 Hz, H-8)); ^{13}C NMR (100 MHz, $CDCl_3$): δ 30.9 (C-1), 34.6 (C-5), 35.3 (C-6), 55.4 (OMe), 114.1 (C-9), 119.5 (C-3), 128.7 (C-7), 129.9 (C-8), 130.5 (C-4), 158.8 (C-10), 193.0 (C-2).

(*E*/*Z*)-9-(4-Hydroxyphenyl)-1-(4-methoxyphenyl)-2,6,7-trithianona-4-ene (15)

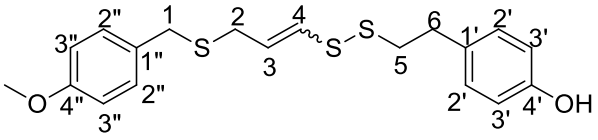

Potassium hydroxide (0.258 g, 4.62 mmol) was added to a solution of vinyl thioacetate (**15**) (0.777 g, 2.89 mmol) in methanol (15 mL) at -40 °C and the reaction was stirred for 30 mins under N_2. The temperature was lowered to -78 °C and then thiosulfonothioate (**3**) (1.249 g, 4.05 mmol) in methanol (3 mL) was added. The reaction temperature was allowed to rise up to room temperature and the reaction was stirred overnight. The reaction was quenched with water (10 mL), the methanol removed under reduced pressure and the residue re-suspended in DCM (10 mL). The aqueous layer was extracted using DCM (3 x 15 mL) and the combined organic extracts were washed with brine (2 x 10 mL). After subsequent removal of solvent under reduced pressure the residue was purified by column chromatography using MeOH and DCM as eluent, to yield (**15**) (0.864 g, 79 %) as a 4 : 5 mixture of *E* : *Z* isomers.

E/*Z* mixture: R_f = 0.4 (Hexane / EtOAc = 85 / 15), IR ν_{max}/cm^{-1} ($CHCl_3$): 3152 (ArOH), 663 (C-S); HRMS (ES) *m/z*: 379.0849 [M+ H] $^+$, $C_{19}H_{23}O_2S_3$ requires 379.0860.

***Z*-isomer**: ^{1}H NMR (400 MHz, $CDCl_3$): δ 2.95 (4H, m, H-5, H-6), 3.25 (2H, dd, *J* = 7.6 Hz, 0.8 Hz, H-2), 3.72 (2H, s, H-1), 3.82 (3H, s, OMe), 5.05 (1H, brs, OH), 5.73 (1H, m, H-3), 6.28 (1H, dt, *J* = 9.2 Hz, 1.0 Hz, H-4), 6.75 (2H, dd, *J* = 8.4 Hz, 4.4 Hz, H-3'), 6.87 (2H, dd, *J* = 8.8 Hz, 2.2 Hz, H-3"), 7.08 (2H, t, 8.4 Hz, H-2'), 7.22 (2H, m, H-2"); ^{13}C NMR (100 MHz, $CDCl_3$): δ 29.5 (C-2), 34.8 (C-5) 35.6 (C-1), 40.6 (C-6), 55.4 (OMe), 114.2 (C-3"), 115.6 (C-3'), 128.3 (C-3), 129.9 (C-2'), 130.2 (C-2"), 130.7 (C-1"), 132.0 (C-1') 132.4 (C-4), 154.3 (C-4'), 158.8 (C-4").

***E*-isomer**: ^{1}H NMR (400 MHz, $CDCl_3$): δ 2.95 (4H, m, H-5 and H-6), 3.10 (2H, dd, *J* =7.2 Hz, 1.0 Hz, H-2), 3.65 (2H, s, H-1), 3.82 (3H, s, OMe), 5.05 (1H, brs, OH), 5.89 (1H, m, H-3), 6.10 (1H, dt, *J* = 14.8 Hz, 1.2 Hz, H-4), 6.76 (2H, dd, *J* = 8.4 Hz, 4.4 Hz, H-3'), 6.87 (2H, dd, *J* = 8.8 Hz, 2.2 Hz, H-3"), 7.08 (2H, t, 8.4 Hz, H-2'), 7.22 (2H, m, H-2"); ^{13}C NMR (100 MHz, $CDCl_3$): δ 32.9 (C-2), 34.7 (C-5), 34.8 (C-1), 39.8 (C-6), 55.4 (OMe), 114.1 (C-3'), 114.2 (C-3"), 115.5 (C-3'), 128.2 (C-3), 128.4 (C-4), 129.9 (C-2'), 130.2 (C-2"), 130.7 (C-1"), 132.1 (C-1'), 154.3 (C-4'), 158.8 (C-4").

(*E/Z*)-9-(4-Hydroxyphenyl)-1-(4-methoxyphenyl)-2,6,7-trithianona-4-ene-2-oxide (**15**)

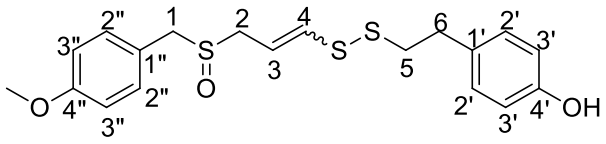

The sulfide (**14**) (0.382 g, 1.00 mmol) was dissolved in DCM (3 mL) and the temperature lowered to -78 °C at which point *m*-cpba (0.268 g, 77 % in H_2O, 1.20 mmol) was added. The reaction was stirred for 5 hrs under N_2 at -78 °C and then quenched with 1 M $NaHCO_3$ (5 mL). The aqueous layer was extracted with DCM (3 x 10 mL), the combined organic extracts washed with H_2O (2 x 10 mL), saturated $NaHCO_3$ (10mL) and brine (10 mL). The organic extracts were dried over $MgSO_4$, the solvent removed under reduced pressure and the residue purified by column chromatography using EtOAc and hexane as eluent. The title compound (**15**) (0.234 g, 68%) was isolated as a 1 : 1 mixture of *E : Z* isomers as a light brown oil.

R_f = 0.6 (Hexane / EtOAc = 40 / 60), IR ν_{max}/cm^{-1} ($CHCl_3$): 3152 (ArOH), 1325 (S=O), 663 (C-S); HRMS (ES) *m/z*: 393.0646 $[M- H]^+$, $C_{19}H_{21}O_3S_3$ requires 393.0653.

***Z*-isomer**: ^{1}H NMR (400 MHz, $CDCl_3$): δ 2.91 (4H, m, H-5 and H-6), 3.48 (1H, ddd, *J* = 13.5 Hz, 7.5 Hz, 0.9 Hz,, H-2a), 3.54 (1H, ddd, *J* = 13.5 Hz, 7.5 Hz, 0.9 Hz, H-2b), 3.80 (3H, s, OMe), 3.94 (2H, s, H-1), 5.72 (1H, m, H-3), 6.57 (1H, dt, *J* = 9.6 Hz, 0.9 Hz, H-4), 6.75 (2H, dd, *J* = 8.8 Hz, 1.4 Hz, H-3'), 6.90 (2H, dd, *J* = 9.0 Hz, 0.8 Hz, H-3"), 7.02 (2H, m, H-2'), 7.20 (2H, d, *J* = 9.0 Hz, H-2"); ^{13}C NMR (100 MHz, $CDCl_3$): δ 34.8 (C-5), 40.8 (C-6), 49.6 (C-2), 55.5 (OMe), 57.0 (C-1), 114.7 (C-3"), 115.7 (C-3'), 118.3 (C-3), 121.6 (C-1"), 129.9 (C-2'), 131.0 (C-1'), 131.4 (C-2"), 138.9 (C-4), 154.9 (C-4'), 160.1 (C-4").

***E*-isomer**: ^{1}H NMR (400 MHz, $CDCl_3$): δ 2.91 (4H, m, H-5 and H-6), 3.32 (1H, ddd, *J* = 13.2 Hz, 8.1 Hz, 0.9 Hz, H-2a), 3.44 (1H, ddd, *J* = 13.2 Hz, 8.1 Hz, 0.9 Hz, H-2b), 3.80 (3H, s, OMe), 3.96 (2H, s, H-1), 5.83 (1H, m, H-3), 6.25 (1H, dt, *J* = 14.7 Hz, 0.9 Hz, H-4), 6.76 (2H, dd, *J* = 8.8 Hz, 1.0 Hz, H-3'), 6.90 (2H, dd, *J* = 9.0 Hz, 0.8 Hz, H-3"), 7.01 (2H, m, H-2'), 7.23 (2H, d, *J* = 9.0 Hz, H-2"); ^{13}C NMR (100 MHz, $CDCl_3$): δ 34.8 (C-5), 40.4 (C-6), 53.0 (C-2), 55.5 (OMe), 56.4 (C-1), 114.7 (C-3"), 115.7 (C-3'), 116.3 (C-3), 121.5 (C-1"), 129.9 (C-2'), 131.0 (C-1'), 131.4 (C-2"), 135.0 (C-4), 154.9 (C-4'), 160.1 (C-4").

4-((*tert*-Butyldimethylsilyl)oxy)butan-1-ol (16)

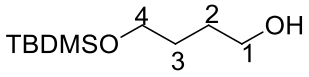

TBDMSCl (1.53 g, 13.5 mmol) in DMF (5 mL) was added dropwise to a stirring solution of butane-1,4-diol (1.22 g, 13.5 mmol) and imidazole (1.72 g, 25.2 mmol) in DMF (20 mL),. The reaction was allowed to proceed at room temperature under N_2 for 3 h at which point the reaction was quenched with H_2O (40 mL). The aqueous layer was extracted using EtOAc (40 mL x 3) and the combined organic extracts were washed with H_2O (40 mL x 10) to remove the DMF. The extracts were dried over $MgSO_4$, the solvent removed under reduced pressure and the residue purified by column chromatography using mixtures of EtOAc and hexane to yield a colourless liquid (**16**) (1.92 g, 69 %).

R_f = 0.4 (Hexane / EtOAc = 30 / 60), IR ν_{max}/cm^{-1} (CH_2Cl_2): 3400 (O-H), 1099 (C-0); ^{1}H NMR (400 MHz, $CDCl_3$): δ 0.00 (6H, s, 2 x Si(CH_3)), 0.84 (9H, s, Si(CH_3)$_3$), 1.57 (4H, m, H-2 and H-3), 3.06 (1H, brs, OH), 3.58 (4H, m, H-1 and H-4); ^{13}C NMR (100 MHz, $CDCl_3$): δ -5.20 ($SiCH_3$), 18.3 ($SiCMe_3$), 26.0 (SiC(CH_3)$_3$), 29.8 (C-3), 30.0 (C-2), 62.6 (C-4), 63.3 (C-1).

4-((*tert*-Butyldimethylsilyl)oxy)butyl 2-chloroacetate (17)

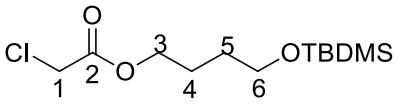

Alcohol (**16**) (1.55 g, 8.72 mmol) and triethylamine (2.50 mL, 17.9 mmol) were dissolved in dry DCM (20 mL), the temperature was lowered to -20 °C then chloroacetyl chloride (1.03 mL, 10.5 mmol) was added via a syringe. The reaction was allowed to proceed for 10 min under N_2 and then quenched with 0.25 M $NaHCO_3$ (10 mL). The aqueous layer was extracted with DCM (3 x 20 mL), the combined organic fractions were washed with H_2O (3 x 10 mL) and then brine (10 mL). The crude residue was dried over $MgSO_4$, the solvent removed under reduced pressure and the residue purified by column chromatography using mixtures of EtOAc and hexane. The title compound (**17**) was isolated as a colourless oil (1.77 g, 72 %).

R_f = 0.85 (Hexane / EtOAc = 70 / 30), IR ν_{max}/cm^{-1} (CH_2Cl_2): 1755 (C=0), 1098 (C-0); ^{1}H NMR (400 MHz, $CDCl_3$) : δ 0.04 (6H, s, 2 x Si(CH_3)), 0.89 (9H, s, Si(CH_3)$_3$), 1.57 (2H, m, H-5), 1.72 (2H, m, H-4), 3.63 (2H, t, *J* = 8.2 Hz, H-6), 4.04 (2H, s, H-1), 4.21 (2H, t, *J* = 8.8 Hz, H-3); ^{13}C NMR (100 MHz, $CDCl_3$): δ -5.20 ($SiCH_3$), 18.4 (SiC), 25.3 (C-5), 26.1 (SiC(CH_3)$_3$), 29.2 (C-4), 41.0 (C-1), 62.6 (C-6) 66.4 (C-3), 167.5 (C-2).

(*E*/*Z*)-9-(*p*-(4-((*Tert*-butyldimethylsilyloxy)butyloxycarbonylmethyoxy)phenyl)-1-(*p*-methoxyphenyl)-2,6,7-trithianona-4-ene (**18**)

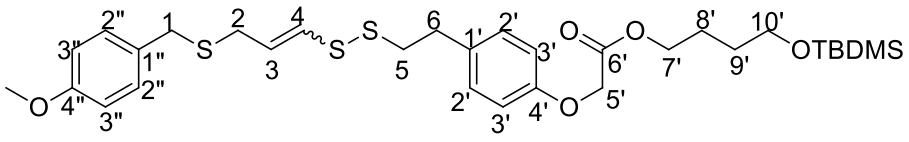

Phenol (**15**) (150 mg, 0.40 mmol) and potassium carbonate (109 mg, 0.80 mmol) in acetonitrile (3 mL) were stirred for 10 min and the chloroacetate (**17**) (222 mg, 0.80 mmol) was added. The reaction was stirred at 40 °C under N_2 for 72 h, at which point the solvent was removed under reduced pressure and the residue suspended in EtOAc (10 mL) and H_2O (10 mL). The aqueous layer was extracted using EtOAc (3 x 10 mL), the combined organic extracts washed with H_2O (3 x 10 mL), brine (10 mL) and dried over $MgSO_4$. The solvent was removed under reduced pressure and the residue purified by column chromatography using EtOAc and hexane as the eluents. The title compound (**18**) was isolated as a yellow oil (113 mg, 45 %) as an *E*: *Z* mixture (7: 5).

R_f = 0.5 (Hexane / EtOAc = 85 / 15), IR *v*max/cm-1 (CH_2Cl_2): 1750 (C=0), 1099 (C-0), 705 (C-S);

***Z*-isomer:** ^{1}H NMR (400 MHz, $CDCl_3$): δ 0.05 (6H, s, 2 x $Si(CH_3)$), 0.91 (9H, s, $Si(CH_3)_3$), 1.55 (2H, m, H-8'), 1.73 (2H, m, H-9'), 2.93 (4H, s, H-5 and H-6), 3.24 (2H, d, *J* = 7.6 Hz, H-2), 3.62 (2H, m, H-10'), 3.68 (2H, s, H-1), 3.79 (3H, s, OMe), 4.23 (2H, t, *J* = 6.6 Hz, H-7'), 4.59 (2H, s, H-5'), 5.71 (1H, dt, *J* = 9.2 Hz, 7.6 Hz, H-3), 6.24 (1H, dt, *J* = 9.2 Hz, 1.2 Hz, H-4), 6.84 (4H, m, H-3' and H-3"), 7.10 (2H, t, *J* = 7.2 Hz, H-2'), 7.24 (2H, d, *J* = 8.8 Hz, H-2"); ^{13}C NMR (100 MHz, $CDCl_3$): δ -5.28 ($SiCH_3$), 18.3 (SiC), 25.4 (C-8'), 26.1 ($SiC(CH_3)_3$), 29.2 (C-9'), 29.6 (C-2 and C-5), 34.9 (C-1), 40.6 (C-6), 55.4 (OMe), 62.6 (C-10'), 65.4 (C-7'), 65.8 (C-5'), 114.2 (C-3"), 115.0 (C-3'), 128.5 (C-3), 129.8 (C-2'), 130.2 (C-2"), 132.3 (C-4), 133.2 (C-1'), 156.8 (C-4'), 158.9 (C-4"), 170.0 (C-6').

***E*-isomer:** ^{1}H NMR (400 MHz, $CDCl_3$): δ 0.05 (6H, s, 2 x $Si(CH_3)$), 0.91 (9H, s, $Si(CH_3)_3$), 1.55 (2H, m, H-8'), 1.73 (2H, m, H-9'), 2.93 (4H, s, H-5 and H-6), 3.09 (2H, dd, *J* = 8.4 Hz, 1.0 Hz, H-2), 3.62 (4H, m, H-1 and H-10'), 3.79 (3H, s, OMe), 4.23 (2H, t, *J* = 6.6 Hz, H-7'), 4.59 (2H, s, H-5'), 5.89 (1H, m, H-3), 6.09 (1H, dt, *J* = 14.4 Hz, 1.0 Hz, H-4), 6.84 (4H, m, H-3' and H-3"), 7.10 (2H, t, *J* = 7.2 Hz, H-2'), 7.21 (2H, d, *J* = 8.8 Hz, H-2"); ^{13}C NMR (100 MHz, $CDCl_3$): δ -5.28 ($SiCH_3$), 18.3 (SiC), 25.4 (C-8'), 26.1 ($SiC(CH_3)_3$), 29.2 (C-9'), 29.6 (C-5), 33.0 (C-2), 34.8 (C-1), 39.8 (C-6), 55.4 (OMe), 62.6 (C-10'), 65.4 (C-7'), 65.8 (C-5'), 114.2 (C-3"), 115.0 (C-3'), 128.2 (C-4), 128.2 (C-3), 129.8 (C-2'), 130.2 (C-2"), 133.2 (C-1'), 156.8 (C-4'), 158.9 (C-4"), 170.0 (C-6').

6.3 Biological Experimental

Cell Culture

The oesophageal cancer cell-line was derived from a biopsy of primary oesophageal squamous cell carcinoma of South African origin. WHCO1 cells were incubated at 37 °C in a humidified atmosphere under 5 % CO_2 and cultured in Dulbecco's Modified Eagle Medium (DMEM) containing 10 % Fetal bovine serum (FBS) and 1 % penicillin-streptomycin. Cells were grown in 150 mm e plates and split 1: 12 every four days. The splitting procedure, briefly, involved removing cell media and washing cells with 10 mL PBS (Phosphate buffer saline, pH 7.4). Cells were then incubated in trypsin (3 mL) at 37 ° C for 1-2 min. Trypsin was deactivated by adding media (3 mL). Thereafter detached cells were transferred to a sterile 12 mL conical tube containing media (3 mL) and centrifuged at 40 000 rpm for 4 min. Upon removal of the media-trypsin solution, the cells were quickly re-suspended in media (6 mL).

MTT Assay

On day 1, WHCO1 cells were seeded in 96-well plates, at 2500 cells per well suspended in DMEM (90 µL). Cells were allowed to attach and recover overnight

On day 2, a 150 mM stock solution of the compound in high purity DMSO (99.9%) was prepared. The solutions were sonicated at 37 °C for 10 min to ensure complete dissolution. The stock was then further diluted in DMSO to give the following series of concentrations: 0, 0.3, 0.58, 1.17, 2.34, 4.68, 9.38, 18.75, 37.5, 75.0 and 150 mM. The solutions were then subjected to a further 100-fold dilution into media. Thereafter, 10 µL of the compound solution was added to the cells, to give final concentrations of 0, 0.3, 0.58, 1.17, 2.34, 4.68, 9.38, 18.75, 37.5, 75.0 and 150 µM in the cells and final DMSO concentrations of 0.1 %. The negative controls were cells treated with 0.1 % DMSO alone and cells treated with media alone. All experiments were performed in quadruplicate. The cells were then incubated with the compound for 48 h.

On day 4, 10 µL of MTT (5mg/mL) solution was added to each well and the cells incubated for a further 4 h. Thereafter 100 µL of solubilization reagent (10% SLS in 0.01 M HCl) was added to each well and the cells incubated overnight.

On day 5, the absorbance was measured at 595 nm using the Multiskan FC multi-well reader (Thermo Scientific). The background media reading was subtracted using readings from wells containing media and reagents only (no cells). The spectrophotometric data was analysed using Graphpad prism 6, fitted to a sigmoidal dose-response curve, non-variable slope from which the IC_{50}

determined. Each compound IC_{50} is calculated as the mean of at least three independent determinations +- standard deviation.

REFERENCES

1. Rivlin, R., *J. Nutr*. **2001**, *131*, 951S-954S.
2. Keys, A., *Am J Clin*. **1995**, *61*, 1321S-1323S.
3. Rahman, K. *Ageing Res. Rev*. **2003**, *2*, 39–56.
4. Yogeshwer, S.; Neetu K. *Cancer Lett*. **2007**, *247*, 167–181.
5. Cavallito, C.; Bailey, J. *J. Am. Chem. Soc*. **1944**, *66*, 1950-1951.
6. Iciek, M.; Kwiecien I.; Wlodek, L. *Environ Mol Mutagen*. **2009**, *50*, 247-265.
7. Stoll, A.; Seebeck, E. *Helv. Chim. Acta*. **1948**, *31*, 189-210.
8. Brodnitz, M.H.; Pascale, J.V.; van Derslice L. *J. Agric. Food Chem*. **1971**, 19, 273–275.
9. Block, E.; Ahmad, S.; Catalfamo, J.L.; Jain, M.K.; Apitz-Castro, R. *J. Am. Chem. Soc.* **1986**, *108*, 7045-7055.
10. Block, E.; Ahmad, S. *J. Am. Chem. Soc*. **1984**, *106*, 8295-8296.
11. Naznin, M. T.; Akagwa, M.; Okukawa, K.; Maeda, T.; Morita, N. *Food Chem*. **2008**, *106*, 1113-1119.
12. Apitz-Castro, R.; Badimon, J. J.; Badimon, L. *Thromb. Res.* **1994**, *75*, 243–249.
13. Apitz-Castro, R.; Escalante, J.; Vargas, R.; Jain, M.K. *Thromb. Res.* **1986**, *42*, 303-311.
14. Apitz-Castro, R.; Badimon, J.J.; Badimon, L. *Thromb. Res*. **1992**, *68*, 145-155.
15. Jamaluddin, M.P.; Krishnan, L.K.; Thomas A. *Biochem. Biophys. Res. Commun*. **1988**, *153*,479-486.
16. Wagner, H.; Wierer, M.; Fessler, B. *Planta. Med*. **1987**, *53*,305-306.
17. Naganawa, R.; Iwata, N.; Ishikawa K., Fukuda, H., Fujino, T.; Suzuki, A. *Appl. Environ. Microbiol.* **1996**, *62*, 4238-4242.
18. Yoshida, S.; Kasuga, S.; Hayashi, N.; Ushiroguchi, T.; Matsuura H.; Nakagawa, S. *Appl. Environ. Microbiol*. **1987**, *53*, 615.
19. San-Blas, G.; San-Blas F.; Gil, F.; Marino L.; Apitz-Castro, R. *Antimicrob. Agents Chemother*. **1989**, *33*, 1642-1644.
20. Singh, U.; Pandey, V.; Wagner, K.; Singh K. *Can. J. Bot*. **1990**, *68*, 1354-1356.
21. Urbina, J.; Marchan, E.; Lazardi, K.; Visbal, G.; Apitz-Castro, R.; Gil, F.; Aguirre T.; Piras, M. *Biochem. Pharmacol*. **1993**, *45*, 2381.
22. Williams, D.; Edwards, D.; Hamernig, I.; Jian, L.; James, A.; Johnson, S.; Tapsell L. *Food Res. Int.*, **2013**, *52*, 323-333.
23. Yang, J.; Della-Fera, M.; Nelson-Dooley C.; Baile, C. *Obesity*. **2006**, *14*, 388-397.
24. Yang, J.; Della-Fera, M.; Hausman, D.; Baile, C. *Apoptosis.* **2007**, *12*, 1117-1128.
25. Tanaka, T. *J. Exp. Clin. Med*. **2013**, *5*, 89-91.

26. http://www.thymic.org/uploads/reference-sub/03chemopric.pdf
27. Patrick, G.L. An Introduction to Medicinal Chemistry, Oxford University Press, 4th ed, 2009.
28. Elledge, S. *Science* **1996***, 274*, 1664-1672.
29. Elmore, S. *Toxicol Pathol.* **2007**, *35*, 495–516.
30. Sjöström, J.; Mäkelä, T., Apoptosis and the Cell Cycle in Human Disease. Wiley Online Library **2006**, 1-6.
31. Shukla, Y.; Kalra, N. *Cancer Lett*. **2007**, *247*, 167–181.
32. Ishikawa, K.; Naganawa, R.; Yoshida, H.; Iwata, N.; Fukuda, H.; Fujino T.; Suzuki, A. *Biosci. Biotech. Biochem*. **1996**, *60*, 2086–2088.
33. (a) Dirsch, V.; Gerbes, A.; Volmar, A. *Mol. Pharmacol*. **1998**, *53*, 402. (*b*) Li, M.; Ciu, J-R.; Ye, Y.; Min, J-M.; Zhang, L-H.; Wang, K.; Gares, M.; Cros, J.; Wright M.; Leung-Tack, J. *Carcinogenesis* **2002**, *23*, 573. (*c*) Taylor, P.; Noriega, R.; Farah, C.; Abad, M-J.; Arsenak, M.; Apitz, R., *Cancer Lett.,* **2006**, *239*, 298. (d) Dirsch, V.M.; Antlsperger, D S.; Hentze H.; Vollmar, A.M. *Leukemia* **2002**,*16***,** 74. (d) Ledezma, E.; Apitz-Castro, R.; Cardier, J. *Cancer Letters* **2004**, *206*, 35-41.
34. Scharfenberg, K.; Wagner, R.; Wagner, K. G. Cancer Lett. **1990**, *53*, 103–108.
35. Tilli, C.M.; Stavast-Kooy, A.J.; Vuerstaek, J.; Thissen, M.; Krekels,G.; Ramaekers, F.; H. Neumann, H. *Arch. Dermatol. Res.* **2003**, *295*, 117-123.
36. Wang, Z.; Xie, C.; Huang, Y.; Wai Kei Lam, C. Chow, M. S. S. *Phytochem. Rev.* **2013**, *October*, 1-15.
37. Hassan, H. T. *Leuk. Res*. **2004**, *28*, 667.
38. Xu, B.; Monsarrat, B.; Gairin, J. E.; Girbal-Neuhauser, E. *Clin. Pharmacol.* **2004**, *18*, 171.
39. Münchberg, U.; Anwar, A.; Mecklenburg, S.; Jacob, C. *Org. Biomol. Chem*. **2007**, *5*, 1505-1518.
40. Gallwitz, H.; Bonse, S.; Martinez-Cruz, A.; Schlichting, I.; Schumacher, K.; Krauth-Siegel, R. L. *J. Med. Chem.* **1999**, *42*, 364-372.
41. Lawson L. D.; Wang Z. J. *Planta. Med*. **1993**, *59S*, A688-A689.
42. Hunter, R.; Kaschula, C. H.; Parker, M. I.; Caira, M. R.; Richards, P.; Travis, S.; Taute, F.; Qwebani, *Bioorg. Med. Chem. Lett.,* **2008**, *18*, 5277-5279.
43. Kampmeier, J. A.; Chen, G. *J. Am. Chem. Soc.* **1965**, *87*, 2602.
44. Han, C. Y.; Ki, S. H.; Kim, Y. W.; Noh, K.; Lee, D.Y.; Kang, B.; Ryu, J.-H.; Jeon, R.; Kim, E. H.; Hwang, S. J.; Kim, S. G. *Antioxid. Redox Signal*., **2011**, *14*, 187-202.
45. Kaschula, C. H.; Hunter, R.; Stellenboom, N.; Caira, M.R.; Winks, S.; Ogunleye, T.; Richards, P.; Cotton, J.; Zilbeyaz, K.; Wang, Y.; Siyo, V.; Ngarande, E.; Parker, M. I. *Eur. J. Med. Chem*., **2012**, *50*, 236-254.
46. Cotton, J. Masters Dissertation, University of Cape Town, 2010.

47. Mabunda, M. Masters Dissertation, University of Cape Town, 2013.
48. a) Brachwitz, H.; Bergmann, J.; Thomas, Y.; Wollny, T.; Langena. B. *Bioorg. Med. Chem*., **1999**, *7*, 1195-1200. b) Chhikara, B. S.; Mandal, D.; Parang, K. *Eur. J. Med. Chem*., **2010**, *45*, 4601-4608.
49. Torssell, K.; Wahlberg, K. *Acta Chem. Scand*., **1967**, *21*, 53-62.
50. Krysin, P.A.; Egorova, T.G.; Vasil'ev, V. G. *Russ. J. Gen. Chem*., **2010**, *18*, 275-283.
51. Khan, A.T.; Mondal, E. *Synlett*., **2003**, *5,* 694-698.